ENCODING OF GRASPING MOVEMENTS IN THE ANTERIOR INTRAPARIETAL AREA OF MACAQUES

Dissertation

zur

Erlangung der naturwissenschaftlichen Doktorwürde
(Dr. sc. nat.)

vorgelegt der

Mathematisch-naturwissenschaftlichen Fakultät

der

Universität Zürich

von

MARKUS ANDREAS BAUMANN

von Wassen, UR

Promotionskomitee

Prof. Dr. Kevan A.C. Martin (Vorsitz)
Prof. Dr. Hansjörg Scherberger (Leiter der Dissertation)
Prof. Dr. Dominik Straumann

Zürich, 2009

Table of contents

List of figures

List of tables

Acknowledgements

There are many people who helped me during the time of my PhD, either by directly contributing to the work or by supporting me in any other way. Many thanks go to:

Dr. Hansjörg Scherberger, my thesis supervisor. He always took the time for discussions when I asked for it, but also gave me a lot of freedom to try things out that I wanted to try.

Marie-Christine Fluet, for sharing almost all the time with me during the time of our PhD, both at work and at home.

All other members of our group at the INI: Sebastian Lehmann, Erk Subasi and Ben Townsend. It was great to have colleagues with whom I could have a lot of good times not only in the lab, but also outside over one or the other beer.

Johanna Höhn and Gisep Bazzell together with the entire team of animal care takers. It was very reassuring for us to know that a team of responsible people was taking care of our monkeys every day.

Prof. Kevan Martin and Prof. Dominik Straumann who agreed to be in my steering committee amd Dr. Daniel Kiper who agreed to be an examiner at my PhD defense.

Last but for sure not least: My parents who continued to support me in many ways throughout a long period of education at the university.

Disclaimer

All experiments involving monkeys were in accordance with the guidelines for the care and use of mammals in neuroscience and behavioral research (National Research Council, 2003) and approved by the cantonal Veterinary Office of Zurich.

Training of the monkeys was performed by Marie-Christine Fluet and myself, sometimes with the help of Bernadette Disler.

Building the setup for doing electrophysiology in behaving monkeys and in particular for the delayed grasping task that was used in the current thesis, was a joint effort of Hansjörg Scherberger, Marie-Christine Fluet and myself.

The software for the control of the behavioral setup and the acquisition of behavioral data was written by myself in LavView.

The surgeries necessary to prepare for the recordings were performed by Hansjoerg Scherberger, with me assisting him.

All data presented in this thesis were collected by myself, in close collaboration with Marie-Christine Fluet.

All software for data anlalysis in MatLab was written by myself.

Summary

The primate hand has developed as an extremely versatile tool to manipulate a wide range of objects with a variety of different grip types, spanning from strong power grips to fine and delicate precision grips. Grasping movements are typically made under visual guidance, and therefore their neural control can perhaps be most easily understood in the framework of visuo-motor transformations. However, the optimal grip type and therefore the shape of the hand during grasping does not only depend on the form of the target object, but also on the intended manipulation, which in turn depends on the context of the action. Therefore, this context has to be incorporated at some point into the visuo-motor transformation.

The parietal lobe plays an important role for the generation of hand grasping movements. Lesions in human parietal cortex lead to optic ataxia, a deficit in hand movement coordination. Recently, neurons in a region of the macaque parietal lobe, the anterior intraparietal area (AIP), were found to fire specifically during the execution of certain grip types. Furthermore, the same neurons were active during mere fixation of the graspable objects. However, the interplay between the visual and motor response in AIP has been poorly studied and the question to what extent AIP encodes also context-specific information for hand grasping is unknown.

To explore these issues, we trained two macaque monkeys to grasp a single object with two different grip types, namely power and precision grip. The correct grip of each trial was instructed by a colored LED which served as context cue. Furthermore, a factor of the 3D object appearance was varied by presenting it in five different orientations. The task was a delayed grasping task, which allowed separating in time the visual instruction phase from the movement execution.

We recorded 571 single-units in AIP of two macaques during this task. While the neural representation of the object orientation was stable over the time of a trial, the number of cells encoding grip type increased from the cue epoch to movement

execution. A classification of cells according to the time of their tuning onset revealed differences in the function and anatomical location of early- versus late-tuned cells. Furthermore, when the grasp type instruction was presented before the object, type information was only weakly represented in AIP, but it was strongly encoded after the grasp target was revealed. We concluded that AIP encodes context specific hand grasping movements to perceived objects, while the encoding of context information is weak in the absence of a grasp target.

Furthermore, we analyzed the coding properties of the local field potential (LFP) during the delayed grasping task. The LFP is a summation signal that represents the net excitatory and inhibitory synaptic and dendritic potential in a 'listening sphere' around the tip of the electrode. Several reasons contributed to an increased scientific interest in the LFP over the last years. Some of these reasons are: (1) The LFP is better correlated with the BOLD signal of fMRI research than spiking activity. (2) The LFP has been proposed as an input signal in future brain-machine interface applications, as it can be stably recorded over extended periods of time. (3) The LFP is thought to be related to local input activity, while spikes represent neural output. A better understanding of the relationship between the LFP and local spiking activity might therefore give new tools at hand to better study the local information processing.

We found that LFPs in AIP were most strongly modulated by the behavioral epoch of the task, but were also frequently selective for the handle orientation and the grip type. When comparing the coding properties of the LFP with the one of multi unit spiking, we found that the power of the gamma band LFP (30-100 Hz) was correlated with spiking activity on the same electrode. Furthermore, the preferred conditions in this band could be explained by the behavior of the spiking activity in a larger listening sphere, if one takes into account the structural organization of single cells within AIP.

In sum, this thesis brings new insights into the mechanisms of visuo-motor transformation for hand grasping movements, by showing how visual, motor and context parameters are combined at the stage of the parietal cortex.

Zusammenfassung

Die Hand der Primaten ist ein extrem vielfältiges Instrument, mit welchem eine grosse Zahl an Objekten mit verschiedensten Greifarten manipuliert werden können. Letztere reichen von festen Kraftgriffen bis zu diffizilen Präzisionsgriffen. Greifbewegungen werden normalerweise unter visueller Kontrolle ausgeführt, weshalb die neuronalen Kontrollmechanismen am besten im Rahmen der visuo-motorischen Transformationen verstanden werden können. Der optimale Grifftyp und damit die Handkonfiguration hängen aber nicht nur von der Form des Zielobjektes ab, sondern auch von der beabsichtigten Manipulation. Diese wiederum hängt vom Kontext der Handlung ab, welcher daher in die visuo-motorische Tranformation einfliessen muss.

Der Parietallappen spielt eine wichtige Rolle bei der Planung von Handbewegungen. Patienten mit Läsionen in dieser Rindenregion leiden an optischer Ataxie, einem Defizit der Koordination von Handbewegungen. Vor kurzem wurden im Anterioren Intraparietalen Areal (AIP), einer Region im Parietalkortex von Makaken, Neuronen gefunden, welche spezifisch aktiv sind bei der Ausführung gewisser Greifarten. Dieselben Zellen sind ausserdem aktiv beim blossen Anblick der greifbaren Objekte. Das Zusammenspiel von visueller und motorischer Aktivität in AIP wurde bisher aber kaum untersucht. Ob AIP auch kontext-spezifische Faktoren kodiert, welche für Greifbewegungen relevant sind, ist ebenfalls unbekannt.

Um diese Fragen zu untersuchen, haben wir zwei Makaken trainiert, ein Objekt mit zwei verschiedenen Griffarten zu fassen, nämlich mit einem Kraft- oder einem Präzisionsgriff. Der korrekte Griff wurde bei jedem Versuch mittels einer farbigen Leuchtdiode instruiert, welche damit als Kontextinformation diente. Ausserdem wurde ein Faktor der 3D Erscheinung des Objektes variiert, indem es in fünf verschiedenen Orientierungen präsentiert wurde. Wir benutzten einen ‘delayed

grasping task', in welchem die Phase visueller Instruktionen zeitlich klar von der Ausführung der Bewegung getrennt war.

Wir zeichneten die Aktivität von 571 Neuronen zweier Tiere auf, während diese die beschriebene Aufgabe ausführten. Die neuronale Repräsentation der Objektorientierung war zeitlich konstant, während die Zahl der Zellen, welche die Griffart kodierten, von der Instruktion zur Bewegungsausführung zunahm. Zellen mit früher Aktivität unterschieden sich von solchen mit später Aktivität sowohl in funktioneller Hinsicht, wie auch in ihrer anatomischen Lokation. Des weiteren war die Kodierung der Griffart stark reduziert, wenn sie instruiert wurde bevor das Zielobjekt dem Tier gezeigt wurde. Wir folgerten aus diesen Resultaten, dass AIP kontext-spezifische Greifbewegungen kodiert, die Kontext-Information aber nur schwach repräsentiert, wenn kein konkretes greifbares Objekt präsent ist.

Des weiteren untersuchten wir die Kodierungseigenschaften des Lokalen Feldpotentials (LFP) während des 'delayed grasping task'. Das LFP repräsentiert die Summe von erregenden und hemmenden synaptischen und dendritischen Potentialen im Umkreis der Elektrodenspitze und hat in letzter Zeit aus verschiedenen Gründen wachsendes wissenschaftliches Interesse erregt. Einige dieser Gründe sind: (1) Das LFP korreliert stärker mit dem BOLD Signal der fMRI Forschung als die Aktionspotentiale von Einzelzellen. (2) Das LFP wurde als Eingangssignal für zukünftige Anwendungen in Hirn-Maschinen-Schnittstellen vorgeschlagen, da es über längere Zeit stabil aufgezeichnet werden kann. (3) Man nimmt an, dass das LFP eher lokalen Input repräsentiert, während die Aktionspotentiale den Output von Neuronen darstellen. Ein besseres Versändnis der Zusammenhänge von LFP und Aktionspotentialen könnte daher hilfreich sein, um die lokale Informationsverarbeitung zu untersuchen.

Unserer Resultate zeigen, dass das LFP in AIP am stärksten durch die verschiedenen Phasen des Tasks moduliert wird, doch ist es oft auch selektiv für die Orientierung und die Art des Griffs. Ein Vergleich der Kodierungseigenschaften von LFP und Aktionspotentialen zeigte, dass die Aktivität im Gamma Band des LFP (30-100 Hz) mit der Anzahl der Aktionspotentiale auf der gleichen Elektrode korreliert.

Die bevorzugte Orientierung und Griffart des LFP in diesem Frequenzband kann erklärt werden durch das Verhalten der Aktionspotentiale vieler Zellen, wenn man die strukturelle Organisation der Zellen in AIP berücksichtigt.

Zusammengefasst gewährt diese Dissertation neue Einblicke in die Funktionsweise der visuo-motorischen Transformationen für Greifbewegungen, indem sie zeigt, wie im Parietalkortex visuelle, motorische und Kontextinformationen kombiniert werden.

1 Introduction

1.1 Overview

The use of the hand plays a crucial role in everyday behavior of humans and non-human primates. The primates' hand has developed as an extremely versatile tool to manipulate a wide range of objects with a variety of different grip types, spanning from strong power grips to fine and delicate precision grips. It is obvious that such a complexity of behaviors pose a difficult control task to the brain. Grasping movements are typically made under visual guidance, making the transformation of visual information into motor commands a crucial step in hand movement planning. Studying this sensorimotor transformation is therefore an important part towards a better understanding of the cortical control of hand grasping movements.

In the first part of this introduction, **Section 1.2**, I will therefore review the literature about the general organization of the cortical systems implicated in visuomotor transformations, with a particular emphasis on the role of the parietal cortex in visuomotor transformation. **Section 1.3** will then focus more specifically on cortical areas that are important for hand grasping, presenting in more depth the current view of the parietal area AIP and frontal area F5.

The specific questions and goals of this thesis will be described at the end of the present chapter (**Section 1.4**).

1.2 Visuomotor Transformation

Goal directed movements on visually perceived objects require that the representation of visual features of the target are transformed into motor signals to the muscles. This process is called visuomotor transformation. The present state of the body, the configuration of the target and the environment all have to be taken into account. Reaching for objects and grasping them are two typical forms of such goal directed movements. Reaching is mainly concerned with spatial arrangements like the relative position of the target to the body and the hand, while the suitable grip type is determined by the intrinsic properties of the object like its size, shape or orientation.

Psychophysical experiments in humans have shown that grasping and reaching are closely linked together (Jeannerod and Biguer, 1982; Jeannerod, 1988). Hand opening and pre-shaping occurs during the reaching movement. Furthermore, if the reaching component is disturbed by a displacement of the target, thereby prolonging the reach movement, the pre-shaping of the hand is interrupted and delayed, in order to synchronize it again with the reaching movement (Paulignan et al., 1991). Nevertheless, electrophysiological recordings in monkeys have shown that on the neuronal level several brain regions and cortico-cortical loops are specialized for the sensorimotor transformation and planning of either the reach or the grasp component of a reach to grasp behavior (for a review, see: Rizzolatti and Luppino, 2001).

In this section, we will review the literature about the general structure of the visuomotor system. A first important issue is the organization of the visual system.

1.2.1 Two visual streams

Humans perceive their vision of the world as one unitary process. However, from a neuroscientific point of view, the situation is more complex and the processing of visual information is distributed across several parallel systems that deal with different aspects of the visual input to the cortex. This idea came from research on

animals, in which parts of the visual system were lesioned. Following experiments on hamsters, Schneider proposed in 1969 an anatomical separation between the processing of a stimulus location and its identification (Schneider, 1969). The former he attributed to the retinotectal system, the latter to the geniculostriate pathway to the visual cortex. Although in subsequent experiments it became clear that many behaviors that include object localization could not be explained by tectal mechanisms alone (Goodale and Murison, 1975), the idea of separated visual pathways persisted in neuroscience.

In 1982, Ungerleider and Mishkin suggested a similar functional division, but mapped it onto two subsystems within the neocortex (Ungerleider and Mishkin, 1982). They proposed that the qualities of an object (e.g. shape, size, color) are processed in a ventral pathway that extends from the visual cortex to the inferior temporal lobe (the 'what' pathway) while the spatial location would be processed in a dorsal pathway leading to the posterior parietal cortex (the 'where' pathway). Their hypothesis was based on a number of studies that had been performed in monkeys. Macaques with lesions in the inferotemporal cortex showed strong impairment in pattern recognition and identification of objects but behaved normally in spatial landmark tasks (Gross, 1973). The opposite was true for monkeys with posterior parietal lesions (Pohl, 1973; Milner et al., 1977; Ungerleider and Brody, 1977). Subsequently this notion of a ventral and a dorsal pathway got strong support by anatomical studies demonstrating that cells projecting to parietal areas and those projecting to temporal areas are remarkably segregated within pre- and extra-striate areas (Morel and Bullier, 1990; Baizer et al., 1991), thus confirming the existence of two separated streams. However, both streams also receive strong input from common regions in the superior temporal sulcus (Morel and Bullier, 1990), indicating that the separation is not an absolute one.

Studies of the behavioral deficits in patients with lesions in the parietal or temporal cortex also supported this hypothesis to some extent. Patients with visual agnosia have problems recognizing familiar objects or faces, while they can navigate through their environment without major problems (Farah, 1990). On the other hand,

people with lesions in the posterior parietal cortex often suffer from optic ataxia, a condition in which they have problems to accurately reach for objects in their surroundings (Balint, 1909; Perenin and Vighetto, 1988). Other symptoms, however, could not be easily explained by the dichotomy of object shape and spatial location as it had been proposed by Ungerleider and Mishkin. Patients with optic ataxia often not only have problems in precise reaching, but also fail to adjust the shape of their hand to the form, size or orientation of an object when trying to grasp it (Perenin and Vighetto, 1988; Jakobson et al., 1991), although these features had been attributed to the ventral stream. Similarly, patients with visual agnosia who failed to recognize the shape or size of an object when asked to describe it, perfectly pre-shaped their hand when grasping for it (Goodale et al., 1991). Such experiments revealed that the same attributes of an object sometimes could and sometimes could not be processed by the patients' brain, depending on the behavior that he or she had to perform. Evidence from a number of such psychophysical studies led Goodale and Milner to propose a reappraisal of the function of the two visual streams. They suggested 'to place less emphasis on input distinctions (e. g. object location versus object qualities) and to take more account of output requirements' (Goodale and Milner, 1992). Indeed, it is plausible that the inputs and processing required for skilled visuomotor behavior are quite different from those that underlie visual perception. Therefore, they proposed that the functional dichotomy that is supported by the two visual streams is rather one that deals with visual perception of objects on one hand (the 'what' pathway, ventral stream) and how to act on them on the other hand ('how' pathway, dorsal stream). Goodale and Milner made this proposal based mainly on psychophysical evidence, but it was in good agreement with electrophysiological findings that had been made previously in macaques. In 1990, Taira and colleagues had described neurons in the parietal cortex of monkeys that specifically deal with those characteristics of an object, that determine how the monkey has to shape its hand to grasp it (Taira et al., 1990). These neurons were insensitive to the location in space of the grasp target, therefore clearly favoring the notion of a 'how' pathway over the one of a 'where' pathway.

This general distinction of a ventral pathway for recognition and a dorsal one for action related visual processing is still the valid hypothesis today. In other words, visuo-motor transformation is seen as being predominantly in the domain of the dorsal pathway.

1.2.2 Posterior Parietal Cortex

As mentioned before, the dorsal visual stream links the occipital visual areas with the posterior parietal cortex (PPC). In humans, early evidence for an important role of the PPC in visuomotor transformations for arm and hand movements came from clinical observations. Patients with lesions of the parietal cortex display optic ataxia, a deficit in the coordination of hand and arm movements under visual guidance (Balint, 1909; Rondot et al., 1977; Jeannerod, 1988; Perenin and Vighetto, 1988). Very similar deficits occur in monkeys with lesions of the posterior parietal cortex (Faugier-Grimaud et al., 1978). In addition, early electrophysiological recordings in the parietal cortex of awake behaving monkeys demonstrated that many neurons in the PPC are related to goal directed, visually guided movements of arm and hand (Hyvarinen and Poranen, 1974; Mountcastle et al., 1975).

Various studies using anatomical and physiological techniques have, over time, led to increasingly more detailed mapping of the PPC. The following two sections will introduce some of these classifications.

1.2.2.1 Cytoarchitectonic classifications

The posterior parietal lobe consists of the inferior parietal lobule (IPL) below the intraparietal sulcus (IPS) and the superior parietal lobule (SPL) above the IPS. Early attempts to subdivide the parietal cortex into distinct regions have focused on cytoarchitectonic criteria. In Brodman's famous map of cytoarchitectonic regions in the cortex, the SPL corresponded to area 5, while the IPL was assigned to area 7 (Figure 1Brodmann, 1905). Vogt and Vogt subdivided both of these regions again into areas 5a and 5b in the SPL, and 7a and 7b in the IPL (Vogt and Vogt, 1919). Later studies used nomenclatures based on letters instead of numbers

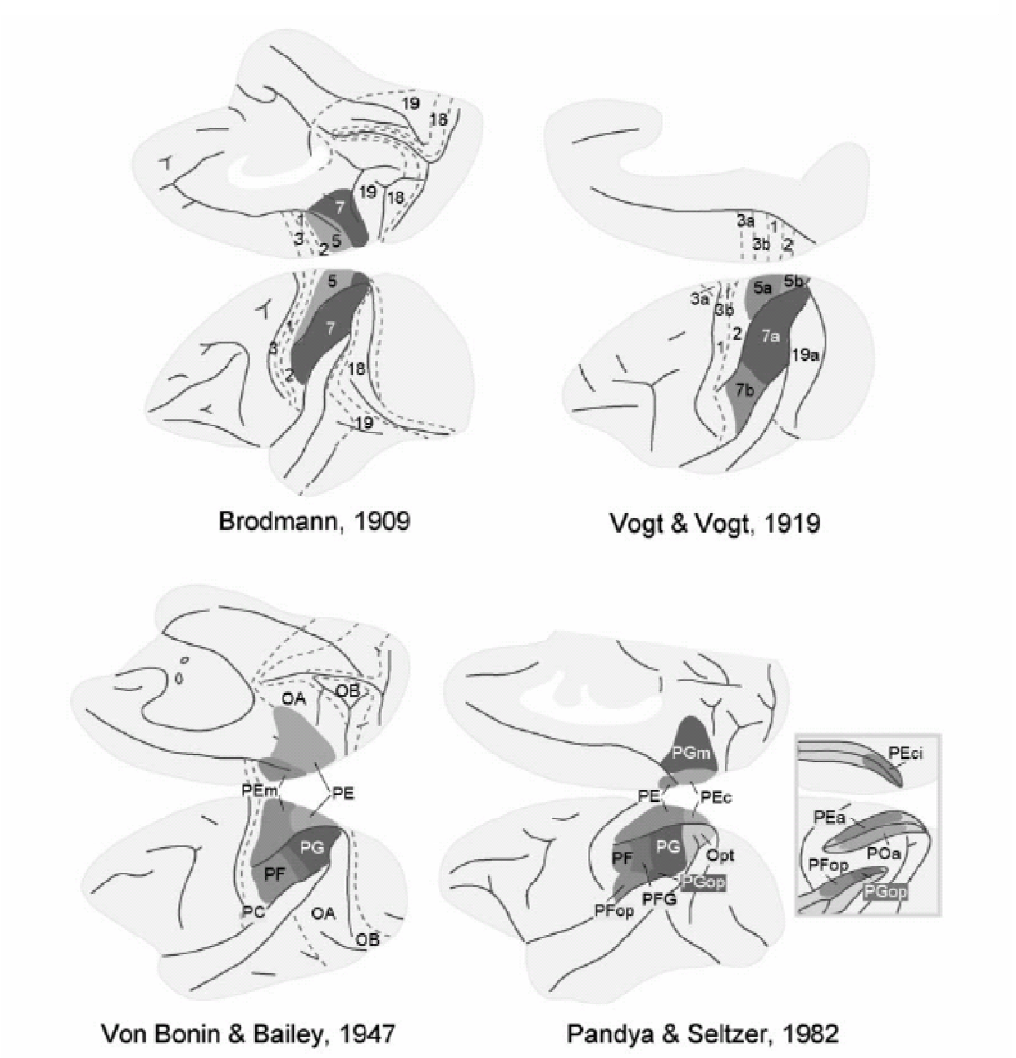

Figure 1-1: Parcellations of the monkey posterior parietal cortex based on cytoarchitectonics

Cercopithecus in Brodmann (1909) and Vogt and Vogt (1919); Macaca in Von Bonin and Bailey (1947) and Pandya and Seltzer (1982). Taken from (Cavada, 2001).

(Bonin and Bailey, 1947; Pandya and Seltzer, 1982). Pandya and Seltzers identified again more subdivisions in the IPL. Despite some similarities in the patterns of these classifications, there are also differences between all of these maps. This is certainly due to the fact that transitions and differences between areas are often subtle and it is hard to define objective and researcher independent criteria for

classifications based on cytoarchitecture alone. Despite this drawback, these nomenclatures are still regularly used, and therefore it is still important to know the names they use for the different areas.

1.2.2.2 Visually responsive areas in posterior parietal cortex

Cytoarchitectonic criteria are of course not the only criterion to define cortical areas and they do not help to assign a function to identified areas. In fact, the present classification of parietal areas is mostly based on the analysis of cortico-cortical connectivity on one hand, and on neurophysiological studies on the other hand. These methods have led to the identification of a number of visually responsive areas along the medial and lateral bank of the IPS (Figure 1-2, inset). Response properties of the neurons in these areas suggest that each of them is concerned with specific spatial analyses that are tailored for the composition of motor plans for different visuomotor behaviors (e.g. reaching, grasping, saccades).

In this chapter, I will very briefly describe the parietal areas with known visual responses. All of them are believed to play important roles in visuomotor behaviors. Area AIP, the parietal area responsible for hand movement planning, will be described in much more detail in Section 1.3, as it is the main topic of this thesis.

1.2.2.2.1 AIP

The anterior intraparietal area (AIP) lies in the rostralmost part of the lateral bank of the intraparietal sulcus (IPS). Neurons in AIP are active during hand grasping movements and show selectivity for particular grip types (Taira et al., 1990). Moreover, many of these neurons are also activated by the visual presentation of graspable objects, when the visual features of the object conform to the preferred grip type of the neuron (Sakata et al., 1995; Murata et al., 2000). AIP is therefore thought to extract and process visual features of objects that are relevant for the planning of a corresponding hand grasping movement.

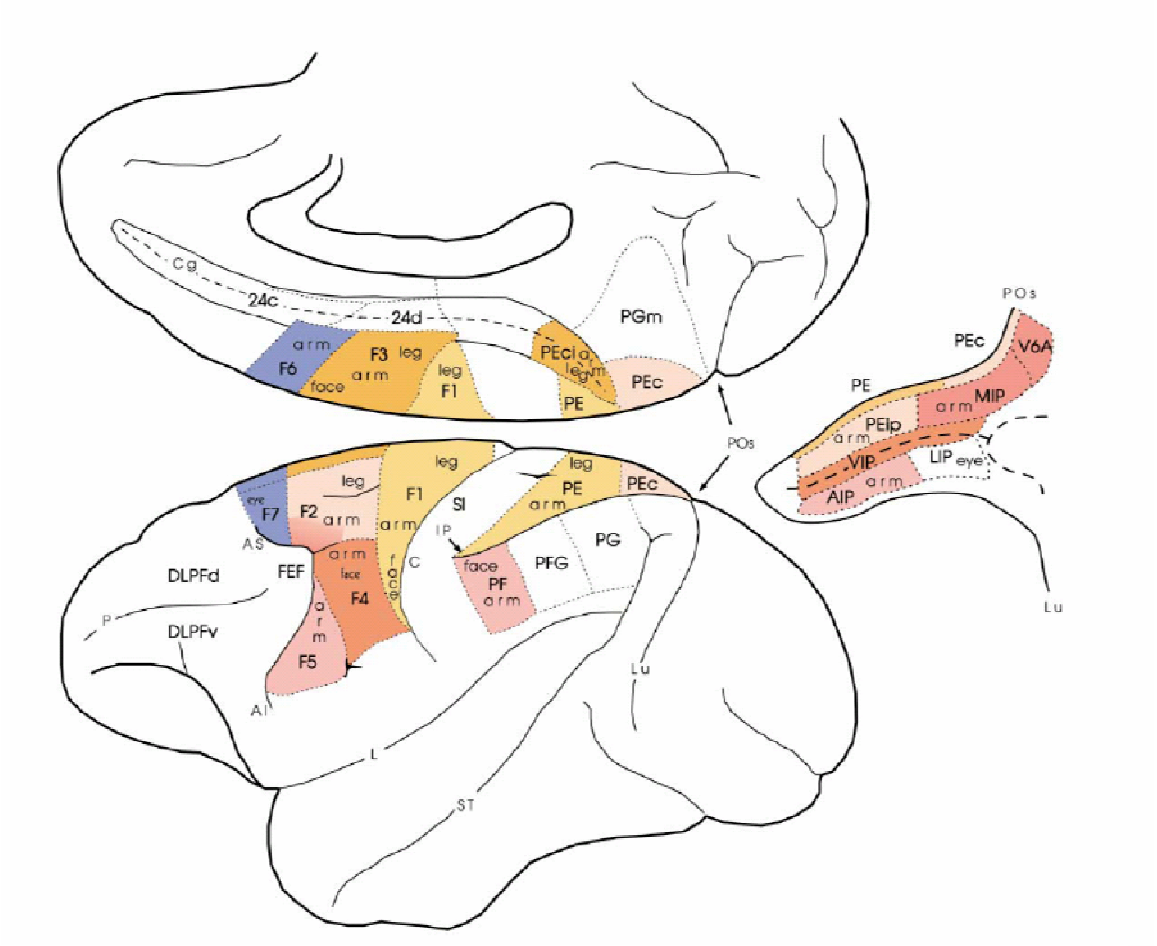

Figure 1-2: Parcellation of the Motor Cortex, Posterior Parietal, and Cingulate Cortices

All parietal areas except those buried within the intraparietal sulcus are defined according to Pandya and Seltzer (1982). The areas located within the intraparietal sulcus (IP) are defined according to physiological data (see text) and are shown in an unfolded view of the sulcus in the right part of the figure.

1.2.2.2.2 MIP

The medial intraparietal area (MIP) occupies the posterior part of the medial bank of the IPS. It is part of the so-called parietal reach region (PRR) which also includes area V6A in the anterior bank of the parieto-occipital sulcus. MIP gets visual input from area PO, with which it is anatomically connected (Colby et al., 1988). In

addition to firing in response to visual stimuli, many MIP neurons are also active during reaching movements (Colby and Duhamel, 1991). Reach related neurons are modulated by the direction of the movement. It has been shown, that this spatial tuning is not only due to the attention to a certain spatial location, but that it encodes specifically the intention or plan to reach to this location (Snyder et al., 1997). When eye movements to the same location are planned, these neurons remain silent. Visually perceived targets are encoded in an eye centered reference frame (Batista et al., 1999). More recently, it was described that PRR neurons also encode reach plans to auditory stimuli (Cohen and Andersen, 2000). Interestingly, a significant proportion of PRR neurons encodes movement goals still in eye-centered coordinates, even when the stimulus was an auditory one. It was therefore proposed that PRR is involved in coordinate transformations to represent movement plans in a common reference frame (Cohen and Andersen, 2000; Andersen and Buneo, 2002). Furthermore, it was demonstrated that PRR neurons are modulated by higher level cognitive signals like motivation (Musallam et al., 2004) and that it is implicated in the autonomous selection of reach plans in the absence of definitive motor instructions (Cui and Andersen, 2007; Scherberger and Andersen, 2007). In summary, while AIP is concerned with hand movements, MIP seems to be important for the planning and controlling of the reach components of upper limb movements.

1.2.2.2.3 LIP

The lateral intraparietal area (LIP) lies on the lateral bank of the intraparietal sulcus, caudal to AIP. LIP gets extensive input from several extrastriate visual areas, including V2, V3, V4, MT, and PO and sends output to saccade related areas like the frontal eye field (FEF), and the superior colliculus (Blatt et al., 1990). Microstimulations with low currents in LIP lead to saccadic eye movements without triggering other body movements (Thier and Andersen, 1996, 1998). Furthermore, injection of the GABA agonist muscimal into LIP lead to deficits in eye movements that are related to high level processing, such as an inability to perform memory saccades or to decide between two saccade targets, while the execution of saccades remains possible (Li et al., 1999).Taken together, this evidence suggests that LIP is

implicated in saccade planning and execution. Recordings in behaving monkeys demonstrated that many LIP neurons burst before saccades (Barash et al., 1991). Some researchers argued that this activity could be explained by modulation of spatial attention alone, without assuming that LIP is implicated in saccade planning (Colby and Goldberg, 1999). However, later experiments dismissed this hypothesis and showed, that LIP indeed codes for eye movement intentions and not only a general spatial attention (Snyder et al., 1997, 1998), although an additional attentional modulation of LIP activity is certainly possible.

In the context of the present thesis it is important to note that LIP sends extensive connections also to AIP. The role of this input to AIP is unclear. One possibility is that these connections are necessary to maintain a spatially accurate representation of the visual field despite eye movements. It is also possible that LIP is implicated in other forms of visual processing, apart from its role for eye movements. In a caudal and ventral sector of LIP, neurons were found that respond to three dimensional visual stimuli (Shikata et al., 1996; Taira et al., 2000; Tsutsui et al., 2001; Tsutsui et al., 2003). This region was then termed CIP, the caudal intraparietal area, but it is possible, that neurons with these properties extend over a wider area of LIP (Nakamura et al., 2001). LIP might therefore also be a source of such 3D information to AIP, but clearly, more research is needed on that subject.

1.2.2.2.4 VIP

The ventral intraparietal area (VIP) occupies the fundus of the IPS, ventral to AIP. It receives strong input of visual areas, particular MT and MST, and from several other sensory areas, including somatosensory, auditory and vestibular cortices (Maunsell and van Essen, 1983; Lewis and Van Essen, 2000). In accordance with these polysensory input connections, electrophysiological recordings in VIP demonstrated responses to visual, tactile, auditory and vestibular stimulation, with individual cells frequently showing bimodal responses (Colby et al., 1993b; Bremmer et al., 1997; Duhamel et al., 1998; Bremmer et al., 2002b; Klam and Graf, 2003). Many of the visually responsive neurons represent stimuli in head-centered

coordinates (Duhamel et al., 1997). Moving stimuli were particularly effective in triggering neural responses (Colby et al., 1993a). Somatosensory receptive fields in VIP are mostly restricted to the face and the head (Duhamel et al., 1998). Neurons with bimodal responses usually combine visual sensitivity with either one of the other modalities. When this second modality is somatosensory, there is usually strong congruence between the tactile and the visual receptive field (Duhamel et al., 1998). For example, a neuron that responds to touch on the right forehead would typically have a visual response field in the upper right quadrant of the visual field. A similar congruence can be seen for neurons that combine visual and vestibular information: such bimodal neurons generally prefer visual motion patterns that simulate head movements corresponding to the vestibular stimulation that drives the same neuron (Bremmer et al., 2002b). Given these functional properties of VIP neurons, it has been suggested that VIP is implicated in the processing of self movements and object movements in near peri-personal space(Bremmer et al., 2002a). While there are so far no reports about VIP responses during active movements, it is interesting to note that electrical stimulation of VIP neurons could evoke avoidance behavior like closing of the eyes or contracting of facial muscles (Cooke et al., 2003). Therefore, VIP might be involved also in defensive behaviors triggered by threatening stimuli in the near extra-personal space.

1.2.3 Parieto-frontal loops

Anatomical studies revealed that different parietal areas show very distinct patterns of connectivity with premotor areas in the frontal lobe. One study, in which neural tracers were injected in parietal and premotor cortex, compared the connections of AIP and VIP with premotor areas (Luppino et al., 1999). It was found that AIP shows strong and specific reciprocal connections with area F5 in the ventral premotor cortex. VIP on the other hand shows selective and also reciprocal connections with area F4. It was therefore concluded that these areas form two segregated parieto-frontal loops. Other studies demonstrated the existence of a similar loop between the parietal area MIP and the dorsal premotor area F2 (Johnson

et al., 1996; Tanne-Gariepy et al., 2002). Other loops have been identified. They are not confined to the visually responsive areas in the parietal sulcus, but also link areas on the convexities of the posterior parietal cortex, where somatosensory responses predominate, with premotor areas. Interestingly, electrophysiological findings of the premotor areas had shown that neurons there show similar characteristics as those in their respective counterparts in the parietal lobe (for a review, see Rizzolatti et al., 1998). There is therefore a multiplicity of largely segregated parietofrontal circuits, linking areas displaying similar functional properties. It is thought that the functional correlate of this anatomical arrangement is that each of these parietofrontal loops is dedicated to a specific aspect of sensorimotor transformation. The parietal areas receive specific sensory information that they transform into information appropriate for the planning of an action. This information is sent to the premotor areas, which might then choose an appropriate motor program.

1.3 Hand movement related areas

In the last section, we have seen the general organization of the visuomotor system and the important role of the dorsal visual stream and the parieto-frontal networks. In the current section we are going to review the literature on some of the parietal and frontal areas that are particularly important for the visuomotor transformation and execution of hand movements in non-human primates. In the parietal cortex this is the anterior intraparietal area (AIP) and in the frontal lobe the areas F5 and the primary motor cortex.

1.3.1 AIP

1.3.1.1 Electrophysiology

Neurons in the inferior parietal lobule that are involved in goal directed, visually guided arm and hand movements were first described by Mountcastle and his colleagues (Mountcastle et al., 1975). They described two broad classes of neurons: 'arm projection' and 'hand manipulation' neurons. More recently, neurons that are related to hand movements were found to be concentrated in the rostral part of the lateral bank of the intra-parietal sulcus (Taira et al., 1990), an area that was later named the anterior intraparietal area (AIP, Gallese et al., 1994). Taira and colleagues trained monkeys to grasp four different objects, each of which required the use of a different configuration of the hand. Most of the task related neurons they found were selectively active for the grasping of one or two of these objects. They were not influenced by the position of the object in space, indicating that their activity was specifically related to the hand, not the arm movement. These grasp related neurons were subdivided into three cell classes, according to their activation during grasping in the light and in the dark: "motor dominant" cells showed no significant difference between the two conditions, "visuomotor cells" showed stronger activation in the light and "visual-dominant" neurons were only active when grasping in the light (Figure 1-3). Visually responsive neurons were further

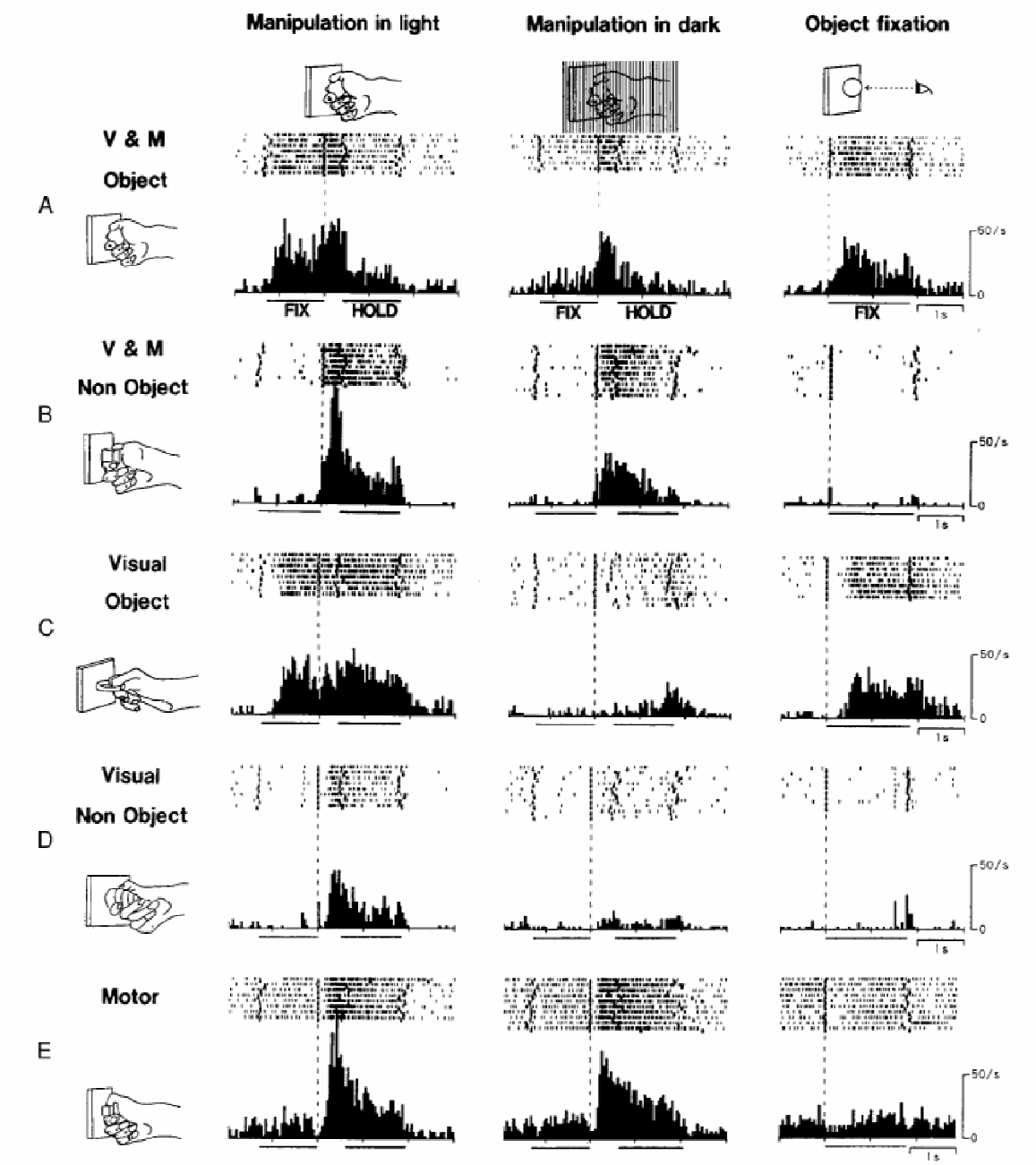

Figure 1-3: Classification of AIP cells according to Sakata

Five types of hand manipulation related neurons under three task conditions. A: Example of object-type visual-motor neuron, B: nonobject-type visual-motor neuron, C: object-type visual dominant cell, D: nonobject-type visual dominant cell, E: motor dominant cell. The lines below the histograms show the mean duration of the fixation period (FIX) and the holding period (HOLD). Between the two, the reach-to-grasp movement is executed. Modified from (Murata et al., 2000)

investigated in subsequent studies of the same group. If they were activated during mere fixation of the graspable object, they were called “object type”, otherwise non-object type” (Sakata et al., 1995). Object type cells were found to represent aspects of the 3D shape ob the graspable objects and some were also selective for the size and/or the orientation (Murata et al., 2000). Furthermore, many of these object type cells preferred the same object during object fixation and during grasp execution. Motor-dominant cells, on the other hand, were found to be more related to the shape of the hand during grasping. Finally, AIP neurons were found to show sustained activity in a delayed grasping task, suggesting that they play a role in the visual memory of 3-dimensional object features (Murata and Kitahara, 1996). Altogether, these electrophysiological findings suggest that AIP neurons play an important role in matching the pattern of the hand movement to visuo-spatial characteristics of the object to be grasped.

1.3.1.2 Inactivation study

The functional relevance of AIP during visually guided hand movements was tested by inactivating it in monkeys (Gallese et al., 1994). Microinjections of muscimol, a GABA agonist, allow a very localized and reversible inactivation. This led to a severe disruption of the pattern of finger movements during the period of preshaping, without error of arm reaching. This incongruous preshaping either led to error trials or to an awkward grasping that was achieved only after several correction movements. These corrections were made under tactile control, after the hand had contacted the object, suggesting that the deficit was restricted to visuomotor control, leaving tactile feedback intact.

This experiment demonstrated the important role that AIP plays in linking the cortical visual system with the premotor and eventually the motor system.

1.3.1.3 Anatomical Connectivity

The electrophysiological results of AIP are in good agreement with the known anatomical connections of this area. First of all, AIP receives visual input via several

higher order visual areas in the parietal cortex, in particular areas LIP, V6A and CIP (Nakamura et al., 2001; Borra et al., 2008; Gamberini et al., 2009). These areas are part of the dorsal visual stream. CIP and V6A represent information on the shape and orientation of visually perceived objects (Sakata et al., 1997; Sakata et al., 1999; Tsutsui et al., 2001; Galletti et al., 2003; Fattori et al., 2009), while LIP might provide AIP with information about impending eye movement (Blatt et al., 1990). However, visual input to AIP is not confined to the dorsal stream. AIP is also connected with ventral visual stream areas in the temporal cortex (areas TEO, TEa, TEp, Borra et al., 2008). These connections might inform AIP about parameters of familiar and identified objects. In this context it is interesting to note that there have been reports about patients with a deficit in hand pre-shaping due to lesions in the parietal cortex that performed much better when they had to grasp known 'meaningful' objects (e.g. pencil) than objects with arbitrary shape and size (Jeannerod et al., 1994).

Furthermore, AIP gets input from other parietal areas, which are not implicated in visual processing. Areas PF, PFG and PG on the convexity of the inferior parietal lobule, as well as the secondary somatosensory area SII in the parietal operculum are connected with AIP (Borra et al., 2008). The IPL convexity areas all receive considerable input from somatosensory areas (Pandya and Seltzer, 1982; Rozzi et al., 2006). These AIP inputs might be surprising, considering that only few neurons in AIP were found to respond to tactile and proprioceptive input (Taira et al., 1990). However, the extent to which AIP neurons are modulated by somatosensory feedback certainly remains to be investigated in future research.

In the frontal lobe, AIP is strongly and reciprocally connected with area F5 (Luppino et al., 1999; Tanne-Gariepy et al., 2002; Borra et al., 2008), an area which exhibits similar activity related to hand movements (Rizzolatti et al., 1988; Murata et al., 1997; Raos et al., 2006; Stark et al., 2007) and is considered to be part of the cortical output structures for controlling the hand due to its projections to primary motor cortex and the spinal cord (Rizzolatti et al., 1988; Luppino et al., 1999; Lemon, 2008).

Finally, AIP is directly connected with the prefrontal cortex (areas 12 and 46, Borra et al., 2008), areas which are believed to be involved in higher order cognitive processing like working memory, rule learning or the representation of abstract concepts (Wilson et al., 1993; White and Wise, 1999; Wallis et al., 2001).

Altogether, these anatomical connections locate AIP right at the interface between sensory, motor and cognitive areas related to hand movement control.

1.3.2 Frontal area F5

As noted before, area AIP displays strong and specific reciprocal connections with a pre-motor region in the posterior bank of the inferior part of the arcuate sulcus (Luppino et al., 1999).

Early electrophysiological recordings in this region had revealed that single units of this pre-motor area are active during and before movements of the distal forelimb (Godschalk et al., 1981; Kurata and Tanji, 1986). These results, combined with anatomical findings that this cortical region receives input from parietal and striate cortex (Pandya and Kuypers, 1969; Pandya and Vignolo, 1971) and projects in turn to the hand and finger region of the primary motor cortex (Pandya and Kuypers, 1969; Muakkassa and Strick, 1979), led to the idea that the post-arcuate cortex of the monkey's frontal lobe might be involved in visuomotor processing. According to Brodman's classification, this region is part of area 6 (Brodmann, 1905). However, a newer classification, using cytoarchitectural and histochemical criteria showed that area 6 can be further subdivided into several distinct areas (Figure 1Matelli et al., 1985). The posterior bank of the arcuate sulcus together with the adjacent cortex on the convexity was termed area F5. In a seminal paper, Rizzolatti and colleagues reported in 1988 that neurons in F5 showed activity that was not specific to movements of individual joints of fingers but to more complete motor acts like 'grasping', 'holding' or 'bringing to the mouth' (Rizzolatti et al., 1988). The most frequent cells were the grasping neurons. While some of these neurons were active for any kind of grasping, even independent of the effector (left hand, right hand or mouth), many others were selectively tuned for a particular grip type, like precision

grip, side grip or power grip. In addition, about half of the grasping related neurons could be activated by the visual presentation of graspable objects. The authors therefore proposed that F5 contains a 'motor vocabulary' where goal directed movements of the distal forelimb are represented. Such an arrangement would drastically reduce the degrees of freedom necessary to code for the various hand shapes. The observed visual activity could then be a sign that this vocabulary can be addressed via visual input derived from the graspable objects. Successive experiments have tested this hypothesis more formally. F5 neurons were recorded while monkeys grasped repetitively one of six different objects either in the light or in the dark. In addition, neuronal activity was recorded during mere fixation of these objects (Murata et al., 1997; Raos et al., 2006). The results showed that activity in F5 is very similar for objects with different geometric shapes when they are grasped with the same grip type, suggesting that the activity of F5 neurons is mainly determined by the type of grip that the animals use and not by the object shape itself, a finding which is consistent with the 'motor vocabulary' hypothesis. Moreover, neurons that were activated also during object fixation in the absence of grasping, showed a strict congruence between the object that elicited the highest activity during grasping and during mere fixation.

In order to test the functional relevance of F5 for visuomotor transformation, Fogassi and coworkers performed a reversible inactivation of F5 by injecting small doses of the gaba agonist muscimol into the area (Fogassi et al., 2001). After inactivation, monkeys displayed pronounced deficits regarding the visuomotor component of the grasp: the usual pre-shaping of the hand during the reaching phase was markedly impaired and kinematic differences that were usually observed between the grasping of small or large objects, disappeared. The general ability to move the hand was, however, spared and monkeys usually succeeded to grasp the object after a series of corrections made with tactile feedback, once the hand had reached the object. Therefore the authors concluded that F5 lesions impaired specifically the visuomotor component of grasping movements. Overall, these symptoms after inactivation were remarkably similar to those after inactivation of

AIP. This is consistent with the notion that AIP and F5 together form a parieto-frontal circuit for sensorimotor transformations specific for hand grasping.

What we will look at in the next section is, how the signals from F5 are relayed to the motoneurons in the cervical spinal cord. F5 does, by itself, send direct projections to the spinal cord. However, in the macaque the contribution of F5 to the cortico-spinal tract is rather weak and, perhaps more importantly, only few of these projections are sent to the cervical enlargement, where the motoneurons controlling the hand muscles are located, but instead they terminate in the upper cervical segments (He et al., 1993). It is therefore likely that the signals of F5 reach the spinal cord via the primary motor cortex.

1.3.3 Primary Motor Cortex

F5 sends strong projections to M1, the primary motor cortex (Muakkassa and Strick, 1979; Matelli et al., 1986). In fact, the connections from F5 constitute the strongest input to the hand and finger area of M1 (Dum and Strick, 2005). M1 is in turn the main source of cortico-spinal projections to the cervical enlargement. More specifically, in a recent experiment in which rabies virus was injected into hand muscles in order to retrogradely and transneurally label cells, it could be shown that hand muscle related cortico-motoneuronal (CM) cells, i.e. cortical projection neurons that make direct contact with motoneurons, are almost entirely restricted to M1 (Rathelot and Strick, 2006). This is important because comparative studies suggested that a high level of manual dexterity depends on the presence of a well developed CM system: CM projections are absent in cats, hardly present in squirrel monkeys with a low level of manual dexterity and more developed in macaques, great apes and humans (Nakajima et al., 2000).

Single unit recordings in M1 revealed that neurons in this area represent many features regarding the dynamics and kinematics of hand movements (Smith et al., 1975; Georgopoulos et al., 1982; Evarts et al., 1983; Porter and Lemon, 1993).

Some recent experiments directly compared the activity of M1 and F5 neurons. These studies reported that while the majority of F5 neurons show ‘extrinsic’ tuning

properties, coding for the goal of an action, often quite independently of the actual muscle movements to achieve this goal, many M1 neurons show tuning that is much more closely bound to the muscle activity (Kakei et al., 2001; Umilta et al., 2008). Furthermore, simultaneous recordings in F5 and M1 revealed that only F5 neurons where tuned for specific grasps well before the movement start. M1 neurons on the other hand lacked this early pre-movement specificity but where strongly involved during the movement execution, often with activity limited precisely to one phase of the grasping movement (Umilta et al., 2007). Last but not least, it could be shown that electrical stimulation in F5 can reliably facilitate the EMG response of intrinsic hand muscles to stimulations in M1 (Cerri et al., 2003).

In summary, these results propose that motor goals or plans that are established in F5 are transformed in M1 into the more segmented and coordinated neural commands necessary for motor execution and are sent to the motoneurons of hand muscles mainly via descending connections originating in M1.

1.4 Goals of the present thesis

To perform grasping movements, the hand is shaped according to the form of the target object. To achieve such a behavior, a visuo-motor transformation has to be preformed, as was described extensively in this chapter. However, it is obvious that most objects can be grasped in several different ways and often, the precise way we grasp an object depends on the final goal of the action, which in turn depends on the action context. The anterior intraparietal cortex (AIP) was shown to be strongly involved in matching the hand configuration to the shape of the object to be grasped, but it is unknown, if it also encodes context specific information for hand grasping. It is possible that AIP 'only' represents all relevant visual object features and that later processing stages like pre-motor cortex then select the ones relevant for the intended manipulation. Alternatively, the representation in AIP might already be tailored to the specific intended manipulation.

In our experiments, monkeys grasped one object with two different grip types, while an LED represented the 'context' information that instructed the animal, which grip type to apply. This way the hand shape was dissociated from the object shape (which was always the same). This allowed us to distinguish between the two above-mentioned hypotheses. These results are described in Chapter 3.

The orientation of an object is one of the features that are certainly relevant to determine, how an object is best grasped. In this respect, one would expect the orientation to be processed in AIP. In terms of the reach to grasp movement, however, the orientation is mainly influencing the wrist orientation and therefore, rather the reach component of the action; and this reach component was reported to be irrelevant for neural response in AIP (Taira et al., 1990). There are only rather anecdotal reports of orientation specific cells in AIP (Taira et al., 1990) and no systematic study on that issue has been performed. In our experiment, the object was systematically presented in one of five different orientations. We can therefore study the orientation selectivity of AIP neurons. These results are also presented in Chapter 3.

Previous electro-physiological studies in AIP used different tasks to compare visuo-motor, motor and visual response: grasping in the light, grasping in the dark and pure fixation. While objects were presented in random order for fixation and grasping in the light, grasping in the dark had to be performed in blocks, with the monkey knowing the object beforehand. Such a design contains several problems, like potentially different attention, motivation or difficulty of the task. In our experiments we used a delayed grasping task, which separated in time the visual object presentation and the movement phase within the same trial. This allowed us to classify neurons according to the temporal appearance of their response and observe the development of the response of these different classes over time, in the course of a trial. These results are also presented in Chapter 3.

The local field potential has previously been reported to encode spatial movement parameters. Several studies of the LFP in parietal areas have been performed using reaching tasks or eye movement tasks (Pesaran et al., 2002; Scherberger et al., 2003a; Asher et al., 2007). The LFP of area AIP has, however, received almost no attention. We recorded LFP together with spiking data and asked, if the local field potential is modulated by the delayed grasping task. Furthermore, we investigated, if the LFP and the neural spiking in AIP show any significant relation. These results are presented in Chapter 4.

2 General Methods

2.1 Experimental setup

Two female rhesus monkeys (*Macaca mulatta*) participated in this study (animals L and J). Procedures and animal care were in accordance with the regulations set by the Veterinary Office of the Canton of Zurich and the Guidelines for the care and use of mammals in neuroscience and behavioral research (National Research Council, 2003).

Animals were habituated to comfortably sit upright in individually adjustable primate chairs with the head post rigidly fixed to the chair. A grasp target was located at a distance of about 30 cm in front of the animal at the level of their chest. The target consisted of a handle that could be grasped with two different grip types, either with a precision grip with index and thumb in opposition or a whole-hand power grip (Figure 2-1A). To detect the contact of the animal's thumb and index finger during precision grips, two touch sensors were placed in small recessions. Their locations were well visible. Power grips were sensed by a light barrier. The handle was rotatable and 5 different handle orientations were tested in this experiment (upright and tilted 25 or 50 deg to the left or right). To illuminate the handle in the dark, two dedicated spotlights were positioned to the left and right of the handle (outside of the animal's reach). A halfway mirror was placed horizontally between the monkey's eye and the grasp target, such that the LED light stimuli used for eye fixation and task instructions (see below) were projected on the center of the handle. The mirror also ensured that the grasp target was only visible when illuminated by the spotlights. Two capacitive touch sensors (model EC3016NPAPL, Carlo Gavazzi, Italy) were fixed to the chair in front of the animal's hips to monitor the hand resting position for both hands. An optical eye tracking system (model AA-ETL-200; ISCAN Inc, Burlington, MA, USA**)** was used to monitor the animal's eye

position. The animal's behavior and all stimulus presentations were controlled in LabView Realtime (National Instruments, Austin, TX, USA) with a time resolution of 1 ms using custom-written software. Finally, an infrared camera was used to monitor the monkeys' behavior continuously throughout the entire experiment.

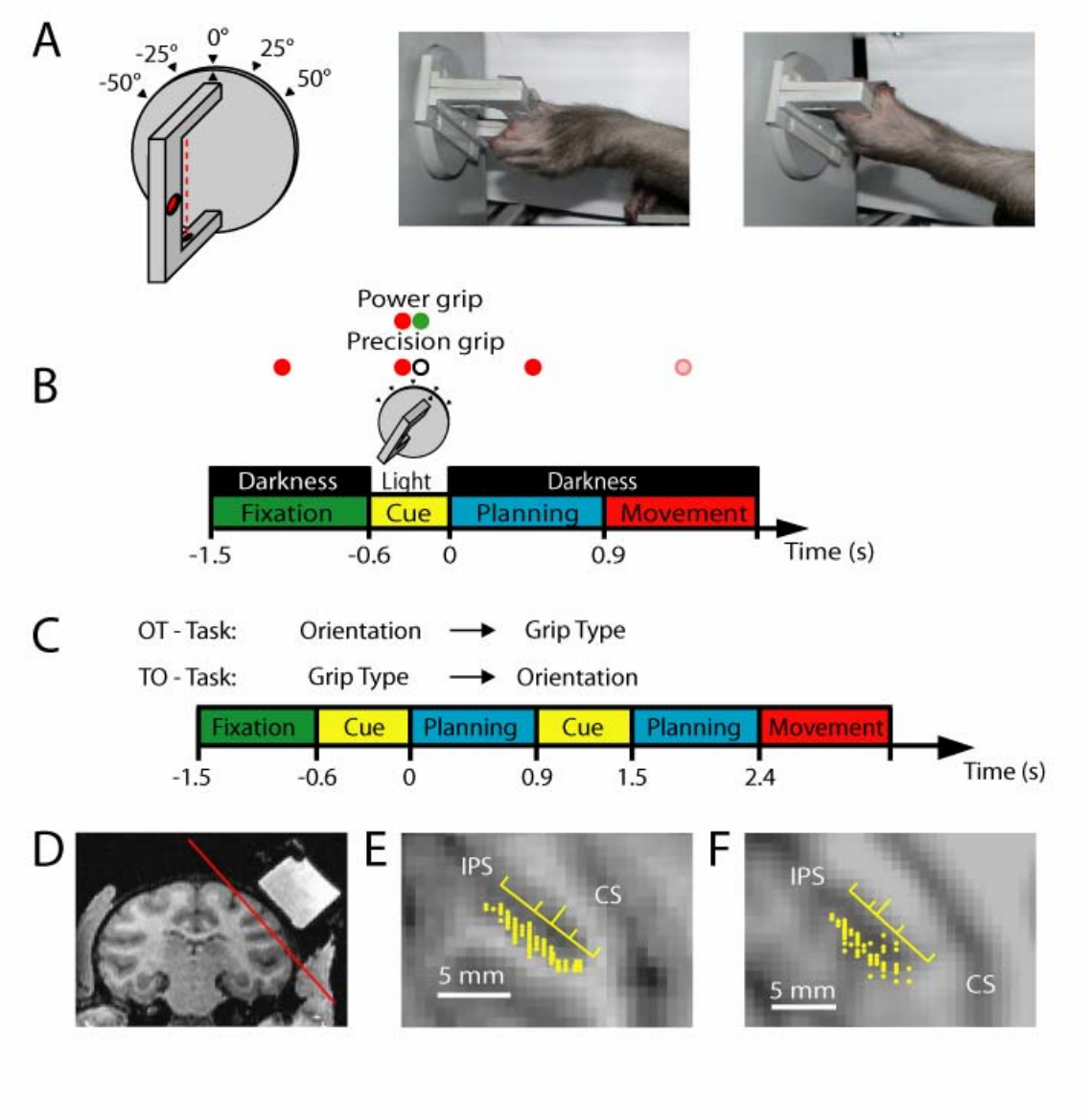

Figure 2-1: Task paradigm and recording penetrations

A: Sketch of the handle (left) and photographs of a monkey performing a precision grip (middle) and a power grip (right). In the drawing, the red dotted line indicates a light barrier for detecting power grips, and the red oval indicates a touch sensor in a groove for sensing precision grips (a second sensor is located on the opposite side of the handle). The handle was presented in 5 different orientations. **B:** Delayed grasping task. Trials were divided into four epochs: fixation, cue, planning and

movement. Monkeys initiated trials by placing both hands on rest sensors and fixating a red LED in the dark. After a variable delay (fixation, 700-1100 ms), the handle was illuminated for 600 ms (cue), revealing its orientation. At the same time, a second colored LED ('context cue') was illuminated, which instructed the animal about the required grip type (power or precision). After a variable delay (planning, 700-1100 ms), the dimming of the fixation light served as the go signal to initiate movement execution. All trial conditions were randomly interleaved. **C:** Cue separation task. Modified task from B, with the cues for grip type and orientation presented consecutively and with each cue followed by a separate planning period. In one version of this task (OT-task), the orientation information preceded the grip type information, while in the other version the cue sequence was reversed (TO-task). **D:** Coronal MRI section (monkey J) with the recording chamber on the right hemisphere filled with contrast medium. The red line indicates the position of the oblique section in E. **E-F:** Maps of recording electrode penetrations (yellow dots) in monkeys J and L, respectively. The yellow ruler indicates the median (long tick mark) and quartiles of the recording distribution along the intra-parietal sulcus (IPS). CS: central sulcus.

2.2 Tasks

Monkeys were trained to perform a *delayed grasping task*, in which they were required to grasp a single object (handle) in one of five possible orientations with either a power grip or a precision grip. This led to a combination of ten task conditions that were presented randomly interleaved. While the orientation of the handle became immediately apparent after illumination, the grip type was instructed to the animal by the color of an additional LED next to the fixation light that was green for a power grip and white for a precision grip.

Monkeys initialized each trial by fixating a red LED and placing both hands on the hand rest sensors while otherwise sitting in the dark (Figure 2-1B). The trial started with a baseline epoch (fixation) of variable length (700–1100 ms, mean: 900 ms), during which the animal had to maintain its resting position in the dark. The following cue epoch (length 600 ms) was dominated by visual input: the grasp target was illuminated, hence revealing the handle orientation, and the additional LED was shown, which informed the animal about the required grasp type (power grip or precision grip). Then, during the planning epoch of variable length (700–1100 ms, mean: 900 ms), the animal could plan, but was not allowed to execute the movement,

until the dimming of the fixation light gave the go-signal to reach and grasp (movement epoch). Planning and movement epochs were again in complete darkness except for the red LED light that the animal had to keep fixating. Only left-hand movements (contra-lateral to the right recording chamber) were allowed. All correctly executed trials were rewarded with a fixed amount of juice, and the animal could initiate the next trial after a short inter-trial interval (1500 ms). Error trials were immediately aborted without giving a reward. To maintain a high motivation for reward, animals were restricted from access to water up to 24 hours prior to the training and recording sessions.

Animals were also trained in a modified version of this task, in which the instructions regarding the grip type (colored LED) and the handle orientation (spotlight) were presented sequentially in two distinct cue periods (Figure 2-1C). In this *cue separation task*, each cue epoch (duration 600 ms) was followed by its own planning period (length 600–1000 ms, mean: 800 ms) before the movement was executed. Animals were trained to perform this cue separation task in two variations: either with the object orientation shown in the first cue epoch and the grip type instruction in the second (OT-task), or with the grip type instruction presented first and the object orientation in the second cue epoch (TO task). When testing neurons in this cue separation task, trials of both versions (OT- and TO-task) were always run randomly interleaved with each other and with trials of the (standard) delayed grasping task.

2.3 Surgical procedures

To prepare for the recording experiments, a titanium head post was secured in a dental acrylic head cap, and a custom made oval-shaped recording chamber (material PEEK; outer dimensions: 40 x 25 mm) was implanted over the right hemisphere on top of AIP with the skull bone removed underneath the chamber. This allowed the insertion of recording microelectrodes through the dura in subsequent recording sessions without discomfort to the animal. The recording chamber and head post were fixed on the skull with bone cement (Refobacin Plus, Biomet Orthopaedics,

Switzerland) and reinforced with titanium (Synthes, Switzerland) and ceramic bone screws (Thomas Recording, Germany).

All surgical procedures were performed under sterile conditions and general anesthesia (induction with ketamine 10 mg/kg, i. m., atropine 0.05 mg/kg, s.c., followed by intubation, isofluorane 1–2%, and analgesia with 0.01 mg/kg buprenorphene, s. c.). Heart and respiration rate, electrocardiogram, O_2 saturation, and body temperature were continuously monitored, and systemic antibiotics and analgesics were administered for several days after each surgery. Animals were allowed to recover for at least one week before behavioral training or recording experiments recommenced.

2.4 MRI scans

Prior to surgical procedures, a structural magnetic resonance image (MRI) of the brain and skull was obtained from each animal to help guide the chamber placement. For this, animals were sedated (ketamine 10 mg/kg, i. m., atropine 0.05 mg/kg, s.c., and xylazine 0.5 mg/kg, i. m.), supplemented with O2 (1 l/min), and their heart rate, O2-saturation, and end-tidal CO2-level continuously monitored. After placing in the scanner (GE Healthcare 1.5T) in a prone position, T1-weighted volumetric images of the brain and skull were obtained (3D IR-SPGR sequence, acquired voxel size 0.7 mm isometric, TR 7.6 ms, TE 3.16 ms, flip angle 12 deg, 400 ms inversion time) and re-aligned offline in stereotaxic coordinates using AFNI 3.0 (for details see: Scherberger et al., 2003b). The stereotaxic location of the tip of the right intraparietal sulcus was then obtained (approximate location: 8 mm anterior, 22 mm lateral) to guide the placement of the recording chamber over AIP.

Weeks after chamber implantation, a second MRI scan was obtained with the recording chamber filled with an MRI sensitive contrast medium (Gadolinium solution diluted in saline 1:2000). This allowed the mapping of cortical structures in the coordinates of the chamber, which greatly facilitated to target AIP with subsequent electrode penetrations (Figure 2-1D-F).

3 Context specific grasp movement representation in the macaque anterior intraparietal area

The content of this chapter has been published in Journal of Neuroscience:
Baumann MA[1], Fluet MC[1], Scherberger H[1,2] (2009) Context-specific grasp movement representation in the macaque anterior intraparietal area. J Neurosci 29:6436-6448.

(1) Institute of Neuroinformatics, University of Zürich and ETH Zürich, Zürich, Switzerland

(2) Deutsches Primatenzentrum GmbH, Göttingen, Germany

3.1 Abstract

To perform grasping movements, the hand is shaped according to the form of the target object and the intended manipulation, which in turn depends on the context of the action. The anterior intraparietal cortex (AIP) is strongly involved in the sensorimotor transformation of grasping movements, but the extent to which it encodes context-specific information for hand grasping is unclear. To explore this issue, we recorded 571 single-units in AIP of two macaques during a delayed grasping task, in which animals were instructed by an external context cue (LED) to perform power or precision grips on a handle that was presented in various orientations. While 55% of the recorded neurons encoded the object orientation from the cue epoch on, the number of cells encoding the grip type increased from 25% during the cue epoch to 58% during movement execution. Furthermore, a classification of cells according to the time of their tuning onset revealed differences in the function and anatomical location of early- versus late-tuned cells. In a cue separation task, when the object was presented first, neurons representing power or precision grips were activated simultaneously until the actual grip type was

instructed. In contrast, when the grasp type instruction was presented before the object, type information was only weakly represented in AIP, but was strongly encoded after the grasp target was revealed. We conclude that AIP encodes context specific hand grasping movements to perceived objects, but in the absence of a grasp target, the encoding of context information is weak.

3.2 Introduction

Humans and other primates are able to perform a wide range of complex hand movements and shape their hands both according to the target object, as well as depending on the intended manipulation. Since grasping movements are typically made to visually perceived targets, their neural control can perhaps be most easily understood in the framework of visuo-motor transformations. However, such a framework needs to incorporate the fact that the same object, depending on internal goals or external context cues, can lead to different types of actions.

It has long been known that the parietal lobe plays an important role for the generation of hand grasping movements. Lesions in human parietal cortex lead to optic ataxia, a deficit in hand movement coordination (Balint, 1909; Jeannerod et al., 1984), while in the monkey, single-unit activity in the parietal lobe has been associated with the generation of hand movements (Hyvarinen and Poranen, 1974; Mountcastle et al., 1975). More recently, the group of Sakata described a region of the macaque parietal lobe, the anterior intraparietal area (AIP), which contains neurons that specifically encode the shape of the hand during grasping (Taira et al., 1990; Sakata et al., 1995; Sakata et al., 1997; Murata et al., 2000). Moreover, the functional relevance of AIP for hand grasping was shown by inactivation (Gallese et al., 1994) and strong direct and reciprocal connections have been demonstrated between AIP and the ventral premotor area F5 (Luppino et al., 1999; Borra et al., 2008), an area that is also involved in hand movement control (Rizzolatti et al., 1988; Murata et al., 1997; Raos et al., 2006; Stark et al., 2007). Finally, there is evidence

for a human homologue of AIP (Binkofski et al., 1998; Culham et al., 2003; Shikata et al., 2008).

In all these electrophysiological studies of AIP, a particular object was always grasped with the same grip. However, in everyday situations, several grip types are often possible for the same object, and we select an appropriate grip according to the intended goal of the manipulation. Such a goal-dependent grip selection can be regarded as a rule-based sensorimotor transformation, which has been attributed to the frontal cortex (White and Wise, 1999; Hoshi et al., 2000; Wallis et al., 2001; Amemori and Sawaguchi, 2006). However, signals representing action selection and task rules for eye and arm movements have also been found in the parietal cortex (Gottlieb and Goldberg, 1999; Kalaska et al., 2003; Gail and Andersen, 2006; Scherberger and Andersen, 2007).

In this study, we recorded single-unit activity in AIP while monkeys were instructed by an external context cue to grasp a handle either with a power or a precision grip. Additionally, we systematically varied a parameter of the object shape, by presenting it in five different orientations. The majority of neurons in AIP encoded the object orientation as well as the instructed grip type. We classified neurons according to the time of their tuning onset and found differences in function and anatomical distribution of early and late tuned cells.

3.3 Methods

3.3.1 Neural recording

Single unit (spiking) activity was recorded using glass-coated tungsten electrodes (impedance: 1-2 MΩ at 1000 Hz) that were positioned by a 5-channel micromanipulator (MiniMatrix, Thomas Recording, Germany) that was directly attached to the recording chamber. Neural signals were amplified (x400), digitized with 16 bit resolution at 30 kS/s using Cerebus Neural signal processor (Bionics Inc., Salt Lake City, UT, USA), and stored to disc together with the behavioral data. To coarsely monitor the tuning properties of the recorded neurons during data acquisition, spike detection was performed in real-time (Cerebus hardware) and analyzed for various task conditions using Matlab (MathWorks Inc, Natick, MA, USA). However, all quantitative analysis reported here was performed offline as described below.

3.3.2 Data analysis

Raw data traces were bandpass filtered (600-8000 Hz) using Matlab and spikes were extracted and sorted using Offline Sorter (Plexon Inc, Dallas, TX, USA). The quality of single unit isolation was assessed with the following criteria: (1) the separation of waveform clusters in projections onto the first three principle component axes, (2) the homogeneity of waveforms, and (3) the presence of a refractory period in the interspike interval (ISI) distribution. A retrospective analysis revealed that less than 0.26% of all ISIs were shorter than 1 ms. Single units were included in our database if they were stably recorded for at least 7 trials per condition in the delayed grasping task (total of 70 trials) and at least 5 trials per condition in the cue separation task (total of 150 trials).

Peristimulus time histograms (PSTH) for the visualization of spike rates were generated by replacing each spike with a kernel function and then averaging all such

functions across all spikes and trials. To obtain PSTHs that are continuous as well as causal (i.e., the PSTH at any given time point is not influenced by spikes that occur in the future), we chose the kernel to be a gamma-distribution function, hence replacing each spike at time t_s with the time-shifted function:

$$R(t) = \begin{cases} (t - t_s)^{\alpha-1} * \beta^{\alpha} * \exp(-\beta(t - t_s))/\Gamma(\alpha) & \text{if } t \geq t_s \\ 0 & \text{if } t < t_s \end{cases} .$$

The shape ($\alpha = 1.5$) and rate parameter ($\beta = 30$) were chosen to achieve little delay (kernel peak at 16 ms) and a standard deviation of approximately 40 ms. It is important to note that PSTHs were only used for illustration; all quantitative analysis was based on exact spike counts. To obtain population averaged PSTHs, individual histograms were averaged across the cell population. For this, preferred and non-preferred conditions were defined as follows:

For each neuron, the preferred grip type and orientation were determined from the mean firing rates in the delayed grasping task taken in the time interval from the cue onset to the end of the movement epoch, which was then averaged across all trials of the same grip type or the same object orientation, respectively. The preferred grip type was then defined as the grip for which the mean rate was largest while the off type was defined as the other grip. Likewise, the preferred orientation was defined as the object orientation for which the firing rate was maximal, while the off-orientation was taken as the object orientation at 75° angular distance from the preferred one. For neurons with preferred orientation of 0°, we randomly chose +50° or -50° as the off-orientation, since no 75° condition existed. This definition was chosen to select the off-orientation not exclusively from the two extreme orientations (±50°). However, all results stayed essentially the same if the off-orientation was defined as the orientation with maximal angular distance to the preferred orientation, or as the orientation with the lowest firing rate.

To test whether neurons were significantly tuned for grip type and/or orientation in a particular task epoch (fixation, cue, planning, or movement), we first determined in each trial the mean firing rate (spike count / length of epoch) and then applied a

two-way ANOVA with group factors grip type and orientation. This compared the rate variance within conditions to across conditions. Neurons were considered to be significantly tuned for grip type or orientation for p values less than 0.01, and if they fired at least 5 spikes/s in the preferred condition.

In addition, tuning significance for grip type and orientation was tested at multiple time points *t* using a 2-way ANOVA on the spike count in a 200-ms window centered around *t*. This test was repeated in time steps of 50ms (sliding window ANOVA). Due to the variable length of the planning period, trials were first aligned to cue offset up until 0.6 s after cue offset; after that they were aligned to movement start (release of the hand rest button). Criteria for significant tuning were the same as for the ANOVA analysis of the fixed time epochs.

For the tuning analysis in the cue separation task, we applied the same 2-way ANOVA as in the (standard) delayed grasping task, but with a significance level of $p<0.05$ due the lower number of trials per condition (minimum 5, average 6.8; standard task: min. 7, avg. 9.8). Since the cue separation task contained 2 planning periods of variable length, trials were aligned to the cue offset of the first and second cue as well as to the movement start (hand rest release), and realignments were placed 0.6 seconds after each cue offset.

To estimate the time when the number of significantly tuned cells for grip type or orientation sharply increased (during the cue and movement epoch), we determined the time in each epoch when the increase became half maximal. For this, we first computed a linear interpolation of the number of significantly tuned cells (as obtained from the sliding window ANOVA) in steps of 2 ms (using Matlab command interp). We then determined, for each epoch, the time when this curve became half-maximal with respect to a baseline level. This baseline was set to 0 for the cue epoch and to the value of the curve at the time of the go-signal for the movement epoch. To assess significance of possible time shifts in the increase of grip type and orientation tuning, we used a Monte Carlo procedure, in which 1000 repetitions of the same analysis were performed with random shuffling of the labels

'grip type tuned' and 'orientation tuned', in order to determine the null distribution and its associated significance level.

Furthermore, we quantified the time in the task when each neuron first became significantly tuned for grip type or orientation. We called this the *tuning onset* of grip type and orientation tuning, and defined it as the first time when a neuron wa significantly tuned in the sliding window ANOVA in at least five consecutive steps. If this occurred, tuning onset was set to the center of the first window; if not, it was set to infinity. Using this quantitative measure, we classified each neuron, separately for grip type and orientation, in one of the four categories: (1) early, (2) middle, (3) late, or (4) no tuning onset, corresponding to the tuning onset falling in the cue, planning, or movement epoch, or never occurring.

Furthermore, we quantified the number of cells preferring each of the two grip types and five grip orientations separately for the different task epochs. For this, the same definition of preferred grip type and orientation was used as for the calculation of population PSTHs, except it was restricted to the task epoch in consideration.

Finally, we applied a receiver operating characteristic (ROC) analysis (Britten et al., 1992) to various task epochs to assess for each individual cell, how well its firing rates during precision grip trials could be discriminated from those during power grip trials. We calculated the area between the ROC curve and the no-discrimination (diagonal) line as a measure of discriminatory power. To remove interaction effects of superimposed orientation tuning, we computed this measure separately for each orientation and averaged the five results. Significance levels were assessed by performing a Monte Carlo analysis for each cell as explained above, this time with random shuffling of the labels for power and precision grip between trials. The 95^{th} percentile of the resulting distribution was then taken as the significance level.

3.4 Results

We recorded a total of 571 single cells in two monkeys (Monkey L: 299 cells, monkey J: 272 cells) while the animals performed the delayed grasping task. Results were essentially the same for both animals and are therefore reported together.

Both monkeys performed the task with high accuracy. Errors due to the execution of the wrong grip type occurred only in about 5% of all trials. Observation of the animals via infrared camera during task performance revealed that the handle was approached with the hand pre-shaped and in the matched orientation. Analysis of the movement times also suggested that the animals did not approach the target in a 'standard' orientation and then adjusted the hand orientation based on sensory (tactile) feedback information: the influence of the object orientation on the movement time was quite small to allow for such feedback adjustments. The median movement times for precision grips/power grips were 0.53s/0.22s (-50deg orientation), 0.47s/0.21s (-25 deg), 0.46/0.21s (0 deg), 0.47/0.21s (+25 deg), and 0.53s/0.21s (+50 deg). No pre-shaping occurred before the go-signal, and the hands were kept motionless on the sensor pads.

3.4.1 Tuning for grip type and orientation

A large majority of cells were modulated by the delayed grasping task. Three typical neurons are shown in Figure 3-1. Neuron A showed a sharp increase of its firing rate immediately after the movement instruction was given (cue epoch), in particular for objects oriented to the right (+25/+50 deg), and more strongly for power grips than for precision grips. This activity pattern was preserved throughout the task until the movement was executed. The example neuron was therefore modulated by grip type and orientation in all three task epochs (cue, planning, and movement). Note that the timing of the early rise for trials with rightward orientations of the handle was identical for both grip types (left and right panel), before the curves separated shortly afterwards.

A second type of neuron is depicted in Figure 3-1B. It showed a clear modulation of its firing rate with object orientation immediately after cue presentation, while throughout the cue and planning epoch its activity was identical for power and precision trials. However, during movement execution (starting immediately after handrest release) the firing rate of precision trials increased with respect to power trials. Therefore this neuron represented the object orientation from the object presentation onward, while grip type modulated the neuron only during movement execution.

Finally, neuron C in Figure 3-1 did not respond at all after cue presentation, neither for the grip type nor for the object orientation. However, it responded vigorously during movement execution with a strong peak for precision grips while being indifferent to object orientation.

Figure 3-1: Example neurons and population firing rate

Three example neurons with different tuning onsets. For each neuron, precision grip trials are shown on the left panel and power grips on the right panel. Different colors indicate various handle orientations, for which spike rasters (on top) and averaged firing rates (at bottom) are shown individually. The dotted line within the movement epoch indicates the release of the hand rest button (movement start). All trials are aligned to both the end of the cue epoch and the start of the movement (arrow heads below); gaps in the curves (at around 0.6 s) indicate the realignment. A: Neuron that exhibits tuning for the handle orientation and the instructed grip type starting in the cue period and extending until movement execution. B: Neuron with tuning for the handle orientation starting in cue, but with significant grip-type modulation only during movement execution. C: Neuron showing no response during cue presentation and movement planning, but with a strong selectivity for precision grips during movement execution without significant orientation tuning. D: Population firing rate across all 571 neurons for each combination of the cells' preferred and non-preferred grip type and orientation.

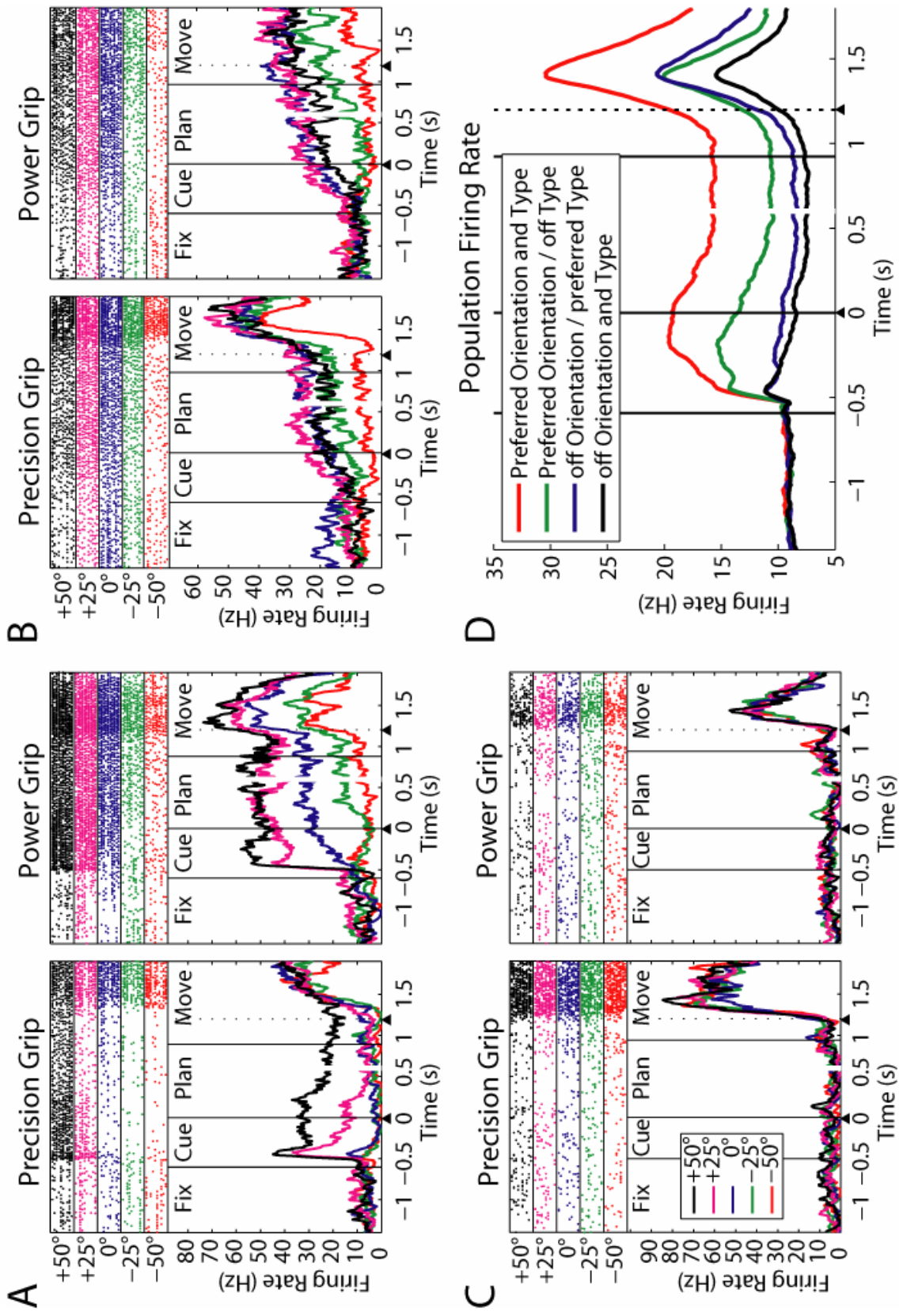
A
B
C
D
Precision Grip
Power Grip
Fix
Cue
Plan
Move
Time (s)
Firing Rate (Hz)
+50°
+25°
0°
−25°
−50°
Population Firing Rate
Preferred Orientation and Type
Preferred Orientation / off Type
off Orientation / preferred Type
off Orientation and Type

These examples illustrate the variety in our dataset. As a summary, Figure 3-1D shows the population firing rate across all 571 neurons for each neuron's preferred and non-preferred grip type and orientation. Both grip type and object orientation were well represented in the population during cue presentation and remained so until the movement was finished. Importantly, this was true even if the definition of the preferred and non-preferred condition was based on the activity during the movement epoch alone, indicating that this finding is not a selection artifact.

To quantify the number of cells with a particular tuning in each task epoch, we performed, for each cell, a 2-way ANOVA with factors grip type and orientation on the firing rates within each task epoch (Table 3-1). We found that in the course of the trial, these two variables behaved distinctively (Figure 3-2A). During the cue period the fraction of neurons showing specificity for the object-cued factor, i.e. the object orientation, accounted for 55% of all cells, and this ratio stayed roughly constant throughout the planning and movement epochs. In contrast, only about 25% of the cells showed selectivity for the context-cued variable (grip type) during the cue period; however this value increased to 37% during the planning epoch and 58% during movement execution, reaching a level that was eventually similar to the number of orientation tuned cells.

Of the cells which did not show tuning for either grip type or orientation, more than half (cue: 57%, planning: 62%, movement: 68%) displayed significant rate variations (increase or decrease) when compared to the baseline activity in the fixation epoch (2-tailed t-test, $p=0.01$). Presumably, some of these neurons could be tuned for other objects or grip types than the ones we tested in this study.

Orientation Tuning				Grip type Tuning			
Cu	Pla	Mo		Cu	Pla	Mo	
+	+	+	30%	+	+	+	12%
+	+	-	11%	+	+	-	4%
+	-	+	6%	+	-	+	3%
+	-	-	8%	+	-	-	6%
-	+	+	7%	-	+	+	15%
-	+	-	3%	-	+	-	6%
-	-	+	12%	-	-	+	28%
-	-	-	23%	-	-	-	26%

Table 3-1: Cell classification by tuning in task epochs

Legend: Left: List of cell classes (different rows) according to the presence (+) or absence (-) of significant orientation tuning in the task epochs: cue, planning, and movement (2-way ANOVA, see methods). Percentages indicate the fractional size of each class in our population (n=571). **Right:** Corresponding classification for grip type tuning.

To further investigate grip type and orientation tuning over time, without constraining the analysis to predefined epochs, we extended the 2-way ANOVA on a sliding window (window width: 200 ms, step size: 50 ms), which revealed marked differences between the two variables (Figure 3-2B). First, the number of orientation selective cells after cue presentation rose considerably earlier than for grip type selective cells. By measuring the time at half height of this increase during the cue epoch, this time difference was found to be about 150 ms in the population ($p << 10^{-3}$, Monte Carlo procedure). This time difference was also observed in individual neurons (e.g., see: Figure 3-1A), perhaps indicating that the processing of an abstract cue took longer than processing of an object cue. During the planning epoch, both fractions of tuned neurons stayed on a plateau, with the orientation fraction slightly larger than type; while during movement execution, the number of grip type specific neurons further increased and actually exceeded the number of

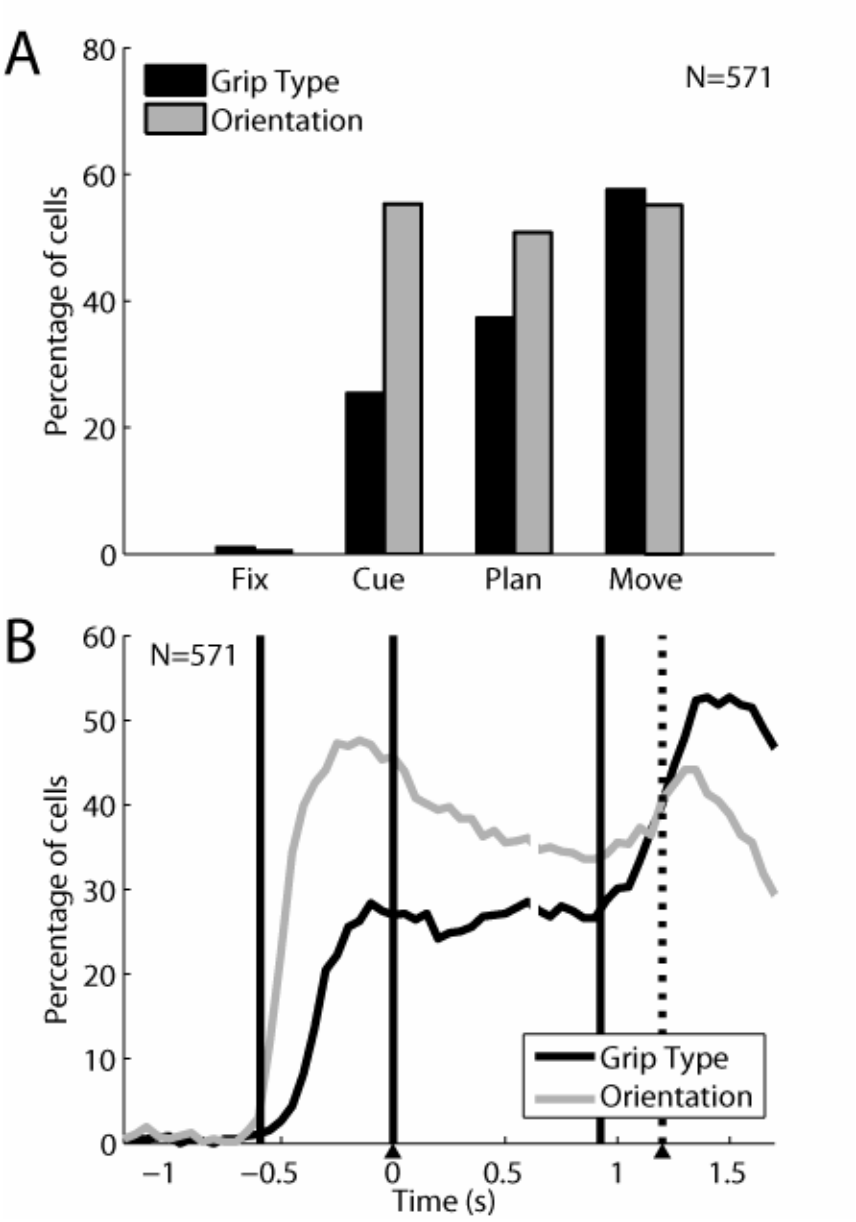

Figure 3-2: Orientation and grip type tuning in the neuronal population

A: Fraction of cells showing tuning for grip type (black) and handle orientation (gray) in the different task epochs (two-way ANOVA; see Methods). Tuning for object orientation was constant from cue to movement, while grip type tuning increased over time. **B:** Percentage of tuned cells in a sliding window (width: 200 ms, centered on each data point). During cue, tuning for orientation started about 150ms earlier than for grip type. Grip type tuning increased in two steps: one during cue and one during the movement epoch. Trials are aligned on cue offset and movement onset (as in Figure 3-1).

orientation selective cells, which was due to neurons that became type specific only during the movement epoch (e.g., as in Figure 3-1B-C). However, no significant time difference was found between the two fractions in this second increase ($p > 0.3$).

In summary, the population analysis showed that the representation of grip type, while already present in the cue period shortly after the instruction was given, strongly increased toward movement execution, both in absolute terms (number of tuned cells) and in relation to the number of cells coding for orientation. These different roles of AIP for the encoding of an object-cued factor (orientation) and a context-cued factor (grip type) are further analyzed in the next section.

3.4.2 Tuning onset

As we have seen in the example neurons (Figure 3-1A-C), some cells were grip type modulated already in the cue period, while others were tuned only during movement execution. Similarly, cells exhibited different onset times for the tuning of orientation. To quantify this effect, we determined each cell's *tuning onset* for grip type and object orientation, respectively (see methods). Figure 3-3 (top row) shows, separately for grip type (left panel) and object orientation (right panel), the time periods when neurons were significantly tuned (black lines). Each neuron is represented by one row, and neurons were sorted (along the y-axis) according to their tuning onset. The graph emerging from the white-black transition depicts the cumulative distribution of the tuning onset, which is shown below in its derivative (histogram) form (bottom panels). For grip type (left panels), the tuning onset distribution was clearly multimodal with a first peak during cue presentation followed by a second peak of similar size after the go-signal, with only a small fraction of cells located in between. For object orientation, the majority of cells had a tuning onset during cue presentation and only a few cells became tuned late in the task.

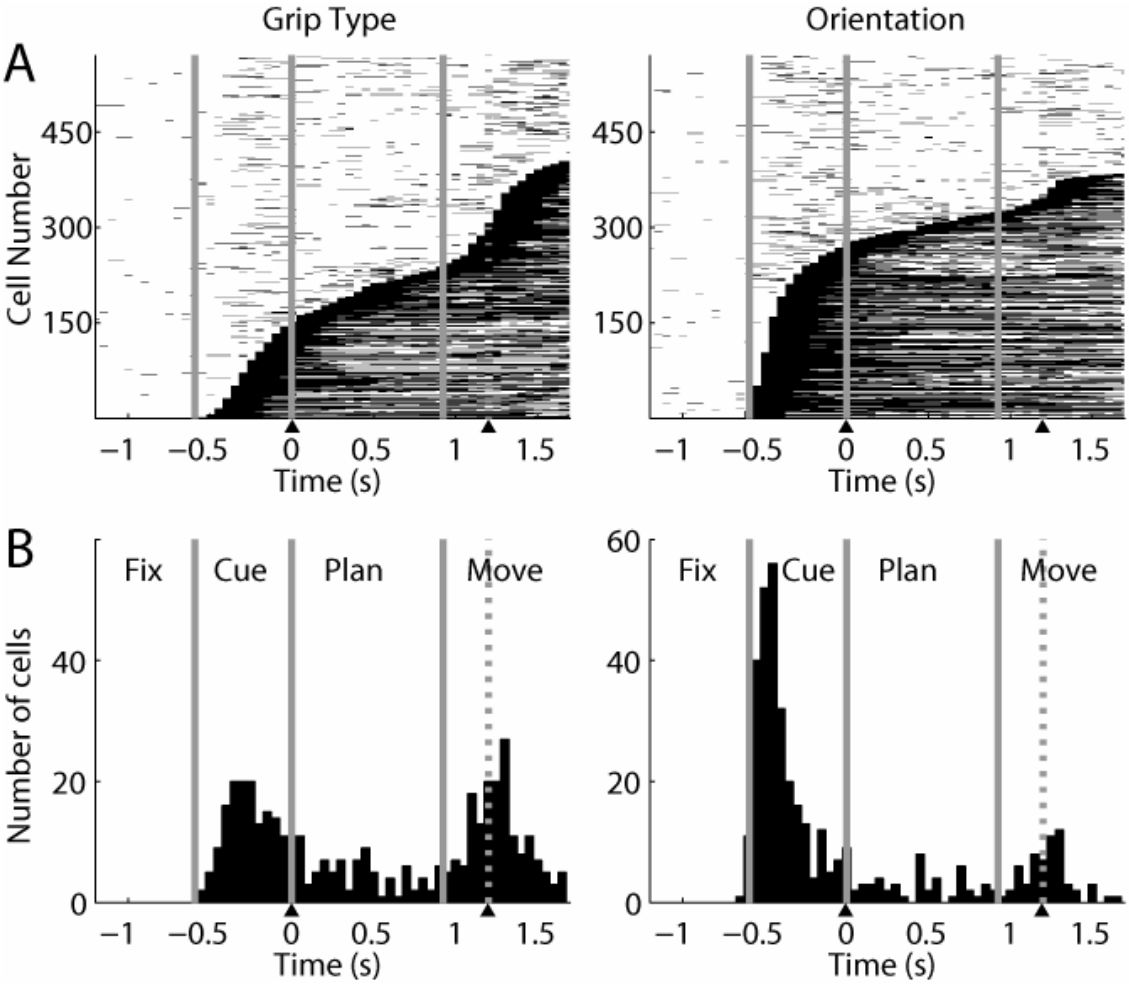

Figure 3-3: Tuning Onset

Times with significant tuning in the neuronal population. **A:** Sliding window analysis (two-way ANOVA) for each cell (y-axis) at each time step (x-axis). Significant grip type (left) and orientation tuning (right) is indicated by black squares ($p < 0.01$). Cells are ordered by tuning onset (first occurrence of five consecutive significant steps). **B:** Histogram of tuning onset for grip type (left) and orientation (right) across the population.

To describe the relationship between the onset of grip-type and orientation tuning, we classified neurons into four groups according to their tuning onset (early, middle, late, and none), separately for grip type and orientation tuning. Early, middle, and late onset corresponded to the cue, planning, and movement epochs. Table 3-2 shows a 4x4 contingency table of the combined tuning onset for grip type

and object orientation. As can be readily seen, this contingency table is not statistically independent (Pearson's $\chi^2 = 88.5$, df = 9, $p << 10^{-3}$).

Object Orientation	Grip Type				
	Cue	Planning	Movement	None	All
Cue	108 [A]	40	53 [B]	77	278 (49%)
Planning	11	14	9	8	42 (7%)
Movement	9	7	37	12	65 (11%)
None	24	18	75 [C]	69	186 (33%)
All	152 (27%)	79 (14%)	174 (30%)	166 (29%)	571 (100%)

Table 3-2: Cell classification by tuning onset

Contingency table of tuning onset for type (columns) and orientation (rows) for all neurons in our population (n= 571). Example neurons for the marked classes (A-C) are shown in Figure 3-1A-C.

During the cue period, neural responses were dominated by the object feature orientation. While about half of the recorded cells (278/571, 49%) showed an early onset of orientation tuning, only 152 cells (27%) signaled the grip type. A considerable part of the orientation-sensitive group was also modulated by the instructed grip (108/278, 39%), leading to the largest class of cells (for an example, see Figure 3-1A). However, neurons that were orientation tuned during the cue period were not always grip type tuned at the same time. In fact, many of these cells only became tuned for the grip type during planning (40) or movement (53; e.g. Figure 3-1B), and others not at all (77). In contrast, cells that were grip type tuned in the cue period were very likely to be also orientation tuned then (108/152, 71%), while the other groups with early type tuning were small. Taken together, this

suggests that during the cue period, grip type coding is only modulating the primary coding of object features.

Only a few neurons had their tuning onset during the planning period. Some cells that were already orientation tuned in the cue became additionally grip type tuned in the planning epoch (40). All other groups were very small. Therefore, most of the activity during the planning period (Figure 3-2A and B) was a continuation of the activity already present during the cue epoch, which is consistent with a role of AIP, and of the parietal cortex in general, in working memory (Mountcastle et al., 1975; Sakata et al., 1995; Murata et al., 2000; Andersen and Buneo, 2002).

Neurons whose tuning began during the movement epoch behaved quite differently from those with early tuning onset. Late onset tuning was directed primarily to the grip type rather than the object orientation. The largest group of these neurons was selective for the grip type but lacked orientation tuning (75; see also Figure 3-1C). A second large group consisted of cells that had developed orientation-selectivity during the cue period and now additionally expressed a late onset tuning to grip type (53, see Figure 3-1B). A third group of neurons developed tuning to both the grip type and the orientation during the movement period (37). These latter neurons accounted for the majority of cells with late orientation tuning. In contrast, neurons that became orientation tuned during the movement period, without tuning to grip type, were very rare (12).

Note that cutaneous tactile information could not have been the major source of input for late-onset cells, because the movement epoch ended when the hand had grasped the object. Also, previous studies found little or no neurons in AIP with somato-sensory responses (tactile or joint-related) (Taira et al., 1990; Murata et al., 2000). Therefore, these cells are most likely related to motor output. Together, our findings indicate that neurons with a late tuning onset, in contrast to early-tuned cells, primarily encode the grip type, and only secondarily (and optionally) the object orientation.

3.4.3 Cue Separation Task

Given these asymmetries between the coding of grip type and orientation in AIP, we also tested a subset of 120 neurons in the *cue separation task*, in which the two task instructions were presented in two cue epochs that were separated by an additional planning period (Figure 2-1C). This cue separation task was run in two versions, with either the object orientation presented in the first cue epoch and the type instruction in the second (OT-task), or the type instruction in the first cue epoch and the orientation in the second (TO-task). In addition, all neurons were also tested in the standard *delayed grasping task*, where similar results were obtained as in the full dataset. This indicated that our subset was representative. An example neuron tested in the cue separation task is shown in Figure 3-4. For clarity of presentation, only 4 task conditions are shown: the preferred (-25°) and the non-preferred orientation (50°) for the two grip types. In the standard task (Figure 3-4A), the neuron was tuned for orientation and grip type in all three epochs, with the highest activity for power grips and the object tilted to -25°. When only the object orientation was revealed during the first cue (OT-Task, Figure 3-4B), the cell showed a clear response to the preferred orientation, independent of grip type. Then later, starting with the second cue, the firing rate was additionally modulated with respect to the instructed grip type. In contrast, when the grip type was instructed first (TO-Task, Figure 3-4C), the cell's firing rate did not reflect this information, but stayed low for all conditions. Only when the object orientation was revealed during the second cue did the neuron respond vigorously and with preference for power grips in the preferred orientation, obviously combining the newly presented orientation information with the grip type information that was given before.

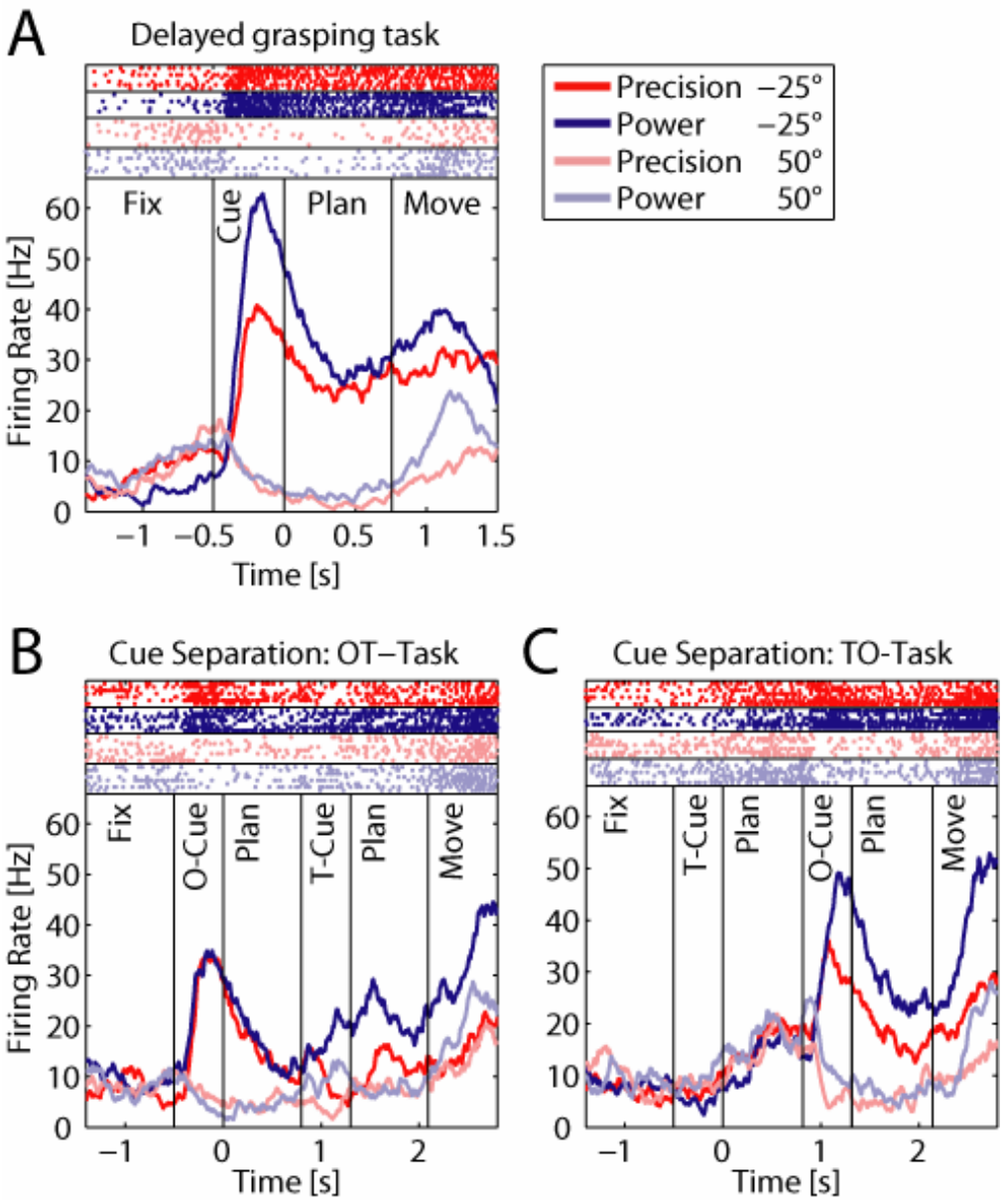

Figure 3-4: Example cell in the cue separation task

Neural activity in the cue separation task. Panels show one example neuron during the delayed grasping task (**A**) and the cue separation task: OT task (**B**), TO task (**C**). Different grip types are shown in red (precision) and blue (power), while the two grip orientations are shown in light and dark color. **A:** The neuron was early tuned for both parameters, showing highest activity for power grips at -25 deg orientation. **B:** In the OT-task, presentation of the object in the -25 deg orientation evoked a strong response, which was then differentially modulated for the two grip types after the second cue. **C:** In the TO-task, the cell did not respond to the type cue when presented in the absence of the object. However, the cell responded vigorously after the orientation cue with a preference for power grips in the preferred orientation.

Such a response pattern, with a strong modulation for orientation when presented first, and a delayed modulation for grip type that kicked in only after the orientation cue was revealed, was typical for many cells, as shown in our population analysis (Figure 3-5). The top panels show the firing rate of the population in 4 conditions (preferred and non-preferred type and orientation). In the first cue of the OT-task (left panel), the population activity increased strongly for both conditions in which the handle was presented in the preferred orientation. This orientation modulation persisted despite some decrease in activity during the first planning period. When the grip type information was subsequently provided in the 2nd cue, the population response decreased for the non-preferred grip type, but remained constant for the preferred grip type instruction. This activity pattern suggests that the neural population in AIP encodes movement plans for both types of actions simultaneously, until the ambiguity between the two grip types is resolved by the type instruction.

The activity pattern in the OT-task also became apparent in the sliding window ANOVA (Figure 3-5B, left). Object orientation was maximally encoded at the end of the first cue. After the second cue, grip type was represented in approximately 35% of all cells, similar to the planning phase of the delayed grasping task. A second increase in grip type selectivity then occurred during movement execution.

The population activity in the TO-task showed a quite different pattern (Figure 3-5A, right panel). Neurons responded weakly to the grip type instruction (first cue), but when the object orientation was presented in the second cue, the population activity became tuned for the object orientation and the grip type at once, similar to the population response in the delayed grasping task (Figure 3-1D). The sliding window analysis (Figure 3-5B, right) showed a reduced number of cells, about 20%, that displayed grip-type selectivity before the object presentation. This selectivity is reflected in the slight increase in population activity of the preferred grip type conditions (red and blue curves) during the first planning epoch (Figure 3-5A, right). Overall however, this modulation was weak; only after the presentation of orientation information in the second cue was there an increase in the number of grip type tuned neurons to a similar level to that observed in the OT-task.

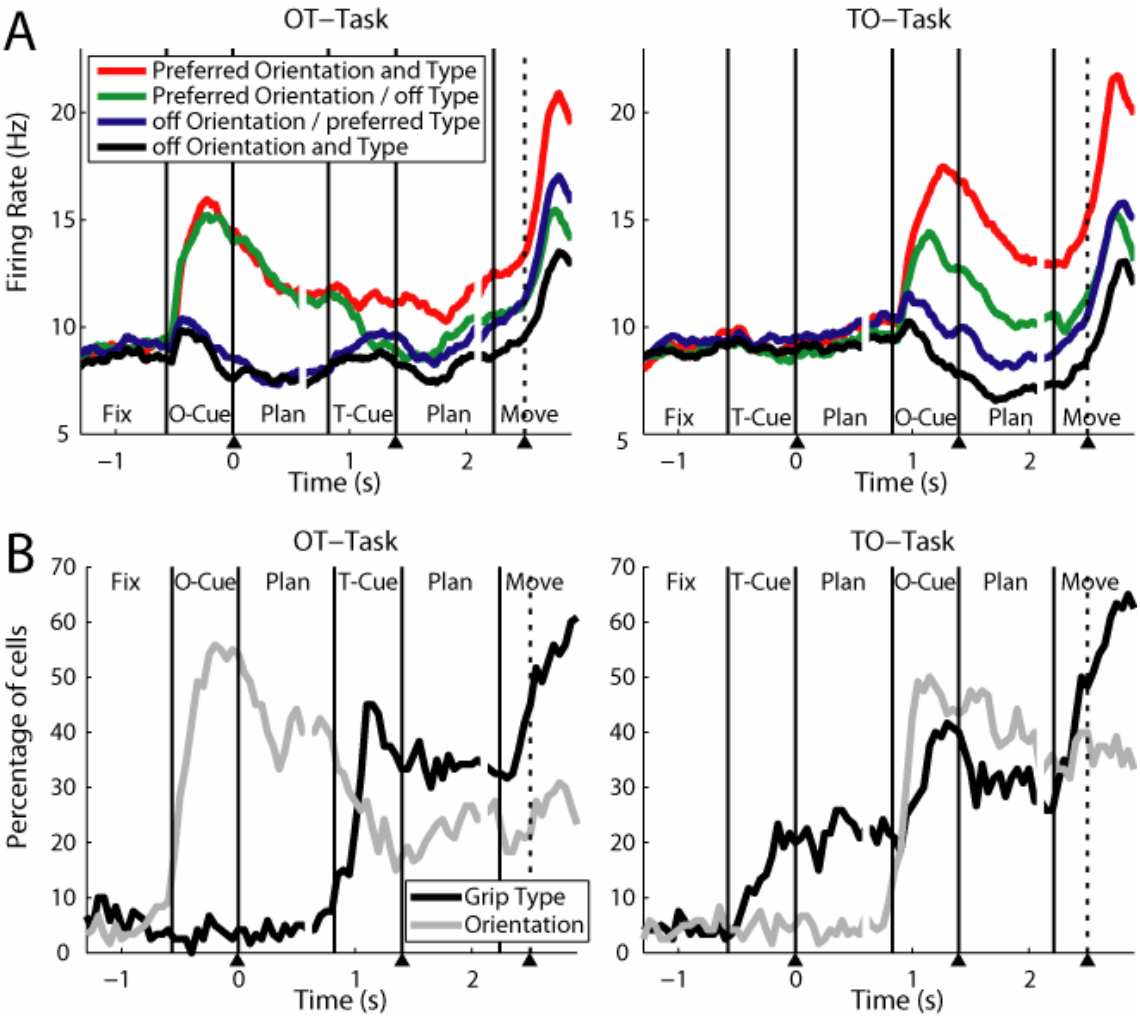

Figure 3-5: Population analysis of the cue separation task

A: Population firing rates in the cue separation task (N=120) with OT-task on the left and TO-task on the right panel. For each cell, its preferred type and orientation was established in the delayed grasping task (not shown). **B:** Fraction of cells that were significantly tuned by grip type and orientation in the course of the OT- and TO-task (sliding window ANOVA as in Figure 3-2B).

Given the weak modulation in the population activity during the first planning of the TO-task, the amount of grip type selectivity in the sliding window ANOVA seems surprisingly high, especially when compared to the level found in the second planning epoch. This could in part be explained by an increased sensitivity of the ANOVA for grip type effects in the absence of orientation information before the

second cue, due to a reduction of within-group variance in the power and precision groups.

To compare grip type effects at different task phases of the TO-task without being influenced by the presence or absence of orientation information, we performed ROC analyses separately for each orientation and averaged the five results (see methods). This allowed us to compute, for each individual cell and any task epoch, how well the firing rates during precision grip trials could be discriminated from those during power grip trials. The result of this analysis showed that only 24 cells (20 %) significantly discriminated between power and precision trials before the object cue, while this value rose to 62 (52%) after object presentation, confirming that many more cells displayed a grip type effect after object presentation. These findings indicate that the representation of grip type is strongly reduced in AIP in the absence of object information, which corresponds well with our cell classification in the full dataset (Table 3-2), where grip type selective neurons during cue were usually orientation tuned as well.

3.4.4 Coding schemes

As we have shown, many neurons in AIP represent the object orientation or the grip type in one or several trial epochs. Here we explore, which grip types and object orientations are preferred in the population, and how these representations change over time.

Figure 3-6A shows the ratio of cells that prefer precision vs. power grip. During the cue period, half of the grip-type specific cells preferred precision grip and the other half power grip. However, later on in the trial, this ratio shifted in favor of precision-preferring cells, such that during movement execution, the ratio of precision- to power-grip preferring cells was about 60 to 40.

A somewhat similar development becomes apparent when looking at the preferred orientation (

Figure 3-6B). During cue presentation, the preferred orientations were fairly evenly distributed with only a slight overrepresentation of the extreme (±50deg) orientations (47% vs. 40% expected from uniform distribution), while during movement execution, the fraction of neurons preferring extreme orientations increased to 59%.

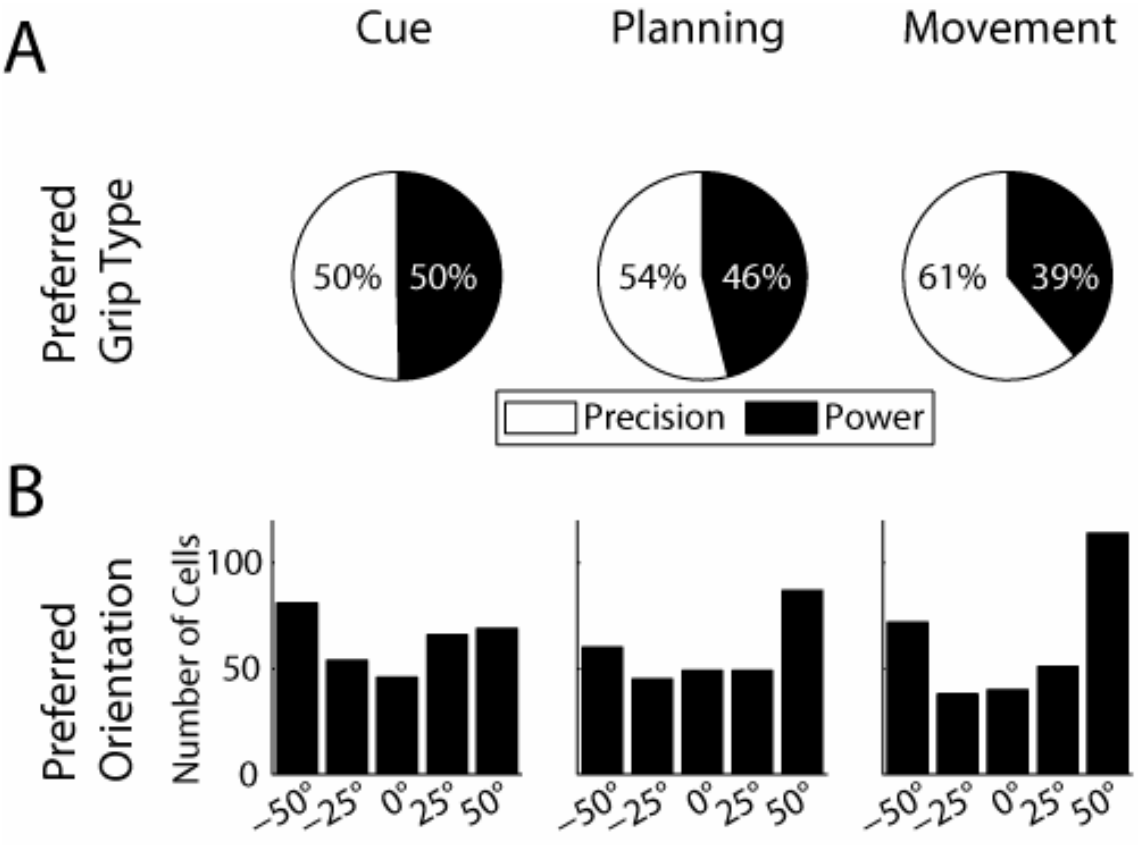

Figure 3-6: Distribution of preferred grip type and orientation in various task epochs

A: Ratio of cells preferring precision (white) or power grip (black). From cue to movement, the fraction of cells encoding precision grip increased substantially. **B:** Number of cells preferring each of the five orientations. In the movement epoch, the distribution shifts in favor of terminal orientations (±50 deg).

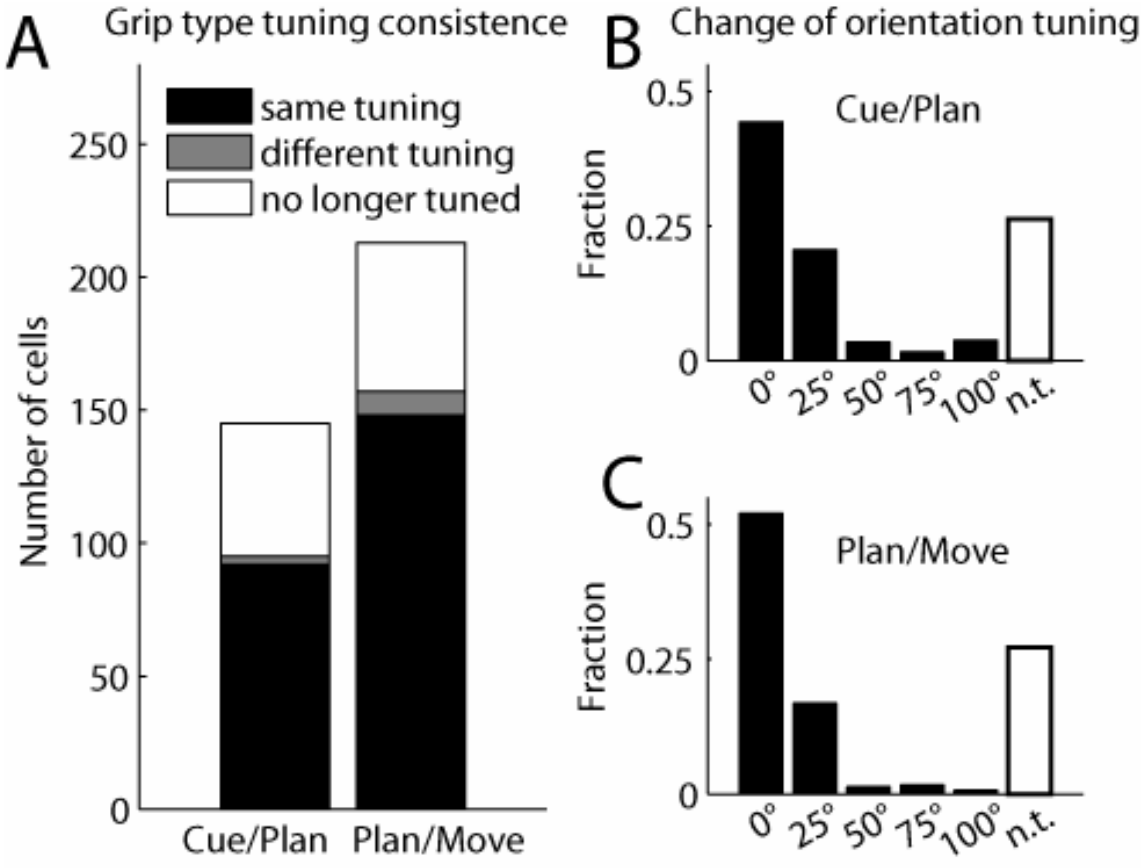

Figure 3-7: Tuning consistency across task epochs

A: Grip type tuning. Histogram bars indicate the number of cells that stay tuned for the same grip (black), change preference to the opposite grip (gray), or lose their tuning (white) when transitioning between consecutive task epochs (cue-planning and planning-movement). **B-C:** Change of orientation tuning in consecutive task epochs: cue-planning (**B**) and planning-movement (**C**). Histograms show the fraction of cells for which the preferred orientations in the two epochs were the same (0 deg shift), neighboring orientations (25 deg), or further apart (50-100 deg), and of cells that lost their tuning (white bars). Preferred orientation shifts of more than 25 deg were rare. In general, cells were tuned consistently over time.

These shifts of preference in the population were not caused by preference changes of individual neurons. Figure 3-7A illustrates the consistency of grip type preference between consecutive epochs. Between adjacent task epochs, only 2% (cue to planning) and 4% (planning to movement) of the cells tuned in one epoch changed their grip type preference between power and precision (gray bars), while the

overwhelming majority of cells remained either tuned for the same grip (black bars; 64% and 70%, respectively) or were no longer significantly tuned (white bars; 34% and 26%). This indicates that in general, the preferred grip type did not change across task epochs but remained constant throughout the task. Similarly, the cell's preferred orientation usually did not change systematically between task epochs, but stayed the same or shifted by one step at most (Figure 3-7B-C).Note that a shift by one is usually not meaningful, since the cell's firing rate was often not significantly different between neighboring orientations.

We demonstrated that the tuning of individual neurons remained largely constant during the task whereas the population tuning shifted at later task epochs toward an over-representation of precision grips and extreme orientations. This apparent discrepancy suggests that different populations of cells with diverse coding schemes might be active at different task epochs. To explore this further, we determined the preferred grip type and preferred orientation separately for the three cell groups of early, intermediate, and late tuning onset. We found, in fact, that the cell group with early-onset grip type tuning preferred precision grips and power grips equally likely throughout the task (in the cue, planning, and movement epoch); in contrast, the cell group with a late tuning onset for grip type (in the movement epoch) had a preference ratio for precision and power grips of 70 to 30 (Figure 3-8A). Similarly, the cell group with the orientation tuning onset during the cue epoch had a fairly constant rate of neurons preferring terminal orientations (±50°) during the course of the task (cue: 49%, planning: 52%, movement: 54% of cells), while neurons with a late onset of orientation tuning mainly preferred extreme orientations (76% of cells; see Figure 3-8B). Moreover, for both grip type and orientation, the middle group behaved similarly to the early group, suggesting that they followed the same scheme as early tuned neurons. Such tuning differences between cells with early and late tuning onset suggest that these cell groups encode different entities earlier in the task during movement instruction, compared to later in the task during movement execution. During movement instruction, similar numbers of neurons are allocated for the representation of the two grip types and for the various object orientations.

However, later in the task, this coding scheme seems to change in favor of a motor representation, in which the precision grip (being more difficult) requires more cortical resources than the power grip while the preponderance of neurons preferring extreme orientations could indicate a push-pull representation for hand rotation in the pronation-supination direction.

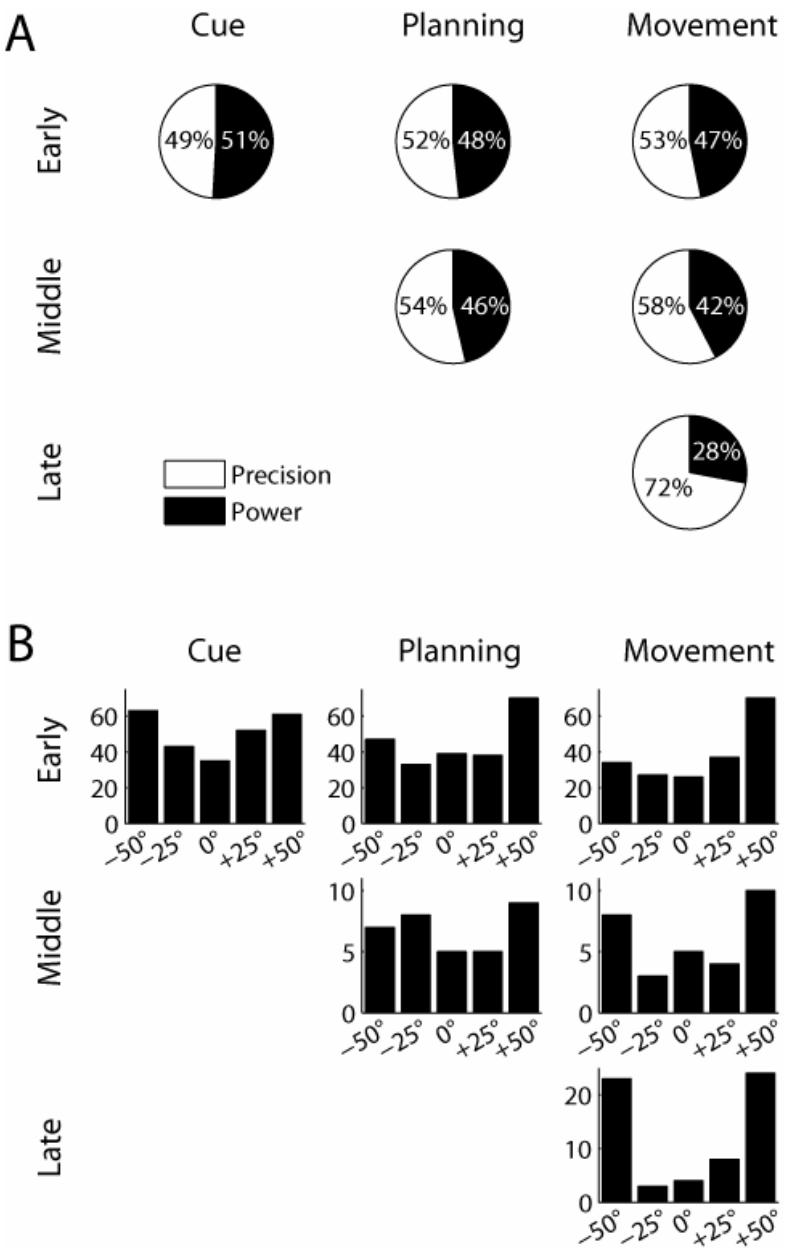

Figure 3-8: Distribution of preferred grip type and orientation in different cell classes

A: Ratio of precision and power preference in cell groups with early (top row), intermediate (middle) and late (bottom) tuning onset for grip type. In all three task epochs, early tuned cells preferred power grips and precision grips approximately equally often. In contrast, ~70% of late tuning cells preferred precision grips. **B:** Number of cells with a particular orientation preference for the three cell classes. In early orientation tuned cells, the portion of cells that preferred extreme orientations (±50 deg) changed little from cue (49%) to movement (53%), while 78% of cells with a late onset of orientation tuning preferred extreme orientations.

3.4.5 Anatomical Organization

Finally, we analyzed if there is a correlation between the reported functional classification (Table 3-2) and the location along the intraparietal sulcus (IPS) where the cells were recorded. For this we projected the recording coordinates of each neuron onto an axis parallel to the IPS and then split the cell population into eight bins, according to the cells' posterior-anterior position on that axis, such that each bin contained the same number of cells. This allowed us to calculate, separately for each bin along the IPS, the fraction of cells that belonged to a particular cell class (e.g., early onset orientation tuned cells). Figure 3-9 displays the result for orientation and grip type tuned cells with early and late tuning onset, respectively. Although all cell classes were present in all bins, the distributions were clearly non-uniform, but instead showed steady gradients. Cells with an early tuning onset (orientation or grip type) were found with a higher probability in the posterior recording sites. In contrast, cells with late tuning onset (orientation or grip type) occurred more frequently in the more anterior segments. To assess the significance of these effects, we compared the occurrence of cell classes in the anterior half of the recordings to those in the posterior half (i.e. to the left and the right of the dashed lines in Figure 3-9; for the anatomical location of the median, see Figure 2-1 E, F). For a cell class that was evenly distributed along the anterior-posterior axis, one would expect to see an even distribution of neurons between the anterior and posterior halves. Instead we found that 60% of all cells with early onset of orientation tuning and 61% of the cells with early onset of grip type tuning were located in the posterior half of the neural population, while 66% of the cells with late onset of orientation tuning and 67% with late onset of type tuning were located in the anterior half. All of these findings were significantly different from the null hypothesis of a uniform distribution (binomial test, $p<0.01$). Additionally, cells that displayed early orientation tuning but late tuning for grip type (as the example cell in Figure 3-1B) did not show such a gradient but were evenly distributed among the different bins. These results suggest the presence of a visuo-motor gradient along the

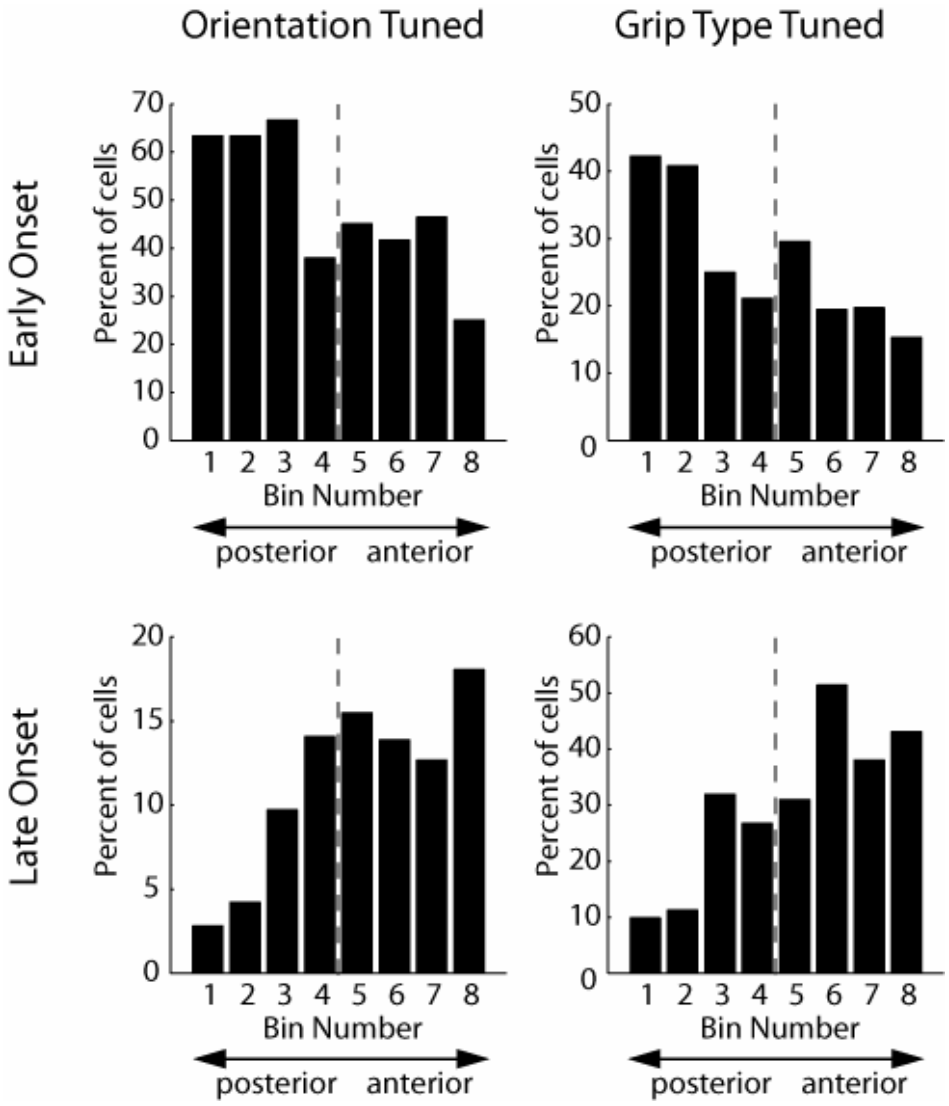

Figure 3-9: Anatomical distribution of different cell classes

Cells (N=571) were distributed into eight bins according to their location along the intraparietal sulcus, such that each bin contained the same number of cells. Bin 1 contained the most posterior and bin 8 the most anterior cells (x-axis). Individual panels show the distribution along the intraparietal sulcus (IPS) for a particular cell class (left: orientation tuned, right: grip type tuned, top: early onset, bottom: late onset). Histograms display the fraction of cells in each bin that belonged to the respective cell class. Early onset cells showed a decreasing, late onset cells an increasing gradient from posterior to anterior. Dotted line: median of the population.

IPS, with cells that show strong responses during the cue epoch being more frequently found in the posterior part of AIP, and cells with predominantly motor responses occurring more frequently towards the tip of the IPS. This fits well with anatomical data of neurons projecting from AIP to F5 that seem to be more frequently located in the anterior part of AIP, as Figure 1 of Borra et al. (2008) suggests. Finally, the presence of cells with sensory and motor representations in one area might facilitate sensorimotor transformation (Cisek and Kalaska, 2005; Optican, 2005; Buneo and Andersen, 2006).

3.5 Discussion

We investigated neural activity in AIP during a delayed grasping task, in which monkeys grasped a single object in various orientations with one of two possible grip types (Figure 2-1). AIP neurons represented the object orientation and the instructed grip type immediately after cue presentation, indicating that AIP integrates 3D-features of graspable objects with contextual information (Figure 3-1, Table 3-1). The representation of grip type was stronger during movement execution than in the cue and planning epochs (Figure 3-2) due to grip-type selective cells that became specifically active during movement (Figure 3-3). Furthermore, grip type selectivity in the cue epoch was mainly found in cells that were also orientation selective, while the opposite was true in the movement epoch (Table 3-2).

In the TO task, the grip type was only weakly encoded in response to the grip type cue alone. In contrast, in the OT task, neurons preferring either grip type were activated simultaneously, after object presentation but before the type was instructed (Figure 3-4, Figure 3-5).

Individual cells generally kept the same preference for grip type and object orientation across task epochs (Figure 3-7). However, at the population level, neurons with early and late tuning onset had different distributions of preferred conditions (Figure 3-8) as well as different anatomical distributions within AIP (Figure 3-9).

3.5.1 Anatomical connectivity of AIP

Our findings are compatible with known anatomical connections of AIP. AIP receives input from parietal visual areas (in particular LIP, CIP, and V6a) and from the inferior temporal cortex (TEa, TEm) (Nakamura et al., 2001; Borra et al., 2008). These areas represent spatial and object orientation information of visible objects (Sakata et al., 1997; Tsutsui et al., 2001; Tsutsui et al., 2002; Galletti et al., 2003). Also, AIP receives connections from the prefrontal cortex (areas 46v and 12l) (Borra

et al., 2008), which might convey contextual information, as we have observed in AIP. Furthermore, AIP is reciprocally connected to area F5 in the ventral premotor cortex (Luppino et al., 1999) which exhibits similar activity related to hand movements (Rizzolatti et al., 1988; Murata et al., 1997; Raos et al., 2006; Stark et al., 2007) and is considered to be part of the cortical output structures for controlling the hand due to its projections to primary motor cortex and the spinal cord (Rizzolatti et al., 1988; Luppino et al., 1999; Lemon, 2008). Together these previous studies locate AIP at the interface between sensory and motor areas related to hand movement control.

3.5.2 Functional classification of AIP neurons

The group of Sakata described three cell classes in AIP based on their activity during grasping in the light and in the dark (Taira et al., 1990; Sakata et al., 1995; Sakata et al., 1997): visual-dominant cells were only active when grasping in the light, visuo-motor cells were preferentially active in the light, and motor-dominant cells were equally active for grasping in the light or dark. Furthermore, visually responsive cells were labeled 'object-type' if they were active in a separate object fixation task, and otherwise classified as 'non-object type' (Sakata et al., 1995; Murata et al., 2000).

Our results confirm and extend this classification. Neurons active in the cue period of the delayed grasping task correspond to Sakata's object-type cells (visual dominant and visuo-motor). These neurons fall in two sub-categories: some are tuned to object orientation without selectivity for grip type, while others are modulated by grip type instruction. Most of these cells remain active during the planning epoch, suggesting a role for working memory or movement planning. Neurons active exclusively during the movement epoch correspond to Sakata's motor-dominant or non-object type/visuo-motor classes.

In contrast to the previous categorization, our classification is based on the tuning onset for object orientation and grasp type during the entire course of the task, not

just during the movement execution, and therefore quantifies the temporal appearance of object features and actions. This might allow us to draw inferences about the functional role of these cells during sensorimotor transformation.

3.5.3 Sensorimotor transformation and context dependency

The parietal cortex has long been known for its role in sensory-motor transformation (Mountcastle et al., 1975; Andersen, 1997; Scherberger and Andersen, 2003). Different subregions are specialized for particular types of actions, like the lateral intraparietal area for eye movements and the parietal reach region for arm reaching. Neurons in these areas are continuously active from stimulus presentation to action execution (Barash et al., 1991; Snyder et al., 1997). Furthermore, they represent not only the target object, but also context information, in order to select an appropriate action for that target (Gottlieb and Goldberg, 1999; Kalaska et al., 2003; Gail and Andersen, 2006; Scherberger and Andersen, 2007).

AIP fits well into this scheme. It is specialized for hand grasping, and its function can be well described within the framework of sensorimotor transformation (Taira et al., 1990; Sakata et al., 1995; Sakata et al., 1997; Murata et al., 2000). Using a delayed grasping task, we found a strong visual component of AIP activity, with 55% of the cells distinguishing a spatial property of the grasp target - its orientation - already in the cue epoch (Figure 3-2A). The activity of the majority of these cells extended to planning and execution (Table 3-1). Furthermore, 25% of the cells discriminated between power and precision grips already in the cue epoch, although the applicable grip type was not provided by the grasp target but by context information from the LEDs. This demonstrates that AIP represents not only the target object but also context information for action selection.

Our results suggest that upcoming hand movements are initially encoded as an object representation that is modulated by the action context, rather than a representation of a particular hand and finger configuration in purely motor terms. Such a context-dependent enhancement of motor-relevant object features has

previously been described as a crucial step in visuo-motor transformation: the remapping from a visual object description onto a representation that is more meaningful in motor terms (Allport, 1987; Rizzolatti et al., 1987; Gail and Andersen, 2006). This view is compatible with several aspects of our findings.

First of all, the neural response during cue was dominated by the spatial object feature. Orientation selective neurons outnumbered the grip type selective ones more than two-fold during cue. In addition, 71% of all grip type selective neurons were also selective for the object feature orientation during cue.

Secondly, in the cue separation task we found no increased activity for an abstract grip type instruction in the absence of an object to be grasped (TO-task), while neural activity in the OT-task was increased immediately after the object orientation cue for neurons preferring either grip type. AIP neurons therefore seem to represent visual object features together with the ambiguities of the grip type until they are resolved by further instructions.

Finally, neural activity during the cue epoch was consistent with a coding scheme that is possibly more suitable for a uniform representation of object features, whereas late onset cells are probably more motor related, as we discuss in the following section.

3.5.4 Possible coding schemes

It has been argued that activity in cortical areas related to sensorimotor transformation reflects the sensory stimuli and context cues during the instruction phase of the task, while during movement execution these areas represent the movement plan independent of the sensory stimuli. This becomes evident in decision experiments for eye and arm movements (Platt and Glimcher, 1999; Gold and Shadlen, 2000; Scherberger and Andersen, 2007) and in anti-saccade and anti-reaching tasks (Everling et al., 1999; Zhang and Barash, 2000; Gail and Andersen, 2006).

Our study supports this view. Neurons with a tuning onset during cue were stimulus-driven and represented the different object features and potential movement plans roughly in a uniformly-distributed fashion. In contrast, neurons with tuning onset during movement execution encoded the grasp type independently of the object orientation, and were more frequently tuned for precision grips and for extreme orientations. These neurons therefore seemed to use a different coding scheme than the visually responsive cells.

We consider late-onset neurons to be closely related to movement execution based on the following arguments: the over-representation of precision grips could be explained by the need of increased neural resources for controlling fine precision grips as opposed to power grips, as observed in other cortical areas (e.g., M1 and F5) (Muir and Lemon, 1983; Lemon et al., 2004; Umilta et al., 2007). Likewise, the over-representation of extreme object orientations could be explained by a motor-related encoding, namely a push-pull representation in pronation/supination coordinates. In contrast, visually responsive cells seem to use a coding which is closer to the visual input, as discussed above.

In summary, AIP neurons are modulated by contextual information about upcoming grasp movements when multiple grip types are possible. The encoding of a motor plan in AIP depends upon the presence of knowledge about a target object, suggesting that hand movements are initially encoded by a goal-dependent modulation of the object representation, while during movement execution neurons seem to represent the grip type as such, independent of the target object.

4 Modulation of the Local Field Potential in AIP

4.1 Introduction

The local field potential (LFP) is a summation signal that represents the net excitatory and inhibitory synaptic and dendritic potential in a 'listening sphere' around the tip of the electrode (Mitzdorf, 1987). Relatively little is known about the relationship between the LFP and local spiking activity and about the meaning of the LFP for local information processing. Nevertheless there has been a growing interest in the study of LFPs over the last years. Several reasons contribute to this trend:

First of all, the LFP has been described to be better correlated with the BOLD signal of fMRI research than single or multi unit spiking (Logothetis et al., 2001; Logothetis and Wandell, 2004). FMRI is to date the dominating non-invasive technique to acquire functional data from the human brain and therefore, a huge body of fMRI literature has accumulated over the last years. However, the interpretation of this data often suffers from the fact, that the neural basis of the BOLD signal is poorly understood and, as Logothetis and colleagues have shown, it can even be uncorrelated with spiking activity (Logothetis et al., 2001). The study of the LFP, even purely descriptive ones, seems therefore very important for the interpretation of fMRI data, for instance when one tries to identify human homologues of known simian cortical areas.

Second, the LFP is easy to record and more stable over long time periods than the spiking activity of single units. Therefore, the LFP has been suggested as an input signal in future brain-machine interface applications (Andersen et al., 2004). Indeed, several studies have reported the potential of the LFP for decoding of behavioral parameters like reach or saccade direction (Pesaran et al., 2002; Mehring et al., 2003;

Scherberger et al., 2005; Asher et al., 2007). However, the informational content of LFPs compared to spiking activity is unclear. While some of these studies reported that the LFP was as informative as spiking activity (Pesaran et al., 2002; Mehring et al., 2003), others found significant drawbacks of the LFP, such as highly non-uniform distributions of preferred directions (Scherberger et al., 2005; Asher et al., 2007). There remain still a lot of unanswered questions regarding the kind of movement parameters that can be retrieved from the LFP, and with how much temporal and spatial precision.

Third, as the LFP originates largely from dendritic and synaptic potentials, it is thought to be related to local input, while the spiking activity represents the output of a recorded cell. A better understanding of the relationship between the LFP and local spiking might therefore give new tools at hand to better study the local processing as opposed to only listening to the output of the cells.

Finally, because the LFP represents mainly rhythmic activity and because it is a summation signal with a larger listening sphere than spiking activity, some researchers have used the LFP and its synchronization across areas to draw conclusions about communication between areas during task performance (Fries et al., 2001; Pesaran et al., 2008). This latter point is not in the scope of the present chapter.

To date, only few studies exist that describe LFPs in parietal planning areas. Two of them (Pesaran et al., 2002; Scherberger et al., 2005) describe the behavior of the LFP during saccade and reach planning. To our knowledge, there is only one study that deals at least partly with LFPs recorded in AIP (Asher et al., 2007 1623). In this study, monkeys had to grasp different objects that were presented in different reach directions. The researchers reported that tuning for reach direction and target object was common.

In the present chapter we first perform a rather descriptive analysis of the coding properties of the local field potential during the delayed grasping task (for the description of the task, see Section 2.2). We found that LFPs in AIP were most strongly modulated by the behavioral epoch of the task. Furthermore, they were

frequently selective for the handle orientation and the grip type. While grip type selectivity increased in the course of the task, orientation selectivity was dominated by different frequencies in the different task epochs. The distributions of preferred conditions varied with the task epoch and were in some cases different for different frequency bands.

In the remainder of the chapter, we compared the coding properties of the LFP with the one of multi unit spiking. We found that the power of the gamma band LFP (30-100 Hz) was correlated with the spiking activity measured on the same electrode and that the preferred conditions in this band, including its variations over task epochs, could be explained by the behavior of the spiking activity in a larger listening sphere, if one takes into account the structural organization of single cells within AIP. Furthermore we found evidence that this latter finding can not simply be explained by possible contamination of the LFP with spike residuals.

4.2 Methods

The LFP data presented in this chapter was recorded simultaneously with the spiking data presented in the previous chapter. General methods like the design of the experimental setup and surgical procedures are therefore the same as described in Chapter 2. All LFP data reported here were recorded during the standard delayed grasping task, which was described in detail in Chapter 2. In the present section, I will focus on specific methods of data analysis of the LFP that have not been described in the previous chapters.

4.2.1 Data analysis

Raw signals were amplified (400x), digitized with 16 bit resolution at 30 kS/s using Cerebus Neural signal processor (Bionics), and stored to disc together with the behavioral data. In order to extract LFPs, raw data traces were then lowpass filtered in MatLab (4^{th} order Butterworth filter with a corner frequency of 200 Hz) and down-sampled to 1kS/s. The resulting data was bandpass filtered a second time, using a Fourier filter (passband: 4-100 Hz). The advantage of the Fourier filter is that the cut-off at the corner frequencies can be designed very steep without having to deal with problems of phase shifts near the cut-off. The disadvantage is that it gets impracticably slow for data recorded at high temporal resolution. Hence the two step filtering procedure with the application of (wider) Butterworth filter first, followed by downsampling and filtering with the narrower Fourier filter.

After filtering, an algorithm was applied to invalidate trials containing artifacts. The origin of such artifacts was not always clear. Some artifacts displayed as sharp peaks in the LFP time course. Sudden movements of an electrode or the entire electrode drive due to slight head movements of the monkey, as well as static electric discharge are the most likely reasons for these artifacts. A second type of artifacts consisted of fast oscillations of around 100 Hz with amplitudes that were several orders of magnitude larger than the amplitude of the 100 Hz component of the LFP. This type of artifact almost certainly originated in oscillations of the electrode within

the guide tube, resulting in so-called microphonic noise. To detect artifacts, the root mean square (RMS) of the data trace was calculated in windows of 50 ms length. This window was time-shifted along the trial in steps of 25 ms. This was done for all trials of a recording site and the median of all RMS values from all the trials of the site was determined. We then removed all trials that contained one or more RMS values that were at least 5 times bigger than this median RMS. Visual inspection of the invalidated trials as well as of accepted trials that came closest to invalidation confirmed, that this criterion was sufficiently reliable in artifact detection.

For spectral analysis we applied multi-taper spectral analysis, which is described in detail elsewhere (Percival and Walden, 1993). For the tapering of the data, we used the discrete prolate sheroidal (Slepian) sequencies, which represent an optimal family of orthogonal tapers. The advantage of the multi-taper method compared to 'pure' Fourier transform is a reduction of variance. The cost for this benefit is a frequency leakage, i.e. a reduced resolution of neighboring frequencies. This leakage is described by a bandpass parameter W. The number of tapers that can be applied is then limited by 2TW-1, where T is the time length (in seconds) of the data segment being analyzed. For the production of spectrograms (see below), we chose W = 5. For the analysis of spectral power in several predefined frequency bands (see below), we reduced the frequency leakage to W = 3.

For the production of spectrograms we applied the multi-taper analysis to data segments taken from a window which was time-shifted along the trial. The window width was 300 ms and consecutive windows were shifted by 100 ms, therefore overlapping by 67%. As for the production of PSTHs in the previous chapter, trials were double aligned: first to the cue offset and then to the moment of handrest release. Realignment occurred 0.6 seconds after the cue offset.

To quantitatively assess if an LFP recording at a given site was significantly tuned (either task modulation or tuning for grip type/orientation), we calculated for each trial the spectral power averaged over entire task epochs (fixation, cue, planning, movement). Furthermore, we defined frequency bands of 5 Hz width each (5-10 Hz, 10-15 Hz, …, 90-95 Hz) and averaged the spectral power over the

frequencies falling into a given band. This way, the spectral power was calculated for each recorded trial, separately for each task epoch and for each of 18 frequency bands. We then applied a one way ANOVA (with factor 'task epoch' and p-level 0.05) to the spectral power in a given frequency band, in order to assess if the spectral power in this band was modulated by the task epoch.

Similarly, tuning for grip type and handle orientation was assessed using a 2-way ANOVA (p-level 0.05) with these parameters. 2-way ANOVAs were calculated separately for the task epochs cue, planning and movement and, again, for each frequency band.

For frequency bands that showed a significant grip type effect, the preferred grip type was defined as the type with the higher spectral power in this band, independent of the handle orientation. Likewise, the preferred orientation was defined as the orientation with the highest spectral power in a certain frequency band.

In order to compare the LFP with spiking activity recorded on the same electrode, we used multi-unit (MU) spiking activity. To extract the MU activity, we first bandpass filtered the raw data traces in the spike band (500-8000 Hz). We then calculated the standard deviation of the distribution of all data points and defined a threshold at -4.5 times this standard deviation. Whenever the data trace crossed this threshold (in the direction towards negative deflection), the time of the threshold crossing was taken to be the time of a spike.

4.2.2 Nomenclature

Apart from the predefined frequency bands of 5 Hz width, we will – for convenience – also use the terms *slow frequency*, as well as *beta frequency* and *gamma frequency band*. The latter names have their roots in the EEG literature and usually refer to the following frequency bands: beta: 13-30 Hz, gamma: > 30 Hz. In human EEG, the frequencies below 13 Hz are usually subdivided into the alpha band (8-12 Hz), the theta band (4-8 Hz), and the delta band (<4 Hz). Here we subsume these bands together, calling them the slow frequencies. Within the gamma band we

refer to the range 30-60 Hz as the *low gamma range* and the range 60-100 Hz as the *high gamma range*.

4.3 Results

We recorded 244 LFP channels in AIP of monkey J and 117 in monkey L. The results for the two animals were largely equivalent as far as the general task modulation of the LFP and its tuning for grip type are concerned. There are, however, discrepancies concerning the orientation tuning, where the results of monkey L do not confirm the findings in monkey J. There are some issues with the LFP recordings made in monkey L, which are potential sources of these differences: Firstly, in many if not most of the recording sessions made in monkey L, there were considerable problems with microphonic noise, probably due to electrode vibrations during task performance. Although we invalidated trials with obvious artifacts, there is of course no method that can reliably tell what effect this noise had on the LFP frequencies we analyze here. The second issue concerns the monkeys' behavior: while monkey J sat always quietly during the planning period, monkey L was more impatient and often shook his body or moved his legs in expectance of the Go-signal. As will be discussed later, such motor behavior is likely to influence the LFP signal, especially the beta-band, were we found the strongest orientation tuning effects in monkey J. For these reasons, we consider the data of monkey J clearly more reliable. I will therefore proceed in this chapter by presenting the results of monkey J. I will pint out the implications of the differences between the monkeys in the discussion part of the chapter.

All results presented in this chapter have been obtained from the standard delayed grasping task. Local field potentials were recorded simultaneously with the spiking data that were analyzed in the previous chapter. Consequently, the behavioral parameters, as for example the movement time or error rate are the same as reported in the result section of Chapter 3.

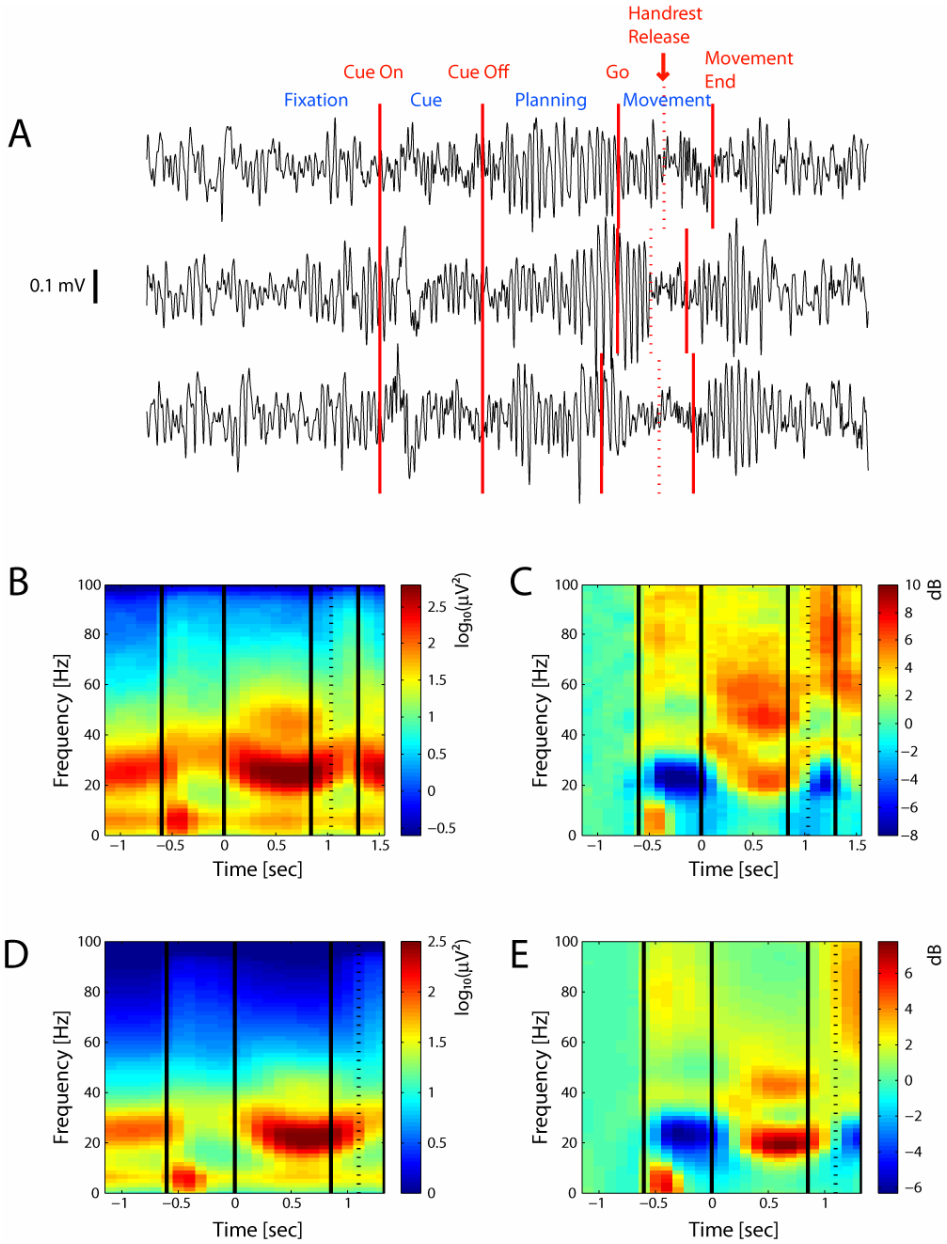

Figure 4-1: Raw LFP traces and spectrograms

A: Raw LFP traces recorded during three single trials. The red lines indicate the events during the trial as indicated above. The blue labels indicate the trial epochs. **B:** Spectrogram of an individual recording site, averaged over all recorded trials. The color code shows the logarithm of the spectral energy of a given frequency (y-axis) at a given time in the trial (x-axis). Trials were double aligned as in Figure 3-1. The black solid and dotted lines indicate the same behavioral and instruction events as the red ones in Figure 4-1A. **C:** Same recording channel as in Figure 4-1B, but each frequency band was normalized to the mean activity of that frequency during fixation. Power changes compared to baseline are expressed in dB. **D and E:** Spectrograms as in B and C, respectively, but averaged over all recorded sites (N = 244).

4.3.1 Task modulation

Figure 4-1A shows raw LFP traces recorded in area AIP during three single trials of the delayed grasping task. Even in such raw traces one can see a modulation of the oscillatory activity depending on the task epoch: During the planning period, oscillations with increased amplitude compared to the other epochs can be seen in each of the three trials. At the time of the handrest release, these large amplitude oscillations disappear and smaller, faster oscillations dominate during the movement epoch until the target has been acquired. However, for quantitative analysis, raw traces are poorly suited because they are composed of a mixture of different frequencies. We therefore applied multi-taper spectral analysis in order to calculate the spectral power at different frequencies (see methods). By performing this frequency decomposition repeatedly for consecutive segments of the trial data, one obtains a spectrogram that allows assessing the modulation over time at different frequencies. A spectrogram from one recording site, averaged over all trials recorded at this site, is shown in Figure 4-1B. Clearly, the strongest spectral power is present in a frequency band between approximately 20 and 30 Hz. These frequencies belong to the beta range (for nomenclature, see methods section). Strong beta activity is present during the fixation period, is then suppressed during the cue period, and reaches its peak during the planning period before it is again suppressed during movement execution. However, task modulated activity is also present in other frequency bands, as can be seen best by the increased spectral power around 40-50 Hz (lower gamma range) during the planning period. Because different frequencies show very different overall levels of spectral power, it is easier to see the task modulation of the LFP when the activity of each frequency is normalized by the activity of that frequency during the fixation period. This is shown in Figure 4-1C, that shows the spectrogram from the same recording site as Figure 4-1B, however with this normalization. Clearly, all frequencies from 30 to 100 Hz (Gamma band) show increased spectral power during the cue, planning and movement epoch, with the lower Gamma band peaking in the planning, and the higher Gamma band in the movement epoch.

This recording site is representative for all recording sites in AIP, as can be seen in Figure 4-1D and E. These two plots again show the raw spectrogram and its normalized form, respectively, but this time averaged over the whole population of 244 LFP sites recorded in AIP.

To quantitatively assess the statistical significance of the observed task modulation, we defined 18 different frequency bands of 5 Hz width each (see methods). For each trial, the spectral power in each of these frequency bands was then calculated separately for the fixation, cue, planning and movement (go signal to target acquired) epochs. For each frequency band we then applied a 1-way ANOVA on these values, to assess, if the spectral power in that band is modulated by the task epoch. This was repeated for each recording site. We found that in all frequency bands, between 92% and 100% of all recorded LFP channels were significantly modulated by the grasping task ($p<0.05$, 1-way ANOVA).

4.3.2 Modulation for grip type and orientation

In the previous section we showed that the large majority of LFP channels show strong modulation in all frequency bands for the different epochs of the task. Next we asked whether the LFP is also tuned for the grip condition, i.e. for the grip type and/or the orientation. We used the same frequency bands as before and calculated the spectral power in each frequency band for every trial and separately for the epochs cue, planning and movement. We then performed 2-way ANOVAs with factors grip type and orientation on the LFP power separately for the different frequency bands and the three epochs. Figure 4-2 shows the results of this analysis. Grip type tuning is relatively weak during the cue epoch, increases to about 15% in most frequency bands during planning and peaks during movement execution, with the higher frequency bands (mainly the gamma range) being most often tuned.

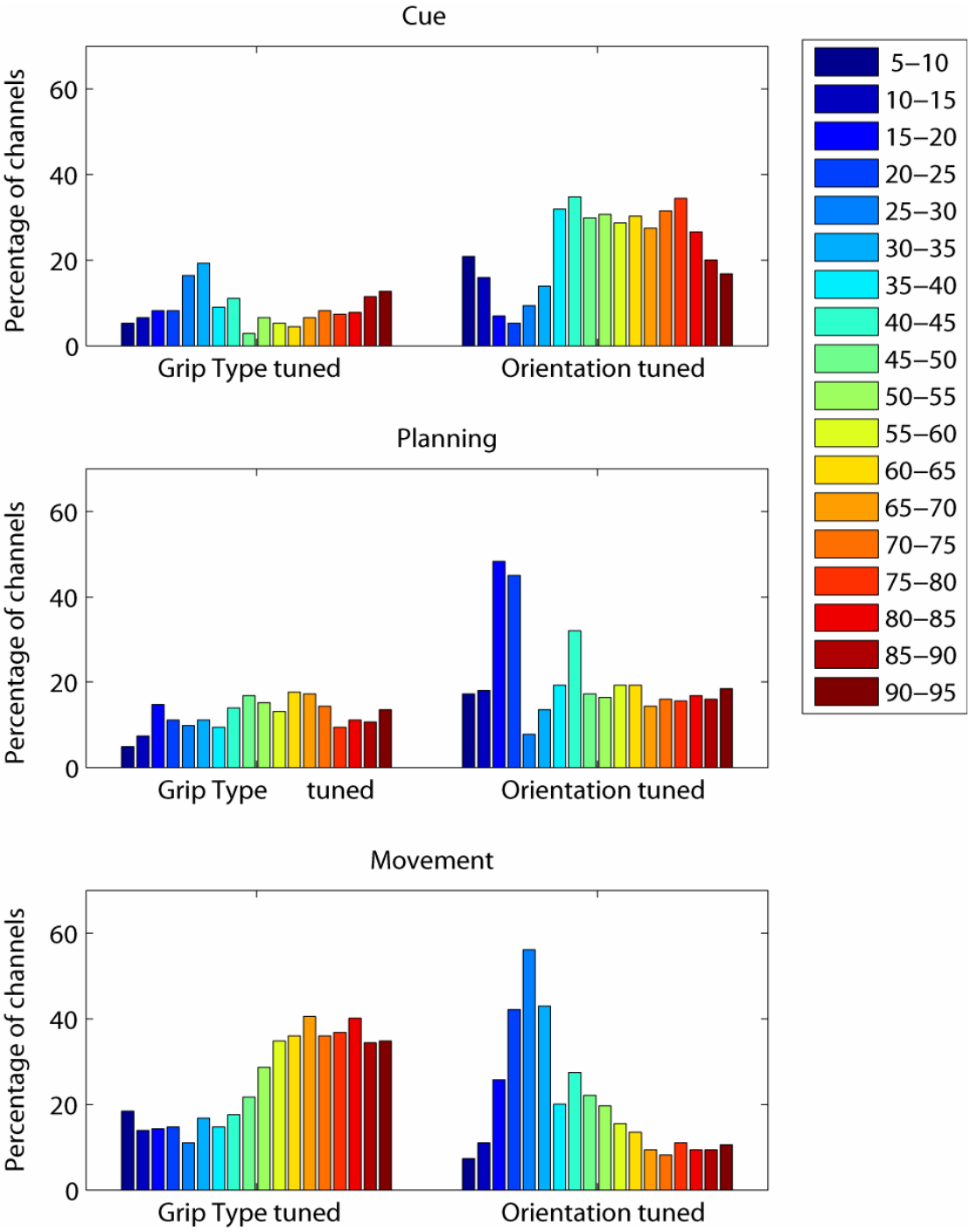

Figure 4-2: Modulation for grip type and orientation in LFP

Percentage of channels that display significant modulation (2-way ANOVA, $p<0.05$) for grip type (left) and orientation (right), separately for the three epochs cue, planning and movement. Grip type and orientation modulation were assessed separately for different frequency bands of 5 Hz width each. These different bands are shown in different colors and the legend shows the corresponding frequency bands in Hz.

This increase in grip type tuning of the gamma LFP in the later epochs is similar to the temporal progression that we saw already for the single units (Figure 3-2A). Overall the fraction of tuned channels in the individual frequency bands stays somewhat lower than the fraction of grip type tuned single units. However, this depends to some degree on the definition of the frequency bands: When stronger averaging is applied, calculating grip type tuning only for the four bands 'slow', 'beta', 'low and high gamma' (see methods), then the fraction of tuned LFP sites is slightly increased and the percentage of sites with tuned gamma LFP becomes very similar to the one of tuned single units.

The picture looks different for orientation tuning: there is strong orientation tuning already during the cue, basically in the whole gamma range (30-100 Hz). In the planning and movement period, orientation tuning in the gamma range is clearly reduced compared to the cue. However, in these later epochs, orientation tuning has not vanished from the LFP, but its peak has shifted to slower frequencies: During planning and movement, strong orientation tuning is present mainly in the beta range (approximately 15-30 Hz). Note that in the spectrogram we saw peak activity in the beta band during the planning period (Figure 4-1D and E). This is the same frequency range as the one with the strongest orientation tuning during the planning period.

Unlike for grip type tuning, the progression of orientation tuning in gamma LFP does not match the progression of tuned single units. While the number of orientation tuned single units was basically constant over the epochs (Figure 3-2A), the percentage of gamma tuned LFP channels decreased strongly in planning and movement. However, in our analysis of single units in AIP we found that the neural response during the cue was mainly driven by the presence of an object in the preferred orientation of the neuron and that grip type tuning at this stage of the trial had only a modulatory effect on the firing rate (Section 3.4.2). In contrast, during movement execution, the main driving parameter for single units was the grip type, and orientation tuning was only secondary and optionally. Therefore, the occurrence of strongly tuned gamma LFP coincides with the main driving input as we identified

it in Section 3.4.2: Object orientation during cue and grip type during movement execution. After the cue, when orientation tuned input is switched off, the orientation tuning of the LFP shifts rapidly to the beta frequency band, possibly indicating that different local processes are responsible for the continued orientation tuning than during the visual input phase.

For each tuned channel/band pair one can define a preferred grip type or orientation, respectively, and ask what the distribution of the preferred conditions is in the population of all recordings. Furthermore, if several frequency bands of one recording site show tuning for one of the parameters (grip type or orientation), one can ask whether their preferred conditions match or not. Similarly, one can compare the LFP tuning to the spike tuning on the same electrode for sites, where both signals have been recorded. These questions we will look at in the following sections.

4.3.3 Distribution of preferred conditions

For each frequency band with significant grip type tuning we defined the preferred grip as the one with the higher spectral power averaged over all trials with the same grip type, thereby pooling the five different orientations together. Similarly, the preferred orientation of frequencies with significant orientation tuning was calculated by pooling over trials of the two different grip types. These definitions are analogous to the ones used to determine the preferred conditions of the spiking activity (Chapter 3).

Figure 4-3 shows, for the different frequencies and task epochs, the fraction of sites that displayed a ‘precision preference’ or ‘power preference’ as percentage of all recorded channels. During the cue, there was a tendency for the beta band to prefer precision grip trials. In the gamma frequencies, however, the number of channels preferring precision grips and power grips were quite similar. In the planning epoch, there was a slight overrepresentation of sites preferring the precision grip throughout all frequencies, with an overall ratio of precision grip sites vs. power grip sites of 3:2. This ratio was very different during movement execution, when

basically all tuned recording sites and frequencies showed stronger LFP activity for the precision grip (ratio of 19:1).

The corresponding results for the preferred orientation are shown in Figure 4-4. During the cue period, the distribution of the preferred orientations was highly non-uniform with a majority of channels preferring the orientation at -25 degrees, i.e. slightly tilted to the left. Channels with a preference for the right tilted object were virtually absent. As mentioned earlier, this tuning was mainly confined to the gamma range. In the planning epoch, the dominating tuning was in the beta range and showed preference mainly for the middle three orientations, whereas the preference distribution in the gamma range shifted more to the right-tilted conditions, compared to the cue epoch. Finally, during the movement epoch, the preference distribution was again very much centered on one orientation as it was the case during the cue epoch, however, the dominating orientation during the movement execution was the one at +25 degrees, i.e. slightly tilted to the right. Highly non-uniform distributions of preferred directions in parietal LFPs have been described before in different tasks which included different directions of reach (Scherberger et al., 2005; Asher et al., 2007). Asher et al. also reported the finding that the distributions of preferred directions can be very different in different task epochs, which seems similar to the different preferred orientations that we find in different task epochs.

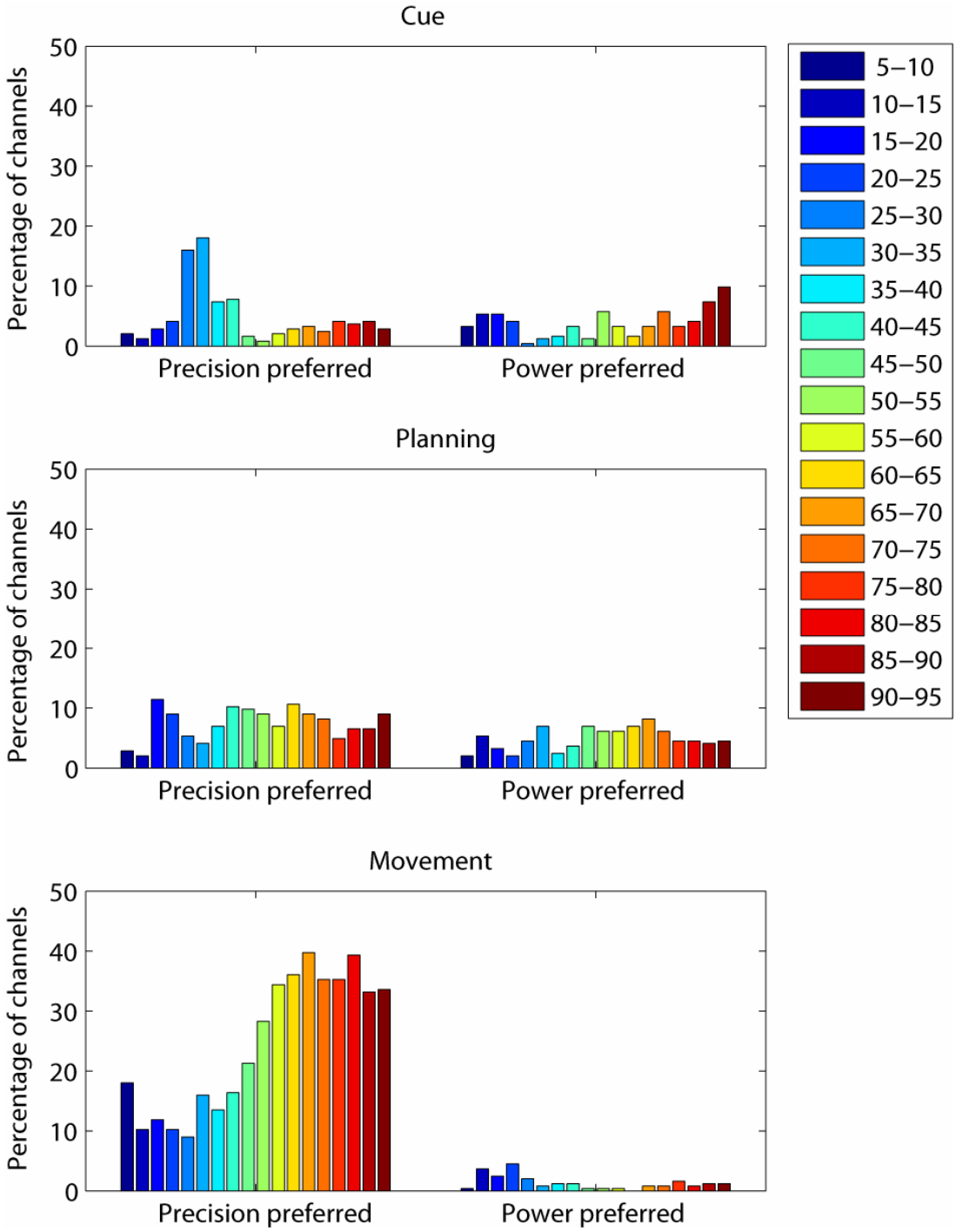

Figure 4-3: Preferred grip type of the different LFP frequencies

Percentage of all channels that show significantly stronger LFP power for precision grips (left) of power grip (right), shown separately for different task epochs (panels) and for different frequency bands (colors). The sum of the two columns in each panel is equal to the number of all channels that show grip type tuning in that epoch (as in Figure 4-2).

Later in this chapter we will look at the question, if and how the pattern of distributions of preferred conditions found in the LFP relates to the spiking activity on the same electrodes. Before that, however, we will compare the different frequency bands with each other and ask, if the tuning preferences of different frequencies at a given recording site are correlated with each other or if different frequencies can show opposite tuning. For this, we computed the correlation of tuning curves of different frequencies. Each tuning curve is a vector with 10 values, containing the average spectral power in a given frequency band for the 10 conditions, with all trials of a given condition being averaged together. The correlation between tuning curves was calculated for all possible combinations of the 18 frequency bands. Figure 4-5 shows the correlation coefficients between different bands, averaged over all recording sites. Clearly, there was a correlation between the different frequency bands within the gamma range during all three epochs. During cue, this extended over all gamma frequencies (30-100 Hz), while during the movement and especially during the planning, the lower gamma range was somewhat less coupled with the higher one while the correlations of the frequencies of about 50-100 Hz with each other stayed as high as before. During planning and movement, there was also correlation between the lower frequencies; in particular there was elevated correlation between the band at 20-25 Hz and the band at 40 Hz. These bands corresponded to two bands of peak planning activity as can be seen in Figure 4-1D. Correlation was basically absent between the low frequencies (including the beta band) and the high gamma band. This is in accordance with the finding of Figure 4-4 that the distribution of preferred orientations can be quite different in the beta range compared to the gamma range, as it was found mainly during the planning period.

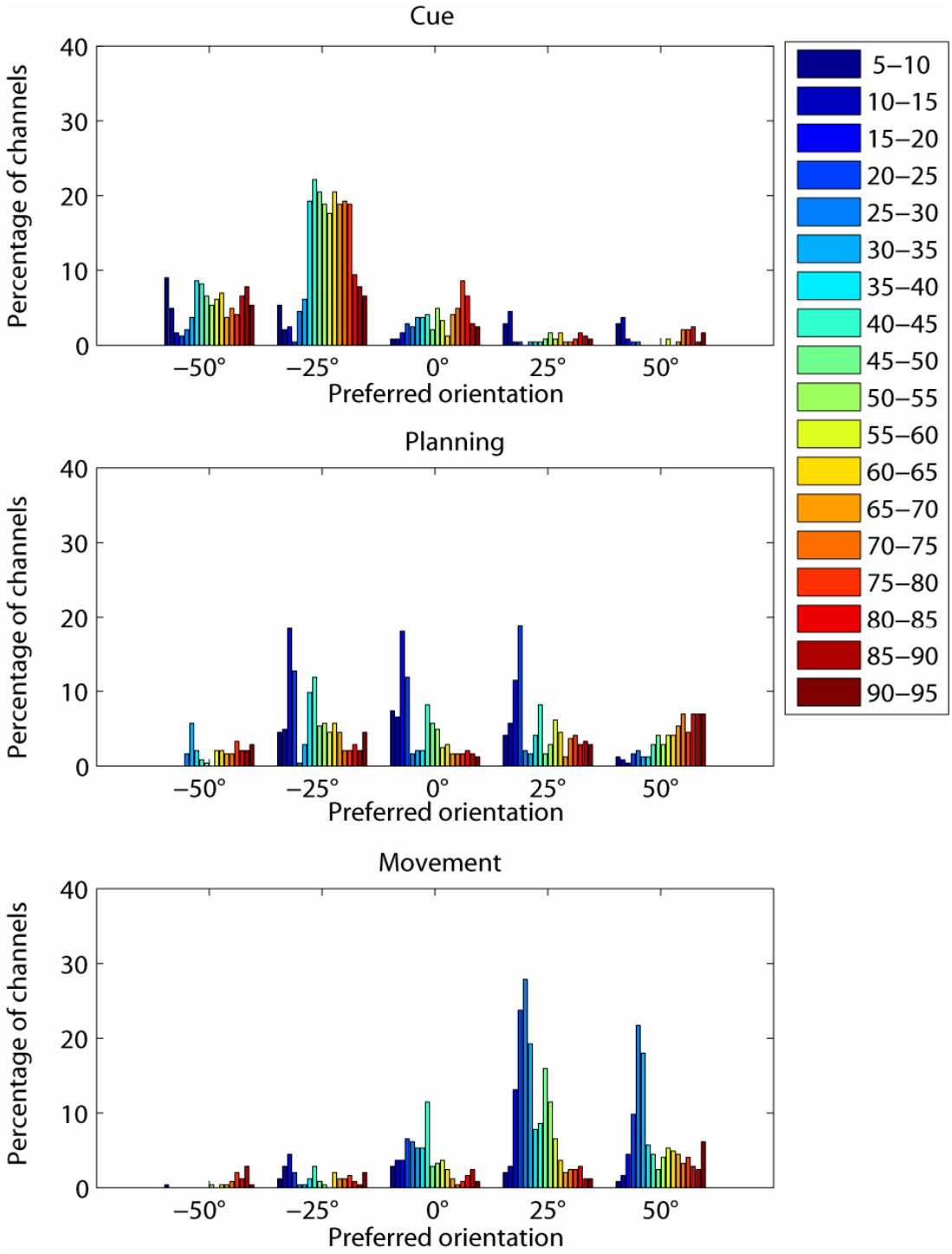

Figure 4-4: Preferred orientation of the different LFP frequencies

Percentage of all channels that prefer each of the 5 different orientations, shown separately for the different task epochs (panels) and for different frequency bands (colors). The sum of the 5 columns in a panel equals to the percentage of orientation tuned channels in that epoch (as in Figure 4-2).

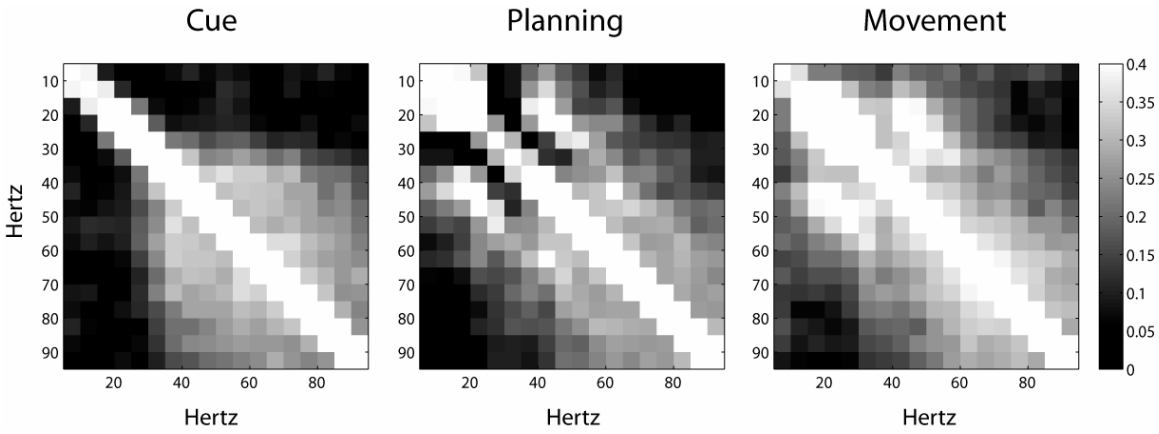

Figure 4-5: Signal correlation between different frequency bands

The shading shows the correlation coefficient, averaged over all recording sites, between the tuning curves of different frequency bands during the task epochs cue, planning and movement. All frequency bands were used for this analysis, not only those with significant tuning.

A different way of looking at the correlation of tuning curves in different frequency bands is to directly compare the preferred grip type and orientation of different frequencies in those recordings where at least two bands show significant tuning. We found that if one band within the gamma frequency range showed significant grip type or orientation tuning, then there was an increased likelihood that other gamma frequencies were tuned for the same parameter. In contrast, significant tuning in the beta frequencies did not coincide with tuning in the higher gamma range more often than expected from their individual likelihood to be tuned. Furthermore, two tuned gamma range frequencies on one electrode tended to prefer the same condition. During planning period for example, if two gamma frequency bands were tuned, they preferred the same grip type in more than 98% of all cases. In contrast, when beta and gamma tuning co-occurred on the same electrode, they shared the same grip type preference in only 76% (again during planning). Similarly for orientation: within the gamma range, in more than 92% of simultaneous tuning, the difference in the preferred orientation was at most one step (25 deg), whereas this was true for only 55% of all pairs if beta range tuning was compared to the high gamma range. This confirms that the gamma range frequencies all show a similar

modulation for the grasp condition, while the beta range is rather independent of the gamma range.

4.3.4 Correlation between LFP and spiking activity

We also calculated the correlation of the different frequency bands' tuning curves with the tuning curve obtained from the multi-unit spiking activity observed on the same electrode. Multi-unit activity was chosen because the LFP by itself is a summation potential and therefore it seems to be reasonable to compare it to the pooled spiking activity on the same electrode, rather than to single units. Figure 4-6A shows the result of this analysis. The low frequencies, up to about 30 Hz showed basically no correlation with the tuning curve of the spiking activity. The gamma band, however, showed a steady increase of the correlation towards higher frequencies. The correlation was approximately the same during all three task epochs cue, planning and movement. During the fixation period it was lower, but still significantly higher than zero, even though the monkey had no knowledge about the upcoming movement at this time. This is an indication that the gamma band LFP and spiking activity are probably not only correlated as far as their tuning curves are concerned, but that also their 'noise' is correlated. (With noise we mean here variability in the firing rate or LFP power that is not explained by the different grasping conditions.) To calculate the strength of this noise-correlation, we computed the trial-to-trial correlation instead of the correlation between tuning curves. From each trial we subtracted the mean activity (spiking or LFP power respectively) of the grasping condition it belongs to, such that the remaining variations were entirely noise, i.e. within condition variations. Figure 4-6B shows the noise correlation between LFP and spikes during the different task epochs. The noise correlation is significantly larger than zero for the gamma frequencies and it is slightly higher during the fixation period than during the other epochs.

Such correlations could either be due to a real correlation of synaptic and dendritic gamma oscillations with the occurrence of a spike, or they might be an effect of spike waveform residuals being present in the LFP, despite the low pass

filtering, as it was also discussed by Asher et al. (Asher et al., 2007). With our experiment the respective contribution of these two factors cannot be disentangled. Nevertheless, there are indications that show that the gamma band activity is not just a summation of such spike residuals: First, if this was the case, gamma band LFP during movement should show more orientation tuning because spiking activity during movement is strongly orientation tuned. Second, the noise-correlation is strongest during the fixation period and weakest during the movement execution, although the spike rate is highest during the movement and therefore, the influence of spike residuals onto the LFP gamma band should be highest. Therefore, gamma oscillations that are not directly spike related must contribute significantly to the gamma band LFP. Finally, the distributions of preferred grip type and preferred orientation in the population are very different for the gamma band LFP than for the single units (Chapter 3), which also shows that the gamma LFP represents something different than just a summation of local spiking.

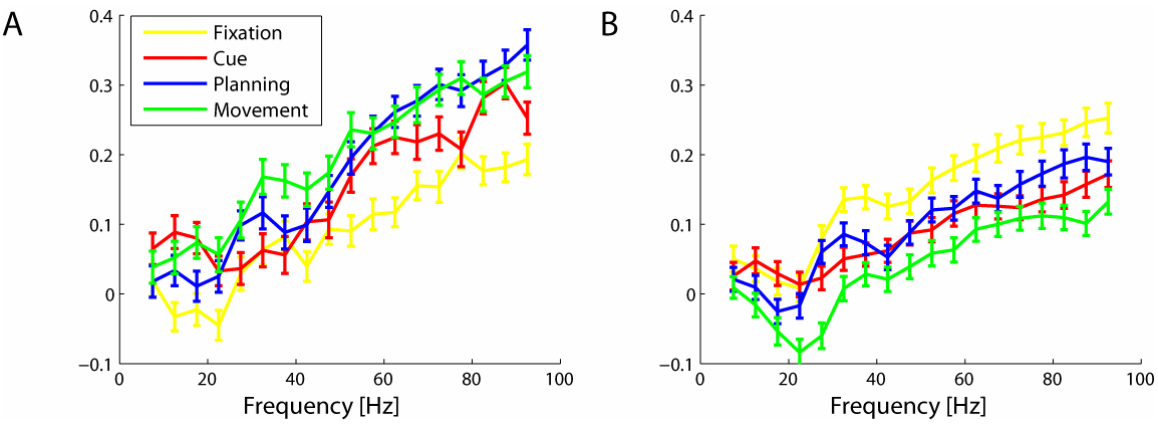

Figure 4-6: Correlation between tuning of LFP and multi-unit spiking

A: Correlation between the tuning curves of the different LFP frequencies (x-axis) with the tuning curve of the multi-unit spiking on the same electrode; average of 244 recordings. Errorbars indicate the standard error. **B:** Trial-to-trial correlation ('noise correlation') of LFP power and multi-unit spiking activity; average of 244 recording sites.

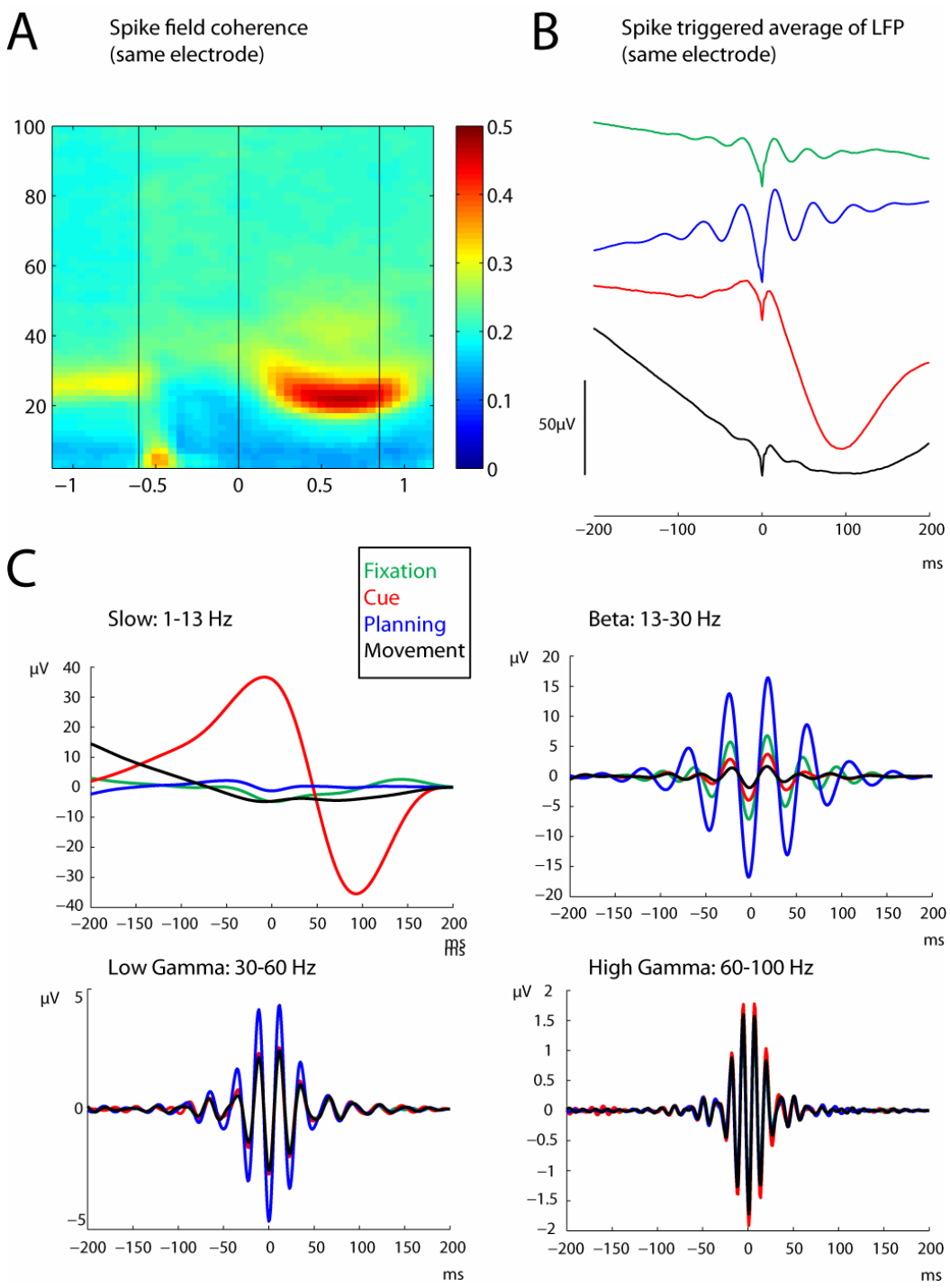

Figure 4-7: Coherence between spikes and LFP (same electrode)

A: Coherence between the MU spiking and the LFP recorded on the same electrode. All plots A-C are population results from 268 recordings. **B:** Spike triggered average (STA) of the LFP. STAs were computed separately for the different task epochs. For color legend, see C. **C:** STAs are shown separately for the different frequency bands of the LFP. The colors within a panel represent again the task epochs.

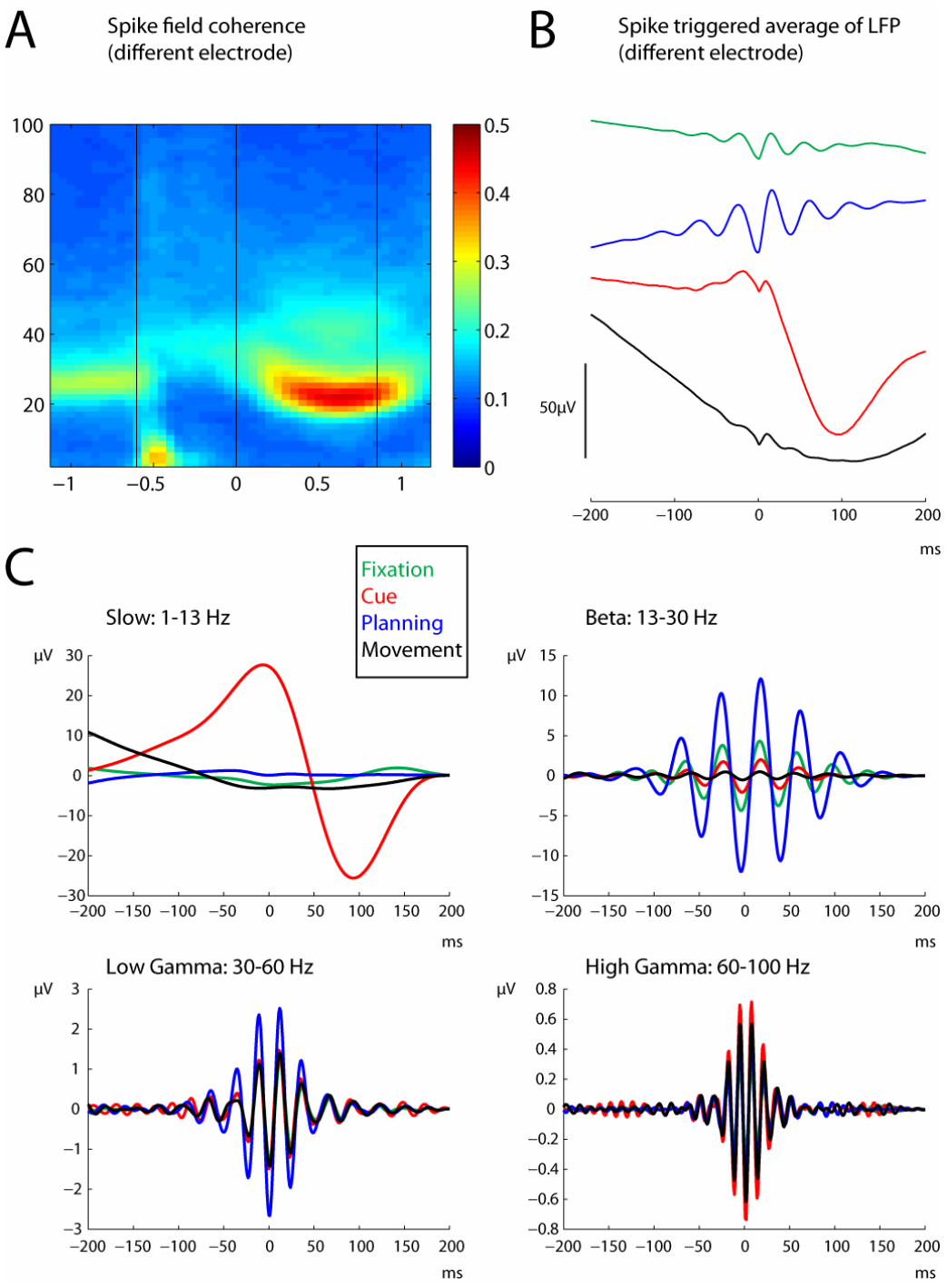

Figure 4-8: Coherence between spikes and LFP (different electrodes)

Same plots as in Figure 4-7 except that for this plot, spike-field coherence as well as Spike triggered averages were computed with MU spikes and LFP recorded simultaneously on different electrodes within AIP. All plots are population results with 478 recorded electrode pairs.

4.3.5 Temporal relationship between spikes and LFP

To investigate, if spikes have a particular temporal relationship with the phase of the LFP oscillations recorded on the same electrode, we computed the coherence between MU-spikes and LFP – the spike-field coherence – in a moving time window. Figure 4-7A shows the spike-field coherence over time, averaged over 268 recordings. The most obvious feature is a very high coherence in the beta band during the planning period, which fits well with the high LFP power in this frequency band during the planning period (Figure 4-1D). This spike-field coherence in the beta band is obviously strongly task modulated, as it is much weaker during the other epochs. Coherence is also elevated in the entire gamma band. This high frequency coherence, however, is almost constant over time and therefore only little task modulated. Furthermore, there is transient coherence in the beginning of the cue in slow frequencies. This latter feature is, however, less interesting. It is due to the fact that a visual evoked potential and peak spiking activity are both time-locked to the cue onset. This feature is the only one that persists if spike-field coherence is computed between shuffled trials (not shown). We will not discuss it any further.

Figure 4-7B shows the spike triggered average (STA) of the LFP. During fixation and planning, it is dominated by the beta frequencies, during cue and movement by slower frequencies that are due to the visual (as mentioned) and motor evoked potentials. Figure 4-7C shows the STA separately for the different frequency bands. Clearly, the beta and gamma frequencies show features which demonstrate that spikes happen preferentially at the troughs of the LFP, i.e. with a phase shift of zero (per definitionem). In the beta and low gamma frequencies, one can also see differences between the epochs, with higher amplitude STAs during the planning, while the high gamma STA was basically the same for all epochs.

The fact that the high gamma coherence was consistent over time raises again the question, if it is due only to spike leakage into the LFP. Indeed, Figure 4-7B shows a clear, sharp feature in all epochs at zero lag, which is most likely the signature of this spike leakage. In order to exclude this possibility, we performed the same analysis as

in Figure 4-7 again, but with spikes and LFP taken from two separate, but simultaneously recorded electrodes. The minimal possible distance between these two electrodes is 300 micrometers and, which ensures that the same spikes will not contaminate both electrodes. The median distance was 530 micrometers. Figure 4-8 shows the results. The spike field coherence of the slow and beta frequency is basically unchanged. The coherence of the (high) gamma range is clearly smaller than in Figure 4-7. However, it is consistently at about 0.12, which is still significantly higher than the 0.05 as it is seen for shuffled trials ($p<0.01$). The sharp features that represented the spike remainder in the STA of Figure 4-7 are no longer present. The STAs for the different frequency bands are qualitatively very similar to the ones when spike and LFP come from the same electrode, only the amplitude, mainly of the higher frequency STAs, are reduced (note the different scales compared to Figure 4-7C).

Altogether, Figure 4-8 proves that the findings of Figure 4-7 cannot be explained only by spike leakage, but that the spike field coherence in all frequency bands is a real feature in our recordings.

4.3.6 Relationship between high gamma LFP and Multi-unit spiking

Given the correlation between spikes and gamma frequency LFP, we asked if and how the gamma LFP could be explained by the spiking activity despite their seemingly very different distributions of preferred conditions. For this we compared the preferred condition of the multi-unit spiking of an electrode with the preferred condition of the high gamma activity of the same electrode. (Spectral power in the whole high gamma range between 60-100 Hz was averaged for this analysis.)

In Chapter 3 (

Figure 3-6) we had seen that grip type tuned single units prefer equally often precision and power grips during cue and that this ratio changes little during planning, but shifts in favor of precision grips (61% precision grip preferring single

units) during movement. Here we used multi-units, not single units, but this temporal development is similar for multi-unit activity (50% for either grip type in cue, 56% precision preferring sites in planning and 73% in movement). These distributions we compared to the ones of the high gamma band LFP (Figure 4-3) and found similar distributions during cue and planning. Indeed, in recordings were both the multi-unit activity and the high gamma LFP were grip type tuned, the preferred type of these two signals largely coincided (cue: 14/15, 93%, planning: 32/34, 94%). However, during movement execution, the distributions of preferred type were different. Although there was an overrepresentation of precision preference in the multi unit spiking activity (73%), this did not match the gamma LFP, where basically all recorded sites preferred precision grip. However, this latter finding might be reconciled with the spiking activity, if one takes into account that the listening sphere for the LFP is much larger than the one for spiking activity. If one assumes that gamma LFP is correlated with the overall spiking activity in its entire listening sphere, than it is possible that within this radius, precision grip cells will always dominate, due to the fact that they are more numerous than power grip preferring cells. In order for this hypothesis to be a possible explanation, precision and power grip cells that are active during movement execution should be rather intermingled, a fact that we can test based on our single unit recordings. In contrast, the grip type tuned cells that are active during cue and planning should be less intermingled, otherwise it would be unlikely that the local spiking on an electrode and the averaged activity in the LFP listening sphere around that electrode would always coincide, as we found it to be the case during cue and planning.

We looked in our single unit data for pairs of neurons that were isolated on the same electrode and that both showed grip type selectivity. We found 15 recordings, were two neurons recorded on the same electrode were both grip type tuned during the cue (i.e. early grip type tuned cells). In all these 15 cases, the two neurons preferred the same grip type. On the other hand, we found 60 recordings were two cells with grip type tuning during movement were present on one recording electrode. Only in 42/60 (70%) of these cases did the preferred type of the two single units match. In other words, this single unit data show that cells that prefer precision

grip during movement execution are intermingled with cells preferring power grips, while the early grip type tuned cells seem to show some order, such that nearby cells have the same preference. This finding allows explaining the grip type preference of the high gamma band LFP with the spiking activity in a wider listening sphere.

Could this explanation be true also for orientation tuning? The distribution of preferred orientations in the LFP was shown in Figure 4-4, where we saw that during cue, the gamma LFP activity of most sites preferred orientation -25 deg, while during movement, most of them preferred +25 deg. In the planning, it was more heterogeneous with a tendency to the rightward tilted object. This distribution is very different from the one of preferred orientations of single units (Chapter 3, Figure 3-9). The distribution of preferred orientations of the multi-unit activity was similar to the one of single units, but the extreme orientations were somewhat stronger overrepresented (Figure 4-9B, 50% in cue, 68% in planning and 72% in movement, 40% would be expected in case of equal representation). This was therefore very different from the preferred orientations of the gamma LFP. However, the fact that more neurons preferred the right tilted orientation than for instance the vertical one, does not necessarily mean that the overall spiking activity in +50 deg trials was higher than in 0 deg trials. If one pools together the activity of several neurons which prefer either the left most or right most tilted orientation, there averaged activity might also be strongest for any orientation in between. Figure 4-9A shows the spiking activity averaged over all 244 sites of recorded multi-units, plotted individually for the trials of different orientations. Indeed, the firing rate in the different orientations is not simply reflecting the number of neurons that prefer that orientation. The plot below, Figure 4-9C, shows the high gamma LFP power in the course of the trial, also separately for the different orientations. The temporal development of the high gamma activity was strikingly similar to the firing rate in Figure 4-9A, showing that the two parameters did not only show a correlation of their tuning (Figure 4-6), but also a temporal correlation. Secondly, despite the fact that the preferred orientations of the gamma LFP were strongly non-uniform (Figure 4-4), Figure 4-9B shows that the overall spectral power was only moderately different for the different orientations. And thirdly and importantly, the pattern of

modulation for the different orientations was very similar in the spiking activity and the high gamma LFP: Orientation -25 deg, which was preferred by most LFP channels in the cue, was also the one with most spiking activity overall, at least in the beginning of the cue. During movement, however, the spiking activity was highest for right tilted orientations, corresponding again to the preferred orientation of LFP channels.

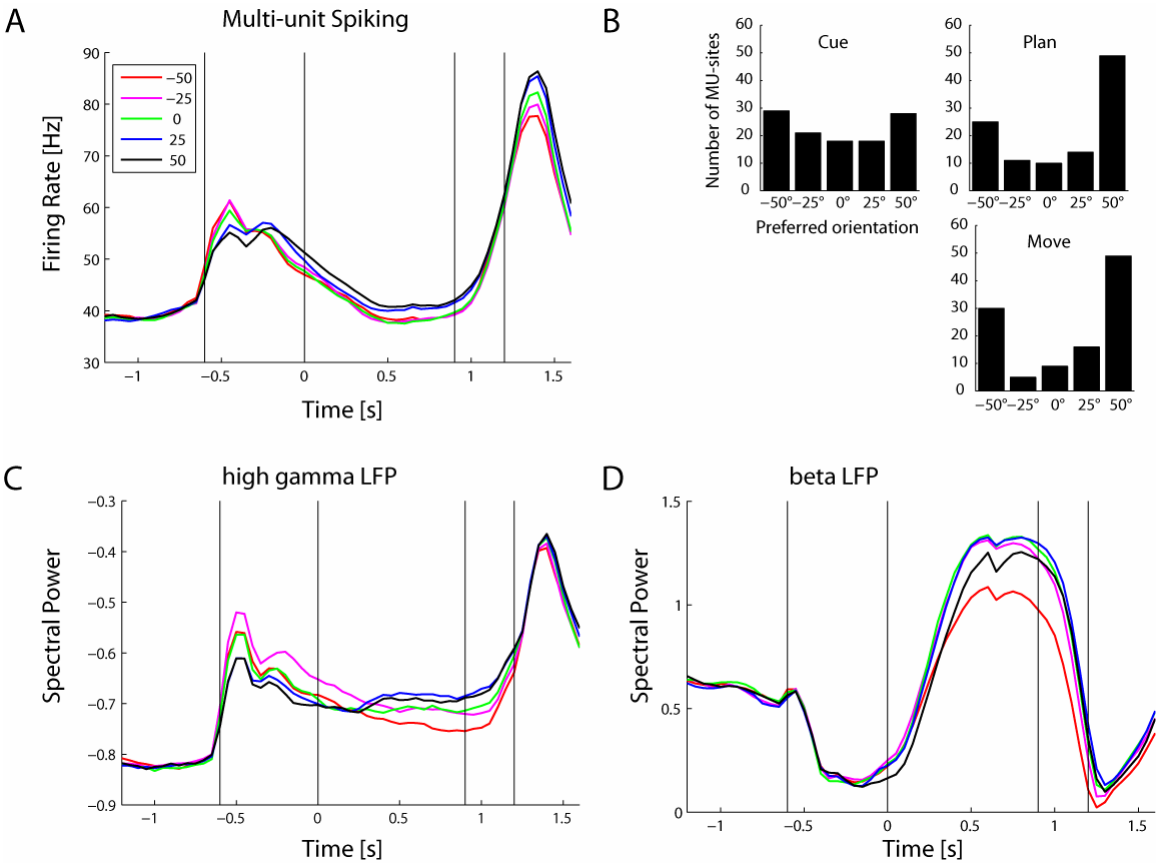

Figure 4-9: Comparison of orientation tuning in MU-spiking and LFP

A: Population averaged firing rate of the multi-unit spiking is displayed separately for trials of the five different orientations. Average over 244 recording sites. **B:** Number of MU recording sites that prefer each of the five different orientations, shown separately for the task epochs cue, planning and movement.
Figure 3-6B showed the same for single units. **C:** Population averaged LFP power of the high gamma range over the course of the trial, shown separately for trials of the five orientations as in A. Averaged over 244 recording sites. **D:** Same as in C, but showing the power in the beta frequency range.

Therefore, it might be possible to explain a big part of the high gamma LFP modulation by the spiking activity in a bigger listening sphere. Our results then propose that within the LFP listening sphere at an individual recording site, an activity averaging occurs that results in similar modulation than the one we obtained by averaging over all spikes of all recording sites. This in turn proposes that cells with different preferred orientations can lie close to each other and are unlikely to be organized in orientation columns. Indeed, in our single cell recordings we could isolate pairs of orientation tuned units on one electrode, where one cell preferred +50 deg and the other one -50 deg. Nevertheless the averaging of single units to multi-unit activity does not result in the same distribution of preferred orientations as the gamma LFP. A wider listening sphere seems to be necessary for this.

Figure 4-9D shows for comparison the temporal development of the beta band LFP for the five different orientations. Unlike gamma activity, this curve does not show any obvious relationship to the spiking activity curve, neither in its temporal structure nor in its orientation tuning.

4.3.7 Comparison with data from monkey L

As pointed out in the introductory section of this chapter, the data presented in this result section is from only one monkey (monkey J). Unfortunately, the LFP recordings in the second monkey contained massive microphonic noise, which most likely originated from vibrations of the electrode in the guide tube. A second issue was the behavior of this monkey, who often did not sit quietly during the planning period, but shook his arms or legs. This behavior meant on one hand that the microphonic noise did not only occur during the movement epoch, but often also during the rest of the trial. Secondly, as we have seen in the results part, movement activity strongly influences the beta activity of the LFP, which is low during movement execution and high during the resting phases. Nevertheless, data from the second monkey does for the most part confirm the data taken from monkey J. We performed similar analyses as in monkey J on parts of monkey L's data, that

contained the least artifacts. The corresponding graphs are shown as supplementary figures in the appendix.

The general task modulation was the same and present in most channels, with the main difference that the overall level of beta activity was much lower in monkey L, in particular during the planning epoch (Figure S 1). Grip type selectivity was also at a comparable level and, importantly, showed a similar distribution of preferred grip type than in monkey J (Figure S 2 and Figure S 3). The big difference was that data from monkey L showed hardly any orientation selectivity (Figure S 2 and Figure S 4). The other important fact we found, the correlation between gamma band and spiking activity, was again similar in both monkeys (Figure S 5).

4.4 Discussion

We investigated the modulation of the local field potential (LFP) during a delayed grasping task, in which monkeys grasped a single object in various orientations with one of two possible grip types. A large majority of LFP recordings were strongly modulated by the different task epochs (Figure 4-1). The strongest spectral power was present in the beta frequency band, but task modulation was found in all frequency bands. We then examined if the LFP is also modulated by the condition of the trial (grip type and orientation). Grip type selectivity was weak during the cue epoch but increased in the course of the trial, mainly during the movement epoch, where it was most prominent in the gamma frequency band (Figure 4-2A). Orientation selectivity, on the other hand, was present in all epochs, but was most prominent in different frequency bands in the different task epochs (Figure 4-2B). The distributions of preferred conditions varied with the task epoch. This was true for the preferred grip type (Figure 4-3) and orientation (Figure 4-4). These distributions were often highly non-uniform and in some cases different for different frequency bands. Analysis of the correlation between different frequency bands revealed, that summarizing them into the four frequency bands ‘slow’, ‘beta’, ‘low gamma’ and ‘high gamma’ is reasonable and that the slow and beta frequencies show a modulation which is independent of the gamma frequencies. (Figure 4-5).

In the remainder of the chapter, we compared the coding properties of the LFP with the one of multi-unit spiking. The spectral power of the gamma band (mainly the high gamma) showed a moderate but significant correlation with the spiking activity measured on the same electrode (Figure 4-6), which was true also for modulations that can not be attributed to the conditions of our task (‘noise correlation’). Spikes tended to happen phase locked mainly to the gamma frequency band of the LFP, but showed some degree of phase preference also for the gamma frequency bands (Figure 4-7 and Figure 4-8). The preferred conditions in the gamma band, including its variations over task epochs, could be explained by the behavior of

the spiking activity in a larger listening sphere, if one takes into account the structural organization of single cells within AIP (Figure 4-9).

The presented data is mainly from one monkey because data from the second monkey was affected by strong artifacts. As far as this data could be analyzed, similar results were obtained for the most part, but two main differences to the data of monkey J were found: In monkey L, power in the beta frequency was much weaker during the planning epoch than in monkey J, and orientation tuning of the LFP was almost absent in monkey L. We think, that the noise and the behavior of that monkey can explain this difference. In monkey J, orientation selectivity was dominated by beta frequencies during the planning and movement epochs. This frequency band was strongly reduced in monkey L, likely as a consequence of her behavior. Furthermore, since we recorded around 50 trials per grip type but only about 20 trials per orientation, the detection of orientation selectivity with statistical tests might suffer more strongly from the added noise than the detection of grip type selectivity. Although these issues might explain the discrepancy, and although the data of monkey J was clearly of better quality, our findings in monkey J regarding the orientation tuning and including the fact that it was dominated by different frequency bands in different epochs, will have to be confirmed in another animal before they can be taken as valid across individuals.

Our finding of a strong modulation of the LFP with the behavioral state matches well with what other people have found in other areas of the parietal cortex (Pesaran et al., 2002; Scherberger et al., 2005; Asher et al., 2007). In fact, Scherberger et al. found that the behavioral state of reaching and eye movements could be decoded better from the LFP than from single unit spiking data in a trial-to-trial decoding analysis in PRR. Furthermore, the dominating frequency band in PRR during a delayed reaching task and in AIP during a delayed reach-to-grasp task was also found to be the beta band (Scherberger et al., 2005; Asher et al., 2007). A recent paper analyzing LFPs from the premotor area F5 and from M1 also reported task modulation in the beta frequency band of the LFP with strong power being present in the delay period and during stable hold, but not during movement execution (Spinks

et al., 2008). Our data therefore fits well with these previous papers and confirm that the LFP is highly informative with respect to the behavioral state that an animal is in.

Previous studies have shown that the LFP also contains information about specific task parameters. In different areas of the parietal cortex, LFPs were shown to be modulated by the direction of a saccade or a reach movement or by different objects that were grasped (Pesaran et al., 2002; Scherberger et al., 2005; Asher et al., 2007). But also in the premotor and primary motor cortex, the LFP was modulated by reach direction and grasping different objects (Mehring et al., 2003; Spinks et al., 2008). Our results provide new information as we have investigated two other parameters, namely the orientation of a grasp and the type of grip, which is used independently of the object. Furthermore, our results come from area AIP, where LFPs have previously not been explored. Our finding that both investigated parameters significantly modulated the LFP, together with the previous reports mentioned above, suggests that the local field potential is modulated by a variety of different task parameters. This would be a prerequisite if LFP signals should be used as an input signal for brain-machine interfaces, as it was sometimes suggested (Andersen et al., 2004). However, the strongly non-uniform distributions of preferred conditions that we found in the LFP might hinder accurate decoding of movement parameters. Such non-uniform distributions were also reported before (Scherberger et al., 2005; Asher et al., 2007). Pesaran on the other hand, who reported that the direction of saccades can be equally well decoded from the LFP than from spikes in LIP, most likely circumvented this problem by decoding only two directions (preferred vs. non-preferred); this although he had actually recorded data from eight directions. The most likely reason why the distributions are so non-uniform is the fact that the LFP at each site averages activity within a sphere containing a large number of cells and therefore represents a strongly averaged signal. A second open question regarding the decoding of LFP signals is, how informative they could be with respect to quickly varying parameters in continuous movements, i. e. the temporal precision. The cycle times of LFP oscillations are in the order of tens of milliseconds. Hence, if several cycles need to be recorded to reach a good decoding performance, quick changes can not be tracked. What are the limits of decoding

continuously varying signals from the LFP? This is still an open question and needs to be addressed in future research. Overall, our data, together with previous reports, suggest that the LFP might be more helpful to detect 'global' task parameters like the general intention to move the hand than for the precise reconstruction or predicition of the planned movement.

A new aspect of our findings was the fact that the frequency band that dominated the orientation tuning shifted very strongly from one epoch to the next. While the orientation tuning was dominated by gamma frequencies in the cue epoch, it shifted to the beta range during planning and movement. Such a shift between different task epochs could potentially indicate that different processes are responsible for this tuning at different moments in the task. During the cue period, AIP most likely gets strong input from extrastriate visual areas that might contribute information about the spatial configuration of objects, like its orientation. In our analysis of single units in AIP, we found that the neural response during the cue was mainly driven by the presence of an object in the preferred orientation of the neuron and that grip type tuning at this stage of the trial had only a modulating effect on the firing rate (Table 3-2). The strong LFP selectivity in the high frequencies during the cue, together with the much lower grip type selectivity at the same time, could therefore reflect this driving input from visual areas. Interesting in that respect is the comparison with the movement epoch. The gamma frequencies of the LFP show strong grip type tuning during the movement and much weaker orientation tuning. Indeed, spiking activity of the cells with late tuning onset was mainly grip type tuned and showed additional orientation tuning only in a minority of neurons. The gamma band activity during movement might therefore reflect a strong input to AIP that is dominated by grip type selectivity. A candidate for an input with such a pattern is F5, where strong grip type selectivity was found during movement, but only weak orientation tuning (Fluet, 2009). Beta frequencies, on the other hand, have recently been suggested to be implicated in coordination across remote cortical areas (Pesaran et al., 2008). In this paper, task modulated synchronization was found between the beta range LFP in PRR and PMd, two areas that are both involved in the planning of reach movements. The authors attributed this effect to cortico-cortical communication, possibly in a

reverberating loop. In our experiment, orientation modulation persists after extinction of the cue, which must be due to memory related processing. This processing might include local rhythms or feedback loops with other cortical areas (possibly F5) and these processes might then be the source of the strongly orientation tuned beta activity that we observe in the planning and execution epochs.

When we correlated the power of the different LFP frequencies with the spiking activity of multi-units on the same electrode, we found a moderate correlation between the signals. This was described before in the parietal as well as pre-motor and motor cortex (Asher et al., 2007; Spinks et al., 2008). It is possible that the gamma LFP reflects synaptic dynamics which are related to the triggering of spikes in the recorded cells. However, there is also the possibility that this effect is an artifact due to the spike waveform residuals being present in the local field potential. Such residuals are certainly present in our data, as can be seen by the occurrence of a sharp 'spike-like' feature at time zero of the spike triggered average of the local field potential (Figure 4-7B). Nevertheless, there are arguments that make it unlikely that the correlation between the signals is due to only this effect. The most important argument is the fact that the trial-to-trial correlation between gamma LFP and spiking is highest during the fixation period and lowest during the movement period. However, spiking activity is highest during the movement and therefore, a correlation which was due to spike residuals only, should be highest during the movement epoch. This shows that oscillations that are not due to spike residuals must contribute significantly to the gamma band LFP. Furthermore, despite the correlation we found, the distributions of preferred grip type and preferred orientation in the population are very different for the gamma band LFP and for single units, which also shows that a summation of the spike residuals alone can not explain the gamma LFP. The question therefore is: how can the correlation between spikes and LFP be explained together with the different distributions of preferred conditions? In other words: Shouldn't the preferred conditions match as well if the two signals show correlation?

We propose that the solution to this question is to assume an LFP 'listening sphere' that is bigger than the listening sphere of the same electrode for (multi-unit) spiking activity. This assumption is rooted in the observation that the preferred conditions of the spikes averaged over all of our recording sites explain better the preferred conditions of the individual LFP recordings than does the preferred condition of the spikes measured locally on the same electrode as the LFP. For example: during the cue period, the preferred orientation of the gamma band of most LFP channels was -25 degrees. This is the orientation which shows the highest spike count over all of our recordings. Individual single- or multi-unit recordings, however, show very different preferred orientations, with the -50 degrees and +50 degrees being most common. We therefore propose that within the listening sphere of each LFP recording, an averaging occurs that gives a similar result as the averaging over all spikes of all our recordings. This would mean that within this listening sphere, neurons with different preferred orientations are intermingled. A hint that this is true comes from the comparison of pairs of single units recorded on the same electrode, which do indeed not have to share their preferred orientation. Importantly, this hypothesis can not only explain the orientation preference of the LFP during cue, but is able to account for the different distributions of preferred orientations in the different epochs, as in the movement epoch, where most LFP sites prefer a rightward tilted handle, this is again in accordance with the orientation that shows the highest overall spike rate. Maybe even more interesting is the comparison of the preferred grip types. Analyzing pairs of single units recorded on one electrode, we found that the early grip type tuned cells show a spatially ordered arrangement in the sense that two nearby early tuned cells show the same grip type preference. Late tuned cells, however, are intermingled with each other and with the early tuned cells independent of the preferred grip type. The preferred grip type of the gamma band LFP during cue and planning, where only early tuned cells are active, corresponds largely with the preference of the locally recorded spikes, as is expected due to the orderly arrangement of cells with similar grip type preference. In the movement epoch, however, basically all LFP channels prefer precision grips, likely because cells during movement are not spatially arranged and therefore, cells with both

preferences will be present in the LFP listening sphere; with the precision preferring cells dominating this sphere as they are overall more numerous. This hypothesis of ours also got support by a recent paper, in which Katzner el al. tried to model the LFP as a weighted sum of spiking responses in a sphere around the electrode (Katzner et al., 2009). In order to do this, they measured the orientation tuning map in V1 of cats using optical imaging and then recorded the LFP at very well defined positions within that map. Their conclusion was that the LFP can be modeled very well by a weighted sum of spiking activity and that 95% of the LFP signal originates in a radius of 250 micrometer around the electrode. Our findings fit very well with their results as far as the gamma band LFP is concerned. However, while Katzner and colleagues found the same to be true also for the beta range of the LFPs, in our data these frequencies showed a very different behavior and were neither correlated with the gamma band nor the spiking activity. This discrepancy between Katzner's finding and our data might have to do with an important difference in the experiments: Katzner et al. performed their experiments in anaesthetized cats. Although we do at this stage not know what the basis of the strong beta activity is in our experiments, it might be related to long range communication as suggested by Pesaran (Pesaran et al., 2008), which in turn might be related to behaviorally relevant phenomena like attention or working memory. Such processes will of course be absent in the anaesthetized animal. This could explain the discrepancy.

If gamma LFP can be modeled by a weighted sum of spiking activity in a sphere around the recording electrode, then reducing the integration radius below optimal will reduce the fit of the model, but some correlation between the modeled and the measured LFP will remain. This is how the correlation that we found between LFP and multi-unit spiking has to be understood. The multi-unit spiking constitutes some of the activity in the listening sphere which contributes to the LFP, but of course represents activity within a smaller radius than that of the LFP.

Our findings together with the elegant work of Katzner et al. propose that the gamma band LFP can serve as a tool, giving some information as to whether the encoded parameter that one is looking at (orientation, grip type,…) shows an orderly

spatial arrangement in the investigated brain region, like orientation selectivity in V1 or early grip type selectivity in AIP, or if cells with different preferences are completely intermingled. In the former case, the gamma band LFP should mostly show a similar preferred condition than single or multi-units recorded on the same electrode, resulting also in a similar distribution of preferred conditions for spikes and LFP. In the latter case, on the other hand, the preferred conditions of the two signals should be largely uncorrelated. In fact, the case of intermingled cells can explain the highly non-uniform distributions of preferred conditions that are often found in the LFP. As in our experiment, where all LFP channels prefer precision grips during movement because late grip type tuned cells are intermingled and precision cells are more numerous, this mechanism could also explain the highly skewed distribution of preferred directions in PRR. There, cells with contra-lateral preference are more numerous, but ipsi-lateral ones exist as well. The LFP channels, however, prefer all a contra-lateral reach (Scherberger et al., 2003a).

In conclusion, we found that the LFP in AIP is modulated by the behavioral epoch of the task as well as by the task parameters orientation and grip type. The gamma band activity of the LFP is correlated with spiking activity and seems to be well explained by averaging spiking activity from a larger listening sphere. This might allow to gain some information band about the spatial arrangement of cells that are tuned for a given parameter.

Appendix

Supplementary Figures

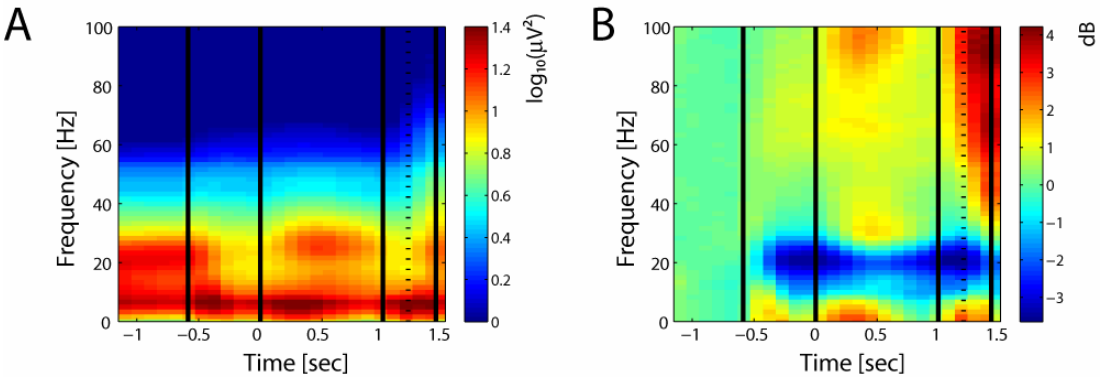

Figure S 1: Spectrograms of monkey L

A: Population spectrogram averaged over all 117 recording sites of monkey L. **B:** Same plot as in A, but with each frequency band normalized to the activity during fixation period. Compare to Figure 4-1D and E.

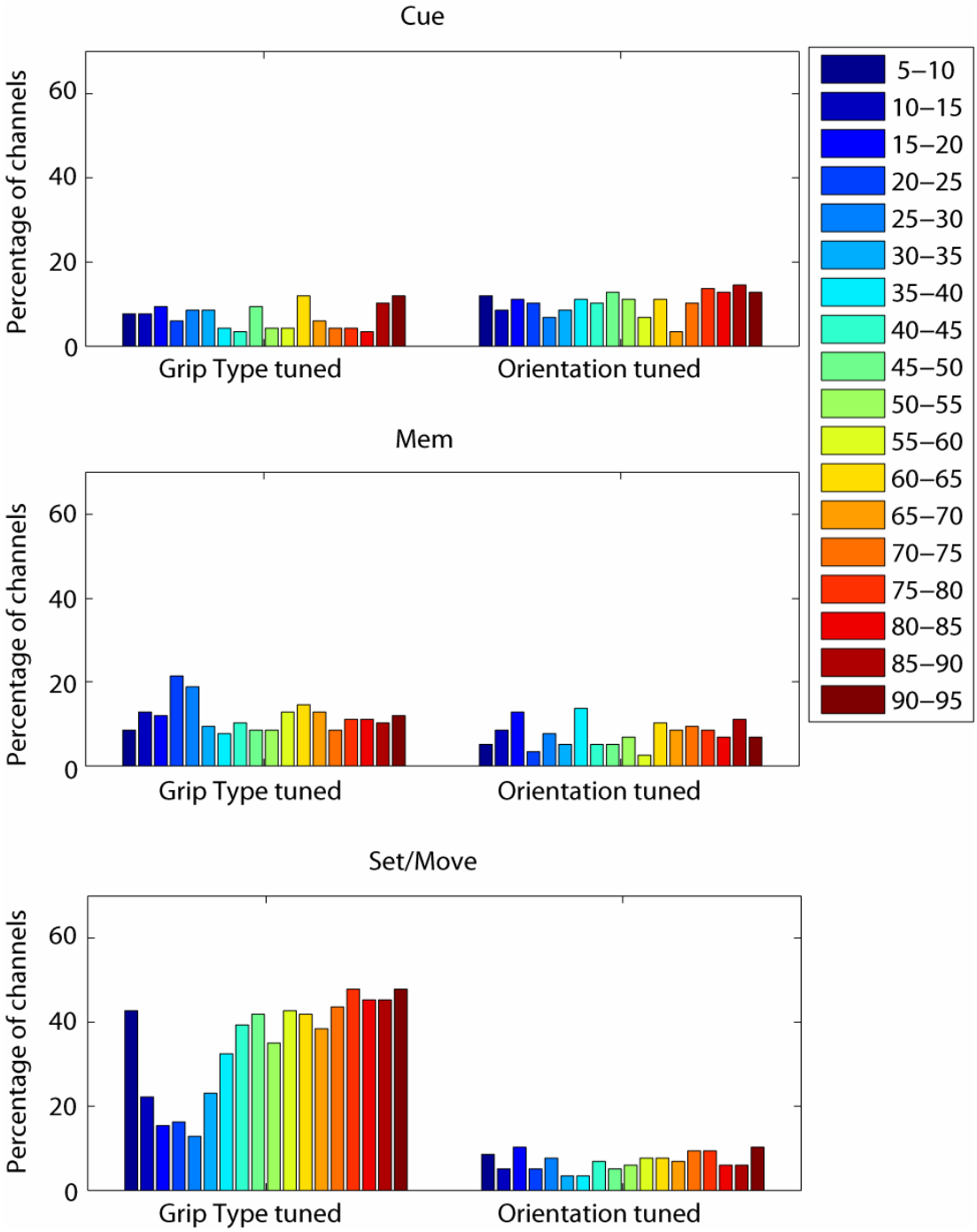

Figure S 2: Modulation for grip type and orientation in LFP of monkey L

Percentage of channels that display significant modulation (2-way ANOVA, $p<0.05$) for grip type (left) and orientation (right), separately for the three epochs cue, planning and movement. Compare to Figure 4-2

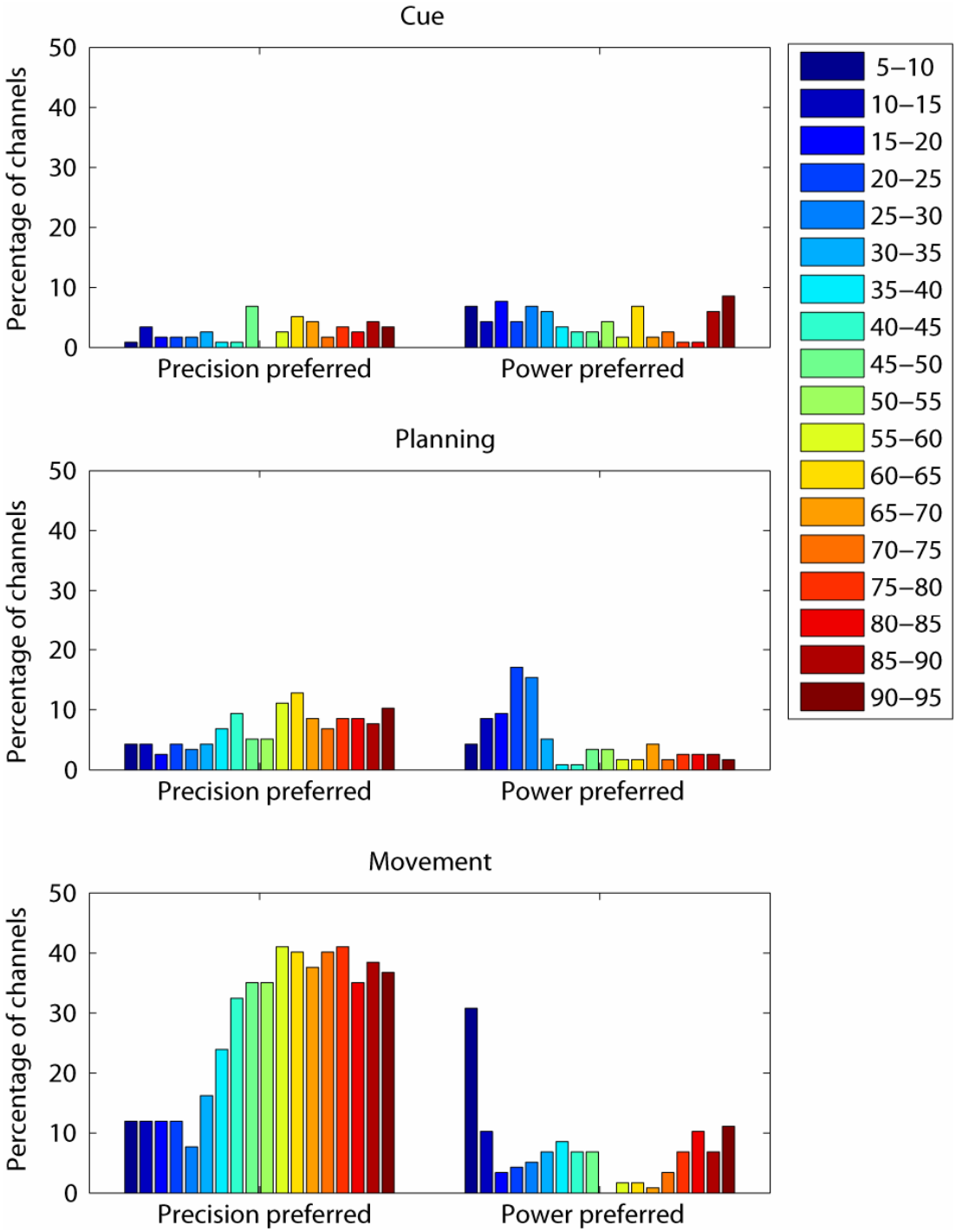

Figure S 3: Preferred grip type of the different LFP frequencies of monkey L

Percentage of all channels that show significantly stronger LFP power for precision grips (left) or power grip (right), shown separately for different task epochs (panels) and for different frequency bands (colors). Compare to Figure 4-3.

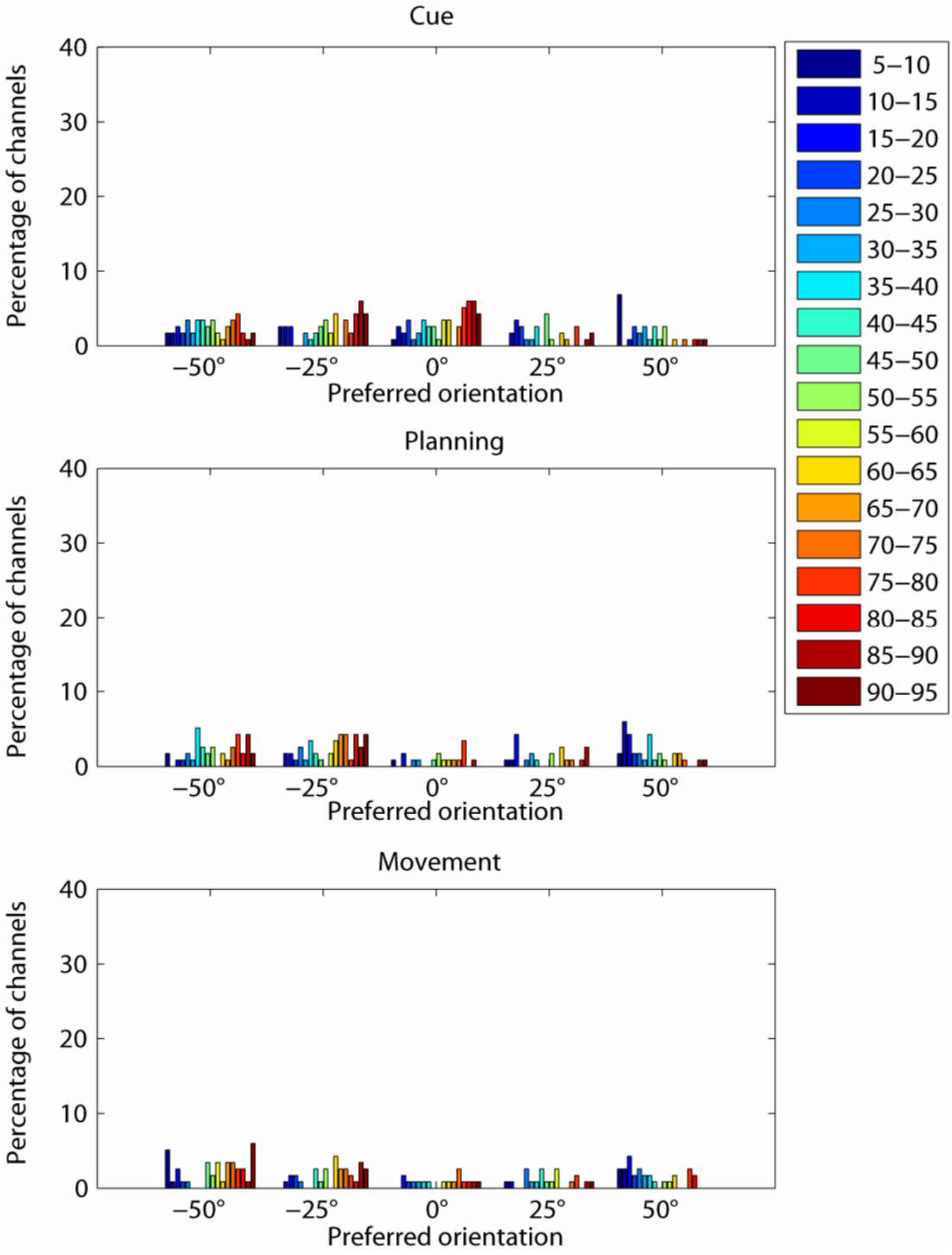

Figure S 4: Preferred orientation of the different LFP frequencies of monkey L

Percentage of all channels that prefer each of the 5 different orientations. As there was almost no orientation tuning in monkey L, no clear distribution can emerge for the preferred orientations. Compare to Figure 4-4.

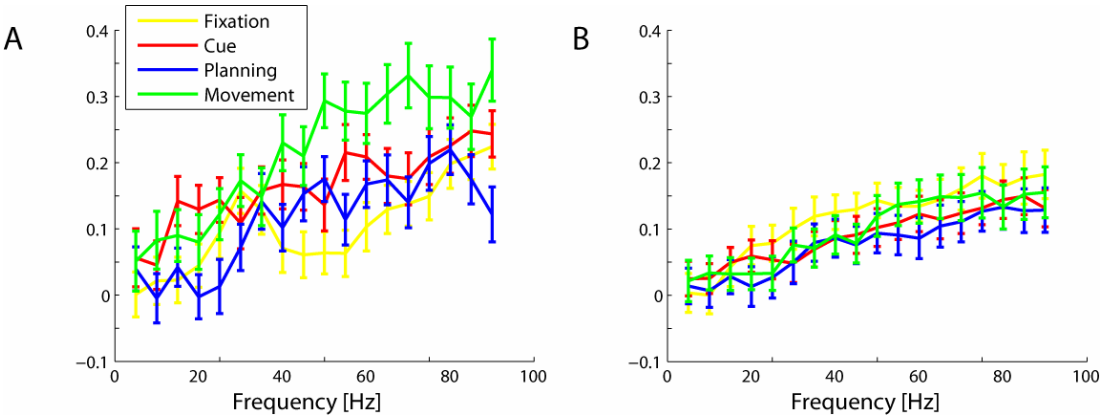

Figure S 5: Correlation between tuning of LFP and multi-unit spiking of monkey L

A: Correlation between the tuning curves of the different LFP frequencies (x-axis) with the tuning curve of the multi-unit spiking on the same electrode; average of 88 recordings. Errorbars indicate the standard error. **B:** Trial-to-trial correlation ('noise correlation') of LFP power and multi-unit spiking activity; average of 88 recording sites. Compare to Figure 4-6.

Data Import

The following code was used to import the raw data into Matlab and build up an easily accessible data structure which contains the data in a trial-by-trial manner. In our case, the following file formats need to be read in:

- proprietary file format of Cyberkinetics (file extensions: '.nev', '.ns1' (…) '.ns5'). All these files can be accessed by opening only the '.nev' file with the Neuroshare Library. However, importing the .ns5 files (with a sampling rate of 30'000 Hz), is incredibly slow this way. We therefore read the ns5 in using the Matlab command fread and parse the retrieved data.
- proprietary file format of Plexon ('.plx'), because we used the Plexon Offline Sorter for spike sorting. The Neuroshare library did not work with our .plx files. We therefore used the Plexon Matlab Library.

The script furthermore has to interpret the code used by the LabView program to encode headers and events. All this data is contained in the Digital Input Channel of the .nev file.

Other issued which added to the complexity of this code:

- in a part of our recordings, no full bandwidth data was recorded. Instead, waveform snippets where extracted together with their timestamps. In later recordings, the entire data stream was recorded at 30 kHz. This script can handle data recorded with either method.
- As Marie-Christine Fluet sorted F5 data and stored it in a plx file, while I sorted AIP data and stored it in a different file, this script has to open two plx files in order to retrieve data from both regions. However, in some recordings only single unit data from one region is present, which has to be checked before.

clear;

```
t1 = fix(clock);



dir = 'E:\Workspace\data\raw\Lilly\Li070126';

fileNo = '0316';
doNS5 = 0;

fileName = 'AIPF5'; % saveName only
errorName = 'errors';
cd(dir);

% files to load
plxAIPfile = ['AIP' fileNo '.plx'];
plxF5file  = ['F5'  fileNo '.plx'];
nevfile = ['raw' fileNo '.nev'];
ns5file = ['raw' fileNo '.ns5'];


plxAIPexist = exist([dir '\' plxAIPfile]) == 2;
plxF5exist  = exist([dir '\' plxF5file])  == 2;
if ~(plxAIPexist | plxF5exist)
    disp('no plx-file')
    return
end


%open the nev-File
ns_SetLibrary('C:\Workspace\Neuroshare\mtools\nsNEVLibrary.dll');
[ns_RESULT, hFile]=ns_OpenFile([dir '\' nevfile]);
if ns_RESULT
    error(['NEV-File nicht gefunden: ' nevfile]);
end
[ns_RESULT, hFileInfo]=ns_GetFileInfo(hFile);

% determine whether the sorting was done on the nev file (plx
contains Digin) or on fbw (plx does not contain Digin)
if plxAIPexist
    try
        [dn, TimeStamp, DiginData] = plx_event_ts(plxAIPfile,257);
        plxAIPhasnames = 1;
    catch
        plxAIPhasnames = 0;
    end
end
if plxF5exist
    try
        [dn, TimeStamp, DiginData] = plx_event_ts(plxF5file,257);
        plxF5hasnames = 1;
    catch
        plxF5hasnames = 0;
```

```
    end
end



if plxAIPexist & plxF5exist
    if plxAIPhasnames ~= plxF5hasnames
        disp('exception');
        keyboard
    end
end


disp([fileName '  --->  ' fileName fileNo '.mat' ]);
if ~doNS5
    disp('not transferring the 30kHz data');
end
disp(' ');


stateTable = ['TrialStart           ';
              'WaitForHandrest      ';
              'OptionalReward       ';
              'Motor                ';
              'FixationPeriod       ';
              'Cue                  ';
              'MemoryPeriod         ';
              'ReactionTime         ';
              'GraspingGo           ';
              'InitiateReward       ';
              'RewardPeriod         ';
              'IntertrialInterval   ';
              'WaitAfterError       ';
              'MovementStart        ';
              'AquireFixation       ';
              'Cue 2                ';
              'Memory 2             ';
              'Motor Overshoot      '];



% Find the entity containing the digital inputs (strobed events) and
% get the Digin Data
for ent = [1:hFileInfo.EntityCount]
    [ns_RESULT, nsEntityInfo(ent)]=ns_GetEntityInfo(hFile,ent);
    if strcmp(nsEntityInfo(ent).EntityLabel, 'digin')
        diginID = ent;
    end
end
diginItems = nsEntityInfo(diginID).ItemCount;
[ns_RESULT, TimeStamp, DiginData, DataSize]=ns_GetEventData(hFile,
diginID,[1:diginItems]);
```

```
%find all trialstart (0), headerstart (255) and headerend (254)
tsInd = find(DiginData==0);
hsInd = find(DiginData==255);
heInd = find(DiginData==254);


% elminate Headers that might come before the first Trialstart
ii = find(hsInd>tsInd(1), 1);
hsInd(1:ii-1) = [];
ii = find(heInd>tsInd(1), 1);
heInd(1:ii-1) = [];


%the following algorithm eliminates incomplete trials (only start or
only
%header)
ii = 1;
while ii<length(tsInd) & ii<=length(heInd)
    if tsInd(ii+1)<hsInd(ii)
        tsInd(ii) = [];
    else
        ii = ii+1;
    end
    if ii<=length(tsInd) & ii<=length(hsInd)
        while tsInd(ii)>hsInd(ii)
            hsInd(ii) = [];
            heInd(ii) = [];
        end
    end
end
while tsInd(end)> heInd(end)
    tsInd(end) = [];
end


% now build the trial structure. In a first step, get the DiginData
task = '';
for tr = 1:length(tsInd)
    header = DiginData(hsInd(tr)+1:heInd(tr)-1)';

    startItem = strfind(char(header), 'success=') + 8;
    endItem = strfind(char(header(startItem:end)), ',');
    trials(tr).header.success = strcmp('TRUE',
char(header(startItem+1:(startItem+endItem(1))-3)));

    startItem = strfind(char(header), 'task=') + 5;
    endItem = strfind(char(header(startItem:end)), ',');
    if ~isempty(startItem)
        trials(tr).header.task =
str2num(char(header(startItem+1:(startItem+endItem(1))-3)));
        if trials(tr).header.task > 0 task = 'cs'; end
    end

    startItem = strfind(char(header), 'graspType=') + 10;
    endItem = strfind(char(header(startItem:end)), ',');
```

```
    trials(tr).header.graspType =
char(header(startItem+1:(startItem+endItem(1))-3));

%     startItem = strfind(char(header), 'positionNo=') + 11 ;
    startItem = strfind(char(header), 'ionNo=') + 6 ;
    endItem = strfind(char(header(startItem:end)), ',');
    trials(tr).header.positionNo =
str2num(char(header(startItem+1:(startItem+endItem(1))-3)));

    startItem = strfind(char(header), 'degPerUnit=') + 11;
    endItem = strfind(char(header(startItem:end)), ',');
    trials(tr).header.DegPerUnit =
str2num(char(header(startItem+1:(startItem+endItem(1))-3)));

    startItem = strfind(char(header), 'angle=') + 6;
    endItem = strfind(char(header(startItem:end)), ',');
    trials(tr).header.angle =
str2num(char(header(startItem+1:(startItem+endItem(1))-3)));

    startItem = strfind(char(header), 'threshold=') + 10;
    endItem = strfind(char(header(startItem:end)), ',');
    if ~isempty(startItem)
        trials(tr).header.pullThreshold =
str2num(char(header(startItem+1:(startItem+endItem(1))-3)));
    end

    startItem = strfind(char(header), 'reward=') + 7;
    endItem = strfind(char(header(startItem:end)), ',');
    trials(tr).header.reward =
str2num(char(header(startItem+1:(startItem+endItem(1))-3)));

    startItem = strfind(char(header), 'rewardDelay=') + 12;
    endItem = strfind(char(header(startItem:end)), ',');
    if ~isempty(startItem)
        trials(tr).header.rewardDelay =
str2num(char(header(startItem+1:(startItem+endItem(1))-3)));
    end

    startItem = strfind(char(header), 'correctTrials=') + 14;
    endItem = strfind(char(header(startItem:end)), ',');
    trials(tr).header.correctTrials =
str2num(char(header(startItem+1:(startItem+endItem(1))-3)));

    startItem = strfind(char(header), 'xGain=') + 6;
    endItem = strfind(char(header(startItem:end)), ',');
    if ~isempty(startItem)
        trials(tr).header.xGain =
str2num(char(header(startItem+1:(startItem+endItem(1))-3)));
    end

    startItem = strfind(char(header), 'yGain=') + 6;
    endItem = strfind(char(header(startItem:end)), ',');
    if ~isempty(startItem)
        trials(tr).header.yGain =
str2num(char(header(startItem+1:(startItem+endItem(1))-3)));
```

```
    end
    startItem = strfind(char(header), 'xOffset=') + 8;
    endItem = strfind(char(header(startItem:end)), ',');
    if ~isempty(startItem)
        trials(tr).header.xOffset =
str2num(char(header(startItem+1:(startItem+endItem(1))-3)));
    end

    startItem = strfind(char(header), 'yOffset=') + 8;
    endItem = strfind(char(header(startItem:end)), ',');
    if ~isempty(startItem)
        trials(tr).header.yOffset =
str2num(char(header(startItem+1:(startItem+endItem(1))-3)));
    end

    startItem = strfind(char(header), 'window=') + 7;
    endItem = strfind(char(header(startItem:end)), ',');
    if ~isempty(startItem)
        trials(tr).header.fixWindow =
str2num(char(header(startItem+1:(startItem+endItem(1))-3)));
    end

    startItem = strfind(char(header), 'allowOut=') + 9;
    endItem = strfind(char(header(startItem:end)), ',');
    if ~isempty(startItem)
        trials(tr).header.allowOut_10ms =
str2num(char(header(startItem+1:(startItem+endItem(1))-3)));
    end

    startItem = strfind(char(header), 'trackOn=') + 8;
    endItem = strfind(char(header(startItem:end)), ',');
    if ~isempty(startItem)
        trials(tr).header.trackOn = strcmp('TRUE',
char(header(startItem+1:(startItem+endItem(1))-3)));
    end

    startItem = strfind(char(header), 'fileName=') + 9;
    endItem = strfind(char(header(startItem:end)), ',');
    if ~isempty(startItem)
        trials(tr).header.taskName =
char(header(startItem+1:(startItem+endItem(1))-3));
    end

    trials(tr).states = [];
    trials(tr).events = [];

    for itm = tsInd(tr):hsInd(tr)-1
        if ( (DiginData(itm) >= 0) && (DiginData(itm) < 128) )
            trials(tr).states(end+1).timeStamp = TimeStamp(itm);
            trials(tr).states(end).newState =
stateTable(DiginData(itm)+1, :);

        elseif ( (DiginData(itm) > 127) && (DiginData(itm) < 192) )
            trials(tr).events(end+1).timeStamp = TimeStamp(itm);
            trials(tr).events(end).pull = bitand(DiginData(itm), 1);
```

```
            trials(tr).events(end).power = bitand(DiginData(itm),
2)/2;
            trials(tr).events(end).precisionLeft =
bitand(DiginData(itm), 4)/4;
            trials(tr).events(end).precisionRight =
bitand(DiginData(itm), 8)/8;
            trials(tr).events(end).handrestLeft =
bitand(DiginData(itm), 16)/16;
            trials(tr).events(end).handrestRight =
bitand(DiginData(itm), 32)/32;
        elseif ((DiginData(itm) > 191) && (DiginData(itm) < 224))
            trials(tr).events(end+1).timeStamp = TimeStamp(itm);
            trials(tr).events(end).EyeIn = bitand(DiginData(itm),
1);
        end
    end
end


% this next test is necessary because of some files where force
% sensor produced hundreds of events:
totalEvents = 0;
for tr = 1:length(trials)
    totalEvents = totalEvents + length(trials(tr).events);
end
if totalEvents/length(trials) > 100
    for tr = 1:length(trials)
        trials(tr).events = [];
    end
    load([savedir 'FileWOEvents.mat']);
    noEvents(end+1, 1:4) = fileNo;
    save([savedir 'FileWOEvents.mat'], 'noEvents');
    disp(['File ' fileNo ' without events because of flickering pull
sensor']);
end


trials(1).elec = [];
% now find the Elecs that have Spiking Data or Analog Data
elecs = []; analogEnt = [];
for nei=1:length(nsEntityInfo)
    if (nsEntityInfo(nei).EntityType == 2 &&
(str2num(nsEntityInfo(nei).EntityLabel(1:3)) >=129) &&
(str2num(nsEntityInfo(nei).EntityLabel(1:3)) <=138))
        elecs = [elecs str2num(nsEntityInfo(nei).EntityLabel(1:3))];
        analogEnt = [analogEnt nei];
    end
    if nsEntityInfo(nei).EntityType == 3 &&
nsEntityInfo(nei).ItemCount > 0 && ...
            (str2num(nsEntityInfo(nei).EntityLabel(end-2:end))
>=129) && (str2num(nsEntityInfo(nei).EntityLabel(end-2:end)) <=138)
        elecs = [elecs str2num(nsEntityInfo(nei).EntityLabel(end-
2:end))];
    end
end
elecs = sort(unique(elecs));
```

```
% get the timeStamps of the startTrials and endTrials
startTrial = TimeStamp(tsInd);
endTrial = TimeStamp(hsInd)+0.8;


% %now get the analog data from the .ns files
% %low sampling rate channels are first imported using Neuroshare
aCh=0; fbwCh=0; fbwEnt = [];
for ent = [128:hFileInfo.EntityCount]
    [ns_RESULT, nsEntityInfo]=ns_GetEntityInfo(hFile,ent);
    if (nsEntityInfo.EntityType == 2) % => analog Channel
        [ns_RESULT, nsAnalogInfo]=ns_GetAnalogInfo(hFile,ent);
        if nsAnalogInfo.SampleRate < 10000
            [ns_RESULT, ContCount,
Data]=ns_GetAnalogData(hFile,ent,1,nsEntityInfo.ItemCount);
            if ismember(ent, analogEnt) % then it is analog Data
from an electrode
                el = find(elecs ==
str2num(nsEntityInfo.EntityLabel(1:3)));
                if ~(elecs(el)>=129 & elecs(el) <=138)
                    error('Es ist etwas faul im Staate Daenemark');
                end
                for tr=1:length(trials)
                    trials(tr).elec(el).ID = elecs(el);
                    trials(tr).elec(el).label = [];
                    trials(tr).elec(el).units = [];
                    trials(tr).elec(el).lfp.source =
nsAnalogInfo.ProbeInfo;
                    trials(tr).elec(el).lfp.samplingRate =
nsAnalogInfo.SampleRate;
                    trials(tr).elec(el).lfp.resolution = 10000/2^16;
                    trials(tr).elec(el).lfp.unit = 'mV';
                    sInd =
ceil((startTrial(tr)*nsAnalogInfo.SampleRate)+1);
                    eInd =
floor((endTrial(tr)*nsAnalogInfo.SampleRate)+1);
                    if eInd > length(Data)
                        eInd = length(Data);
                        disp(['Analog Data cut before end of trial '
num2str(tr)]);
                    end
% %                     % try with Fourier Filter to bandpass 2-
100Hz
% %                     tempLFP =
Data(sInd:eInd)'/nsAnalogInfo.Resolution;
% %                     kHz = nsAnalogInfo.SampleRate/1000;
% %                     if kHz ~= 1
% %                         keyboard
% %                     end
% %                     tempLFP = FouFilter(tempLFP,
length(tempLFP)/kHz,0.05, 0.08, 30, 0);
% %                     trials(tr).elec(el).lfp.filtered = 1;
                    trials(tr).elec(el).lfp.data = tempLFP;
```

```
                    trials(tr).elec(el).lfp.timeStamp = (sInd-
1)/nsAnalogInfo.SampleRate;
                end
            else % then it's one of the other analogChannels (Eye
trace, force sensor)
                aCh = aCh+1;
                for tr=1:length(trials)
                    trials(tr).analogChannels(aCh).source =
nsAnalogInfo.ProbeInfo;
                    trials(tr).analogChannels(aCh).samplingRate =
nsAnalogInfo.SampleRate;
                    trials(tr).analogChannels(aCh).resolution =
10000/2^16;
                    trials(tr).analogChannels(aCh).unit = 'mV';
                    sInd =
ceil((startTrial(tr)*nsAnalogInfo.SampleRate)+1);
                    eInd =
floor((endTrial(tr)*nsAnalogInfo.SampleRate)+1);
                    if eInd > length(Data)
                        eInd = length(Data);
                        disp(['Analog Data cut before end of trial '
num2str(tr)]);
                    end
                    trials(tr).analogChannels(aCh).data =
int16(Data(sInd:eInd)'/nsAnalogInfo.Resolution);
                    trials(tr).analogChannels(aCh).timeStamp =
(sInd-1)/nsAnalogInfo.SampleRate;
                end
            end
        elseif nsAnalogInfo.SampleRate >= 20000
            fbwCh = fbwCh + 1;
            fbwEnt(fbwCh) = ent;
            fbwInfo{fbwCh} = nsAnalogInfo;
        end
    end
end

%create the low pass filter
[b8,a8] = butter(8,300/15000,'low');

% % Full Bandwidth analog Data is imported directly from the ns5-
file using fread
% % open the file and read header data
if doNS5
    try
        fid = fopen([dir '\' ns5file]);
        FileID = char(fread(fid, 8)');
        FileLabel = char(fread(fid, 16)');
        Period = fread(fid, 1, 'int32');
        ChCount = fread(fid,1, 'int32');
        for cc = 1:ChCount
            ChID(cc) = fread(fid,1, 'int32');
        end

        % now read blocks of data, low-pass-filter it, downsample
it, store it to
```

```
        % trial
        fbwData = fread(fid, [ChCount, 1800000], 'int16');
        fbwStart = 1;
        fbwEnd =1800000;
        for tr=1:length(trials)
            sInd = ceil((startTrial(tr)*30000)+1);
            eInd = floor((endTrial(tr)*30000)+1);
            if eInd > fbwEnd
                if sInd > fbwEnd
                    fbwData = fread(fid, [ChCount, 1800000],
'int16');
                    fbwEnd = fbwEnd + 1800000;
                    fbwStart = fbwEnd - 1800000 + 1;
                else
                    fbwData(:, 1:sInd-fbwStart) = [];
                    fbwData = [fbwData fread(fid, [ChCount,
1800000], 'int16')];
                    fbwStart = sInd;
                    fbwEnd = fbwEnd + 1800000;
                end
            end
            if (eInd-fbwStart+1)>length(fbwData)
                eInd = length(fbwData)+fbwStart-1;
            end
            for cc = 1:ChCount
                el = find(elecs == ChID(cc));
                if ~(ChID(cc)>=129 & ChID(cc) <= 138)
                    disp('Es ist wieder etwas faul im Staate
Daenemark');
                end
                trials(tr).elec(el).ID = elecs(el);
                trials(tr).elec(el).label = [];
                trials(tr).elec(el).units = [];
                trials(tr).elec(el).lfp.source =
fbwInfo{cc}.ProbeInfo;
                trials(tr).elec(el).lfp.samplingRate = 1000;
                trials(tr).elec(el).lfp.resolution = 10000/2^16;
                trials(tr).elec(el).lfp.unit = 'mV';
                tempLFP = filtfilt(b8,a8,fbwData(cc, sInd-
fbwStart+1:eInd-fbwStart+1));
% %                 % Try with a Fourier Bandpass Filter: (2-100Hz)
% %                 tempLFP = fbwData(cc, sInd-fbwStart+1:eInd-
fbwStart+1);
% %                 tempLFP = FouFilter(tempLFP,
length(tempLFP)/30,0.05, 0.08, 30, 0);
% %                 trials(tr).elec(el).lfp.filtered = 1;
                trials(tr).elec(el).lfp.data = tempLFP(1:30:end);
                trials(tr).elec(el).lfp.timeStamp = (sInd-
1)/fbwInfo{cc}.SampleRate;
            end
        end
        fclose(fid);
    catch
        disp('no ns5 file');
    end
end
```

```
% now add the neural Data of AIP to the structure
if plxAIPexist
    [nc,names] = plx_chan_names(plxAIPfile);
    [tscounts, wfcounts] = plx_info(plxAIPfile, 0);
    for ch=1:nc
        if plxAIPhasnames
            chname = ['elec' names(ch,end-2:end)];
            elec = str2num(names(ch,end-2:end));
        else
            chname = ['elec' fbwInfo{ch}.ProbeInfo(end-2:end)];
            elec = str2num(fbwInfo{ch}.ProbeInfo(end-2:end));
        end
        if elec >= 129 && elec <= 133
            el = find(elecs == elec);
            for tr = 1:length(trials)
                trials(tr).elec(el).ID = elec;
                trials(tr).elec(el).label = chname;
            end
            unInd = find(tscounts(:, ch+1));
            for un=unInd'
                [nw, npw, ts, wave] = plx_waves(plxAIPfile, ch, un-
1);
                for tr = 1:length(trials)
                    s = find(ts>startTrial(tr),1);
                    e = find(ts<endTrial(tr), 1, 'last');

                    trials(tr).elec(el).units(un).unitID = un-1;
                    trials(tr).elec(el).units(un).timeStamp =
ts(s:e)';
                    trials(tr).elec(el).units(un).waveform =
int16(wave(s:e, :)');
                end
            end
        end
    end
end


% now add the neural Data of F5 to the structure
if plxF5exist
    [nc,names] = plx_chan_names(plxF5file);
    [tscounts, wfcounts] = plx_info(plxF5file, 0);
    for ch=1:nc
        if plxF5hasnames
            chname = ['elec' names(ch,end-2:end)];
            elec = str2num(names(ch,end-2:end));
        else
            chname = ['elec' fbwInfo{ch}.ProbeInfo(end-2:end)];
            elec = str2num(fbwInfo{ch}.ProbeInfo(end-2:end));
        end
        if elec >= 134 && elec <= 138
            el = find(elecs == elec);
            for tr = 1:length(trials)
```

```
                trials(tr).elec(el).ID = elec;
                trials(tr).elec(el).label = chname;
            end
            unInd = find(tscounts(:, ch+1));
            for un=unInd'
                [nw, npw, ts, wave] = plx_waves(plxF5file, ch, un-
1);
                for tr = 1:length(trials)
                    s = find(ts>startTrial(tr),1);
                    e = find(ts<endTrial(tr), 1, 'last');

                    trials(tr).elec(el).units(un).unitID = un-1;
                    trials(tr).elec(el).units(un).timeStamp =
ts(s:e)';
                    trials(tr).elec(el).units(un).waveform =
int16(wave(s:e, :)');
                end
            end
        end
    end
end


% in rare cases, it can be, that an elec does not contain data. This
leads
% to problems. Therefore delete these elecs.
emptyEl = zeros(1, length(trials(1).elec));
for el = 1:length(trials(1).elec);
    if isempty(trials(1).elec(el).ID)
        emptyEl(el) = 1;
    end
end
delID = find(emptyEl);
for tr = 1:length(trials)
    trials(tr).elec(delID) = [];
end


% % sort trials into successful ones and error trials
len = length(trials);
etr = 1;
tr = 1;
while (tr<=len)
    if ~(trials(tr).header.success)
        errorTrials(etr) = trials(tr);
        trials(tr) = [];
        tr = tr - 1;
        len = len - 1; etr = etr + 1;
    end
    tr = tr + 1;
end


NoTrials = length(trials);
% % % % sort CS files into tasks 0, 1 and 2
```

```
if strcmp(task, 'cs')
    clear tempTrials; idTrials0 = [];
    clear trialsCS1;  idTrials1 = [];
    clear trialsCS2;  idTrials2 = [];
    for tr=1:length(trials)
        if trials(tr).header.task == 0
            if exist('tempTrials')
                tempTrials(end+1) = trials(tr);
            else
                tempTrials(1) = trials(tr);
            end
            idTrials0(end+1) = tr;
        elseif trials(tr).header.task == 1
            if exist('trialsCS1')
                trialsCS1(end+1) = trials(tr);
            else
                trialsCS1(1) = trials(tr);
            end
            idTrials1(end+1) = tr;
        elseif trials(tr).header.task == 2
            if exist('trialsCS2')
                trialsCS2(end+1) = trials(tr);
            else
                trialsCS2(1) = trials(tr);
            end
            idTrials2(end+1) = tr;
        end
    end
    trials = tempTrials;
end


save([fileName fileNo], 'trials', 'hFileInfo');
% save([errorName fileName task fileNo ], 'errorTrials',
'hFileInfo');

if strcmp(task, 'cs')
    if exist('trialsCS1') & exist('trialsCS2')
        if length(trialsCS1)>=20 & length(trialsCS2)>=20
            save([fileName task fileNo ], 'trialsCS1', 'trialsCS2',
'idTrials0', 'idTrials1', 'idTrials2', 'hFileInfo');
        end
    end
end


disp(['No of Trials:  ' num2str(NoTrials)]);
disp(['No of Errortrials:  ' num2str(length(errorTrials))]);

t2 = fix(clock);
disp(['Time elapsed:  ' num2str(etime(t2,t1))]);
ns_CloseFile(hFile);
```

References

Allport DA (1987) Selection for action: some behavioral and neurophysiological considerations of attention and action. In: Perspectives on perception and action (Heuer H, Sanders AF, eds), pp 395–419. Hillsdale, NJ: Erlbaum.

Amemori K, Sawaguchi T (2006) Rule-dependent shifting of sensorimotor representation in the primate prefrontal cortex. Eur J Neurosci 23:1895-1909.

Andersen R, Burdick J, Musallam S, Scherberger H, Pesaran B, Meeker D, Corneil B, Fineman I, Nenadic Z, Branchaud E, Cham J, Greger B, Tai Y, Mojarradi M (2004) Recording advances for neural prosthetics. Conf Proc IEEE Eng Med Biol Soc 7:5352-5355.

Andersen RA (1997) Multimodal integration for the representation of space in the posterior parietal cortex. Philos Trans R Soc Lond B Biol Sci 352:1421-1428.

Andersen RA, Buneo CA (2002) Intentional maps in posterior parietal cortex. Annu Rev Neurosci 25:189-220.

Asher I, Stark E, Abeles M, Prut Y (2007) Comparison of direction and object selectivity of local field potentials and single units in macaque posterior parietal cortex during prehension. J Neurophysiol 97:3684-3695.

Baizer JS, Ungerleider LG, Desimone R (1991) Organization of visual inputs to the inferior temporal and posterior parietal cortex in macaques. J Neurosci 11:168-190.

Balint R (1909) Seelenlähmung des "Schauens", optische Ataxie, räumliche Störung der Aufmerksamkeit. Monatsschr Psychiatr Neurol 25:51-81.

Barash S, Bracewell RM, Fogassi L, Gnadt JW, Andersen RA (1991) Saccade-related activity in the lateral intraparietal area. I. Temporal properties; comparison with area 7a. J Neurophysiol 66:1095-1108.

Batista AP, Buneo CA, Snyder LH, Andersen RA (1999) Reach plans in eye-centered coordinates. Science 285:257-260.

Binkofski F, Dohle C, Posse S, Stephan KM, Hefter H, Seitz RJ, Freund HJ (1998) Human anterior intraparietal area subserves prehension: a combined lesion and functional MRI activation study. Neurology 50:1253-1259.

Blatt GJ, Andersen RA, Stoner GR (1990) Visual receptive field organization and cortico-cortical connections of the lateral intraparietal area (area LIP) in the macaque. J Comp Neurol 299:421-445.

Bonin Gv, Bailey P (1947) The neocortex of Macaca mulatta. Urbana,: University of Illinois Press.

Borra E, Belmalih A, Calzavara R, Gerbella M, Murata A, Rozzi S, Luppino G (2008) Cortical connections of the macaque anterior intraparietal (AIP) area. Cereb Cortex 18:1094-1111.

Bremmer F, Duhamel JR, Ben Hamed S, Graf W (1997) The representation of movement in near extra-personal space in the macaque ventral intraparietal area (VIP). In: Parietal Lobe Contributions to Orientation in 3D Space (Thier P, O. KH, eds). Heidelberg: Springer.

Bremmer F, Duhamel JR, Ben Hamed S, Graf W (2002a) Heading encoding in the macaque ventral intraparietal area (VIP). Eur J Neurosci 16:1554-1568.

Bremmer F, Klam F, Duhamel JR, Ben Hamed S, Graf W (2002b) Visual-vestibular interactive responses in the macaque ventral intraparietal area (VIP). Eur J Neurosci 16:1569-1586.

Britten KH, Shadlen MN, Newsome WT, Movshon JA (1992) The analysis of visual motion: a comparison of neuronal and psychophysical performance. J Neurosci 12:4745-4765.

Brodmann K (1905) Beiträge zur histologischen Lokalisation der Grosshirnrinde. Dritte Mitteilung: Die Rindenfelder der niederen Affen. J Psychol Neurol 4:177-226.

Buneo CA, Andersen RA (2006) The posterior parietal cortex: sensorimotor interface for the planning and online control of visually guided movements. Neuropsychologia 44:2594-2606.

Cavada C (2001) The visual parietal areas in the macaque monkey: current structural knowledge and ignorance. Neuroimage 14:S21-26.

Cerri G, Shimazu H, Maier MA, Lemon RN (2003) Facilitation from ventral premotor cortex of primary motor cortex outputs to macaque hand muscles. J Neurophysiol 90:832-842.

Cisek P, Kalaska JF (2005) Neural correlates of reaching decisions in dorsal premotor cortex: specification of multiple direction choices and final selection of action. Neuron 45:801-814.

Cohen YE, Andersen RA (2000) Reaches to sounds encoded in an eye-centered reference frame. Neuron 27:647-652.

Colby CL, Duhamel JR (1991) Heterogeneity of extrastriate visual areas and multiple parietal areas in the macaque monkey. Neuropsychologia 29:517-537.

Colby CL, Goldberg ME (1999) Space and attention in parietal cortex. Annual review of neuroscience 22:319-349.

Colby CL, Duhamel JR, Goldberg ME (1993a) Ventral intraparietal area of the macaque: anatomic location and visual response properties. J Neurophysiol 69:902-914.

Colby CL, Duhamel JR, Goldberg ME (1993b) The analysis of visual space by the lateral intraparietal area of the monkey: the role of extraretinal signals. Prog Brain Res 95:307-316.

Colby CL, Gattass R, Olson CR, Gross CG (1988) Topographical organization of cortical afferents to extrastriate visual area PO in the macaque: a dual tracer study. J Comp Neurol 269:392-413.

Cooke DF, Taylor CS, Moore T, Graziano MS (2003) Complex movements evoked by microstimulation of the ventral intraparietal area. Proc Natl Acad Sci U S A 100:6163-6168.

Cui H, Andersen RA (2007) Posterior parietal cortex encodes autonomously selected motor plans. Neuron 56:552-559.

Culham JC, Danckert SL, DeSouza JF, Gati JS, Menon RS, Goodale MA (2003) Visually guided grasping produces fMRI activation in dorsal but not ventral stream brain areas. Exp Brain Res 153:180-189.

Duhamel JR, Colby CL, Goldberg ME (1998) Ventral intraparietal area of the macaque: Congruent visual and somatic response properties. Journal of Neurophysiology 79:126-136.

Duhamel JR, Bremmer F, BenHamed S, Graf W (1997) Spatial invariance of visual receptive fields in parietal cortex neurons. Nature 389:845-848.

Dum RP, Strick PL (2005) Frontal lobe inputs to the digit representations of the motor areas on the lateral surface of the hemisphere. J Neurosci 25:1375-1386.

Evarts EV, Fromm C, Kroller J, Jennings VA (1983) Motor Cortex control of finely graded forces. J Neurophysiol 49:1199-1215.

Everling S, Dorris MC, Klein RM, Munoz DP (1999) Role of primate superior colliculus in preparation and execution of anti-saccades and pro-saccades. J Neurosci 19:2740-2754.

Farah M (1990) Visual Agnosia: MIT press.

Fattori P, Breveglieri R, Marzocchi N, Filippini D, Bosco A, Galletti C (2009) Hand orientation during reach-to-grasp movements modulates neuronal activity in the medial posterior parietal area V6A. J Neurosci 29:1928-1936.

Faugier-Grimaud S, Frenois C, Stein DG (1978) Effects of posterior parietal lesions on visually guided behavior in monkeys. Neuropsychologia 16:151-168.

Fluet MC (2009) Properties of macaque ventral premotor cortex during grasping. In: Faculty of Science. Zurich: University of Zurich.

Fogassi L, Gallese V, Buccino G, Craighero L, Fadiga L, Rizzolatti G (2001) Cortical mechanism for the visual guidance of hand grasping movements in the monkey: A reversible inactivation study. Brain 124:571-586.

Fries P, Reynolds JH, Rorie AE, Desimone R (2001) Modulation of oscillatory neuronal synchronization by selective visual attention. Science 291:1560-1563.

Gail A, Andersen RA (2006) Neural dynamics in monkey parietal reach region reflect context-specific sensorimotor transformations. J Neurosci 26:9376-9384.

Gallese V, Murata A, Kaseda M, Niki N, Sakata H (1994) Deficit of hand preshaping after muscimol injection in monkey parietal cortex. Neuroreport 5:1525-1529.

Galletti C, Kutz DF, Gamberini M, Breveglieri R, Fattori P (2003) Role of the medial parieto-occipital cortex in the control of reaching and grasping movements. Exp Brain Res 153:158-170.

Gamberini M, Passarelli L, Fattori P, Zucchelli M, Bakola S, Luppino G, Galletti C (2009) Cortical connections of the visuomotor parietooccipital area V6Ad of the macaque monkey. J Comp Neurol 513:622-642.

Georgopoulos AP, Kalaska JF, Caminiti R, Massey JT (1982) On the relations between the direction of two-dimensional arm movements and cell discharge in primate motor cortex. J Neurosci 2:1527-1537.

Godschalk M, Lemon RN, Nijs HG, Kuypers HG (1981) Behaviour of neurons in monkey peri-arcuate and precentral cortex before and during visually guided arm and hand movements. Exp Brain Res 44:113-116.

Gold JI, Shadlen MN (2000) Representation of a perceptual decision in developing oculomotor commands. Nature 404:390-394.

Goodale MA, Murison RC (1975) The effects of lesions of the superior colliculus on locomotor orientation and the orienting reflex in the rat. Brain Res 88:243-261.

Goodale MA, Milner AD (1992) Separate visual pathways for perception and action. Trends Neurosci 15:20-25.

Goodale MA, Milner AD, Jakobson LS, Carey DP (1991) A neurological dissociation between perceiving objects and grasping them. Nature 349:154-156.

Gottlieb J, Goldberg ME (1999) Activity of neurons in the lateral intraparietal area of the monkey during an antisaccade task. Nat Neurosci 2:906-912.

Gross CG (1973) Visual functions of inferotemporal cortex. In: Handbook of Sensory Physiology (R. J, ed), pp 451-482. Berlin: Springer.

He SQ, Dum RP, Strick PL (1993) Topographic organization of corticospinal projections from the frontal lobe: motor areas on the lateral surface of the hemisphere. J Neurosci 13:952-980.

Hoshi E, Shima K, Tanji J (2000) Neuronal activity in the primate prefrontal cortex in the process of motor selection based on two behavioral rules. J Neurophysiol 83:2355-2373.

Hyvarinen J, Poranen A (1974) Function of the parietal associative area 7 as revealed from cellular discharges in alert monkeys. Brain 97:673-692.

Jakobson LS, Archibald YM, Carey DP, Goodale MA (1991) A kinematic analysis of reaching and grasping movements in a patient recovering from optic ataxia. Neuropsychologia 29:803-809.

Jeannerod M (1988) The neural and behavioral organization of goal-directed movements. Oxford: Oxford University Press.

Jeannerod M, Biguer B (1982) Visuomotor mechanisms in reaching wihthin extrapersonal space. In: Analysis of visual behavior (Ingle DJ, Goodale MA, Mansfield RJW, eds), pp 387-409. Cambridge, MA: MIT Press.

Jeannerod M, Michel F, Prablanc C (1984) The control of hand movements in a case of hemianaesthesia following a parietal lesion. Brain 107 (Pt 3):899-920.

Jeannerod M, Decety J, Michel F (1994) Impairment of grasping movements following a bilateral posterior parietal lesion. Neuropsychologia 32:369-380.

Johnson PB, Ferraina S, Bianchi L, Caminiti R (1996) Cortical networks for visual reaching: physiological and anatomical organization of frontal and parietal lobe arm regions. Cereb Cortex 6:102-119.

Kakei S, Hoffman DS, Strick PL (2001) Direction of action is represented in the ventral premotor cortex. Nat Neurosci 4:1020-1025.

Kalaska JF, Cisek P, Gosselin-Kessiby N (2003) Mechanisms of selection and guidance of reaching movements in the parietal lobe. Adv Neurol 93:97-119.

Katzner S, Nauhaus I, Benucci A, Bonin V, Ringach DL, Carandini M (2009) Local origin of field potentials in visual cortex. Neuron 61:35-41.

Klam F, Graf W (2003) Vestibular response kinematics in posterior parietal cortex neurons of macaque monkeys. Eur J Neurosci 18:995-1010.

Kurata K, Tanji J (1986) Premotor cortex neurons in macaques: activity before distal and proximal forelimb movements. J Neurosci 6:403-411.

Lemon RN (2008) Descending pathways in motor control. Annu Rev Neurosci 31:195-218.

Lemon RN, Kirkwood PA, Maier MA, Nakajima K, Nathan P (2004) Direct and indirect pathways for corticospinal control of upper limb motoneurons in the primate. Prog Brain Res 143:263-279.

Lewis JW, Van Essen DC (2000) Corticocortical connections of visual, sensorimotor, and multimodal processing areas in the parietal lobe of the macaque monkey. J Comp Neurol 428:112-137.

Li CS, Mazzoni P, Andersen RA (1999) Effect of reversible inactivation of macaque lateral intraparietal area on visual and memory saccades. J Neurophysiol 81:1827-1838.

Logothetis NK, Wandell BA (2004) Interpreting the BOLD signal. Annu Rev Physiol 66:735-769.

Logothetis NK, Pauls J, Augath M, Trinath T, Oeltermann A (2001) Neurophysiological investigation of the basis of the fMRI signal. Nature 412:150-157.

Luppino G, Murata A, Govoni P, Matelli M (1999) Largely segregated parietofrontal connections linking rostral intraparietal cortex (areas AIP and VIP) and the ventral premotor cortex (areas F5 and F4). Exp Brain Res 128:181-187.

Matelli M, Luppino G, Rizzolatti G (1985) Patterns of cytochrome oxidase activity in the frontal agranular cortex of the macaque monkey. Behav Brain Res 18:125-137.

Matelli M, Camarda R, Glickstein M, Rizzolatti G (1986) Afferent and efferent projections of the inferior area 6 in the macaque monkey. J Comp Neurol 251:281-298.

Maunsell JH, van Essen DC (1983) The connections of the middle temporal visual area (MT) and their relationship to a cortical hierarchy in the macaque monkey. J Neurosci 3:2563-2586.

Mehring C, Rickert J, Vaadia E, Cardosa de Oliveira S, Aertsen A, Rotter S (2003) Inference of hand movements from local field potentials in monkey motor cortex. Nat Neurosci 6:1253-1254.

Milner AD, Ockleford EM, Dewar W (1977) Visuo-spatial performance following posterior parietal and lateral frontal lesions in stumptail macaques. Cortex 13:350-360.

Mitzdorf U (1987) Properties of the evoked potential generators: current source-density analysis of visually evoked potentials in the cat cortex. Int J Neurosci 33:33-59.

Morel A, Bullier J (1990) Anatomical segregation of two cortical visual pathways in the macaque monkey. Vis Neurosci 4:555-578.

Mountcastle VB, Lynch JC, Georgopoulos A, Sakata H, Acuna C (1975) Posterior parietal association cortex of the monkey: command functions for operations within extrapersonal space. J Neurophysiol 38:871-908.

Muakkassa KF, Strick PL (1979) Frontal lobe inputs to primate motor cortex: evidence for four somatotopically organized 'premotor' areas. Brain Res 177:176-182.

Muir RB, Lemon RN (1983) Corticospinal neurons with a special role in precision grip. Brain Res 261:312-316.

Murata A, Gallese V, Luppino G, Kaseda M, Sakata H (2000) Selectivity for the shape, size, and orientation of objects for grasping in neurons of monkey parietal area AIP. J Neurophysiol 83:2580-2601.

Murata A, Fadiga L, Fogassi L, Gallese V, Raos V, Rizzolatti G (1997) Object representation in the ventral premotor cortex (area F5) of the monkey. J Neurophysiol 78:2226-2230.

Murata T, Kitahara M (1996) Acceleration registrography of head movement during alternating inclination of the support platform. Acta Otolaryngol

Acta Otolaryngologica (Stockh).

Musallam S, Corneil BD, Greger B, Scherberger H, Andersen RA (2004) Cognitive control signals for neural prosthetics. Science 305:258-262.

Nakajima K, Maier MA, Kirkwood PA, Lemon RN (2000) Striking differences in transmission of corticospinal excitation to upper limb motoneurons in two primate species. J Neurophysiol 84:698-709.

Nakamura H, Kuroda T, Wakita M, Kusunoki M, Kato A, Mikami A, Sakata H, Itoh K (2001) From three-dimensional space vision to prehensile hand movements: the lateral intraparietal area links the area V3A and the anterior intraparietal area in macaques. J Neurosci 21:8174-8187.

National Research Council (2003) Guidelines for the care and use of mammals in neuroscience and behavioral research. Washington, D.C.: National Academies Press.

Optican LM (2005) Sensorimotor transformation for visually guided saccades. Ann N Y Acad Sci 1039:132-148.

Pandya DN, Kuypers HG (1969) Cortico-cortical connections in the rhesus monkey. Brain Res 13:13-36.

Pandya DN, Vignolo LA (1971) Intra- and interhemispheric projections of the precentral, premotor and arcuate areas in the rhesus monkey. Brain Res 26:217-233.

Pandya DN, Seltzer B (1982) Intrinsic connections and architectonics of posterior parietal cortex in the rhesus monkey. J Comp Neurol 204:196-210.

Paulignan Y, MacKenzie C, Marteniuk R, Jeannerod M (1991) Selective perturbation of visual input during prehension movements. 1. The effects of changing object position. Exp Brain Res 83:502-512.

Percival DB, Walden AT (1993) Spectral analysis for physical applications - multitaper and conventional univariate techniques. Cambridge, MA: Cambridge University Press.

Perenin MT, Vighetto A (1988) Optic ataxia: a specific disruption in visuomotor mechanisms. I. Different aspects of the deficit in reaching for objects. Brain 111:643-674.

Pesaran B, Nelson MJ, Andersen RA (2008) Free choice activates a decision circuit between frontal and parietal cortex. Nature 453:406-409.

Pesaran B, Pezaris JS, Sahani M, Mitra PP, Andersen RA (2002) Temporal structure in neuronal activity during working memory in macaque parietal cortex. Nat Neurosci 5:805-811.

Platt ML, Glimcher PW (1999) Neural correlates of decision variables in parietal cortex. Nature 400:233-238.

Pohl W (1973) Dissociation of spatial discrimination deficits following frontal and parietal lesions in monkeys. J Comp Physiol Psychol 82:227-239.

Porter R, Lemon RN (1993) Corticospinal function and voluntary movement. Oxford: Oxford University Press.

Raos V, Umilta MA, Murata A, Fogassi L, Gallese V (2006) Functional properties of grasping-related neurons in the ventral premotor area F5 of the macaque monkey. J Neurophysiol 95:709-729.

Rathelot JA, Strick PL (2006) Muscle representation in the macaque motor cortex: an anatomical perspective. Proc Natl Acad Sci U S A 103:8257-8262.

Rizzolatti G, Luppino G (2001) The cortical motor system. Neuron 31:889-901.

Rizzolatti G, Luppino G, Matelli M (1998) The organization of the cortical motor system: new concepts. Electroencephalogr Clin Neurophysiol 106:283-296.

Rizzolatti G, Riggio L, Dascola I, Umilta C (1987) Reorienting attention across the horizontal and vertical meridians: evidence in favor of a premotor theory of attention. Neuropsychologia 25:31-40.

Rizzolatti G, Camarda R, Fogassi L, Gentilucci M, Luppino G, Matelli M (1988) Functional organization of inferior area 6 in the macaque monkey. II. Area F5 and the control of distal movements. Exp Brain Res 71:491-507.

Rondot P, de Recondo J, Dumas JL (1977) Visuomotor ataxia. Brain 100:355-376.

Rozzi S, Calzavara R, Belmalih A, Borra E, Gregoriou GG, Matelli M, Luppino G (2006) Cortical connections of the inferior parietal cortical convexity of the macaque monkey. Cereb Cortex 16:1389-1417.

Sakata H, Taira M, Murata A, Mine S (1995) Neural mechanisms of visual guidance of hand action in the parietal cortex of the monkey. Cereb Cortex 5:429-438.

Sakata H, Taira M, Kusunoki M, Murata A, Tanaka Y (1997) The TINS Lecture. The parietal association cortex in depth perception and visual control of hand action. Trends Neurosci 20:350-357.

Sakata H, Taira M, Kusunoki M, Murata A, Tsutsui K, Tanaka Y, Shein WN, Miyashita Y (1999) Neural representation of three-dimensional features of manipulation objects with stereopsis. Exp Brain Res 128:160-169.

Scherberger H, Andersen RA (2003) Sensorimotor transformations. In: The Visual Neurosciences (Chalupa LM, Werner JS, eds), pp 1324-1336. Cambridge, MA: MIT Press.

Scherberger H, Andersen RA (2007) Target selection signals for arm reaching in the posterior parietal cortex. J Neurosci 27:2001-2012.

Scherberger H, Buneo CA, Andersen RA (2003a) Local field potential tuning in the macaque posterior parietal cortex during arm-reaching movements. SocNeurosciAbst 29: 279.16.

Scherberger H, Jarvis MR, Andersen RA (2005) Cortical local field potential encodes movement intentions in the posterior parietal cortex. Neuron 46:347-354.

Scherberger H, Fineman I, Musallam S, Dubowitz DJ, Bernheim KA, Pesaran B, Corneil BD, Gillikin B, Andersen RA (2003b) Magnetic resonance image-guided implantation of chronic recording electrodes in the macaque intraparietal sulcus. Journal of Neuroscience Methods 130:1-8.

Schneider GE (1969) Two visual systems. Science 163:895-902.

Shikata E, Tanaka Y, Nakamura H, Taira M, Sakata H (1996) Selectivity of the parietal visual neurones in 3D orientation of surface of stereoscopic stimuli. Neuroreport 7:2389-2394.

Shikata E, McNamara A, Sprenger A, Hamzei F, Glauche V, Buchel C, Binkofski F (2008) Localization of human intraparietal areas AIP, CIP, and LIP using surface orientation and saccadic eye movement tasks. Hum Brain Mapp 29:411-421.

Smith AM, Hepp-Reymond MC, Wyss UR (1975) Relation of activity in precentral cortical neurons to force and rate of force change during isometric contractions of finger muscles. Exp Brain Res 23:315-332.

Snyder LH, Batista AP, Andersen RA (1997) Coding of intention in the posterior parietal cortex. Nature 386:167-170.

Snyder LH, Batista AP, Andersen RA (1998) Change in motor plan, without a change in the spatial locus of attention, modulates activity in posterior parietal cortex. J Neurophysiol 79:2814-2819.

Spinks RL, Kraskov A, Brochier T, Umilta MA, Lemon RN (2008) Selectivity for grasp in local field potential and single neuron activity recorded simultaneously from M1 and F5 in the awake macaque monkey. J Neurosci 28:10961-10971.

Stark E, Drori R, Asher I, Ben-Shaul Y, Abeles M (2007) Distinct movement parameters are represented by different neurons in the motor cortex. Eur J Neurosci 26:1055-1066.

Taira M, Mine S, Georgopoulos AP, Murata A, Sakata H (1990) Parietal cortex neurons of the monkey related to the visual guidance of hand movement. Exp Brain Res 83:29-36.

Taira M, Tsutsui KI, Jiang M, Yara K, Sakata H (2000) Parietal neurons represent surface orientation from the gradient of binocular disparity. J Neurophysiol 83:3140-3146.

Tanne-Gariepy J, Rouiller EM, Boussaoud D (2002) Parietal inputs to dorsal versus ventral premotor areas in the macaque monkey: evidence for largely segregated visuomotor pathways. Exp Brain Res 145:91-103.

Thier P, Andersen RA (1996) Electrical microstimulation suggests two different forms of representation of head-centered space in the intraparietal sulcus of rhesus monkeys. Proc Natl Acad Sci U S A 93:4962-4967.

Thier P, Andersen RA (1998) Electrical microstimulation distinguishes distinct saccade- related areas in the posterior parietal cortex. Journal of Neurophysiology 80:1713-1735.

Tsutsui K, Sakata H, Naganuma T, Taira M (2002) Neural correlates for perception of 3D surface orientation from texture gradient. Science 298:409-412.

Tsutsui K, Jiang M, Sakata H, Taira M (2003) Short-term memory and perceptual decision for three-dimensional visual features in the caudal intraparietal sulcus (Area CIP). J Neurosci 23:5486-5495.

Tsutsui K, Jiang M, Yara K, Sakata H, Taira M (2001) Integration of perspective and disparity cues in surface-orientation-selective neurons of area CIP. J Neurophysiol 86:2856-2867.

Umilta MA, Brochier T, Spinks RL, Lemon RN (2007) Simultaneous recording of macaque premotor and primary motor cortex neuronal populations reveals different functional contributions to visuomotor grasp. J Neurophysiol 98:488-501.

Umilta MA, Escola L, Intskirveli I, Grammont F, Rochat M, Caruana F, Jezzini A, Gallese V, Rizzolatti G (2008) When pliers become fingers in the monkey motor system. Proc Natl Acad Sci U S A 105:2209-2213.

Ungerleider L, Mishkin M (1982) Two cortical visual systems. In: Analysis of Visual Behavior (J. ID, Goodale MA, W. MRJ, eds), pp 549-586. Cambridge: MIT Press.

Ungerleider LG, Brody BA (1977) Extrapersonal spatial orientation: the role of posterior parietal, anterior frontal, and inferotemporal cortex. Exp Neurol 56:265-280.

Vogt C, Vogt O (1919) Allgemeinere Ergebnisse unserer Hirnforschung. J Psychol u Neurol 25:279-462.

Wallis JD, Anderson KC, Miller EK (2001) Single neurons in prefrontal cortex encode abstract rules. Nature 411:953-956.

White IM, Wise SP (1999) Rule-dependent neuronal activity in the prefrontal cortex. Exp Brain Res 126:315-335.

Wilson FA, Scalaidhe SP, Goldman-Rakic PS (1993) Dissociation of object and spatial processing domains in primate prefrontal cortex. Science 260:1955-1958.

Zhang M, Barash S (2000) Neuronal switching of sensorimotor transformations for antisaccades. Nature 408:971-975.

Curriculum vitae

Personalien

Familienname:	BAUMANN
Vornamen:	Markus Andreas
Geburtsdatum:	9. Oktober, 1976
Bürgerort:	Wassen UR
Natinalität:	Schweiz

Ausbildung

1989-1996	Gymnasium Friedberg, 9200 Gossau SG Matura Typus B
1996-1997	Physikstudium ETH Zürich, Abbruch im 2. Semester und Wechsel auf Medizin
1997-2003	Medizinstudium, Universität Zürich Eidgenössisches Diplom als Arzt
Okt. 2000-2003	MD/PhD Studium parallel zum Medizinstudium mit Prüfungen in Informatik, Physik und Lineare Algebra
2004-2009	PhD am Institut für Neuroinformatik, ETH Zürich und Universität Zürich

Auszeichnungen

2005	MD-PhD Stipendium der SAMW für 3 Jahre
2004	Forschungskredit der Universität Zürich für 2 Jahre

Publikationen

Baumann MA, Fluet MC, Scherberger H: Context-specific grasp movement representation in the macaque anterior intraparietal area. J Neurosci **29:**6436-6448, 2009

Vorträge

Baumann MA, Fluet MC, Scherberger H: Synchronisation of macaque areas AIP and F5 in a delayed hand grasping task. Society for Neuroscience, Annual Meeting 2007. San Diego, CA.